

A THREE-DIMENSIONAL LINEAR ANALYSIS OF
STEADY SHIP MOTION IN DEEP WATER.

A THESIS SUBMITTED FOR THE DEGREE OF DOCTOR OF PHILOSOPHY

BY

JOB JOHANNES MARIA BAAR.

DEPARTMENT OF MECHANICAL ENGINEERING,
BRUNEL UNIVERSITY,
UXBRIDGE, U.K.

NOVEMBER 1986.

To my wife.

To my parents.

ABSTRACT

The investigation of steady ship motion in calm water is a classic problem in ship hydrodynamics, where ship waves and wave resistance are subjects of unquestionable importance. Despite considerable efforts in the past a satisfactory solution of the steady ship motion problem has not been achieved so far. The application of three-dimensional potential flow theory results in an essentially nonlinear problem formulation due to the unknown position of the disturbed free surface. In this thesis consistent linearisation schemes are discarded in favour of the inconsistent Neumann-Kelvin theory. This approximation implies that nonlinear free surface effects are neglected entirely, but the three-dimensional features of the fluid flow and hull geometry are otherwise fully retained.

The Kelvin wave source potential, otherwise known as the wave resistance Green's function, is analysed in great detail. Solutions to the disturbance potential of the steady perturbed ship flow are obtained by means of a Kelvin wave source distribution method. The exact source strength is the solution of a Fredholm integral equation of the second kind. An explicit source strength approximation, valid for sufficiently slender ships operating at fairly low speeds, is investigated. Particular emphasis is placed on computational aspects. Highly accurate and efficient methods for the evaluation of the Kelvin wave source potential are proposed. The developed theory is applied to five different ship forms, viz. a submerged prolate spheroid, Wigley's parabolic ship, a tanker, a fast destroyer and a cruiser. Over a wide range of ship speeds experimental data are compared with theoretical predictions of the steady flow parameters such as wave resistance, wave profiles, pressure signatures and lift force distributions.

CONTENTS

| | <i>page</i> |
|--|-------------|
| ABSTRACT | 1 |
| 1. INTRODUCTION | 4 |
| 1.1 Ship waves and wave resistance | 4 |
| 1.2 Historical remarks | 7 |
| 1.3 The present investigation | 14 |
| 1.4 Outline of thesis | 18 |
| <i>Tables and figures</i> | 22 |
| 2. HYDRODYNAMIC THEORY OF STEADY SHIP MOTION | 24 |
| 2.1 Potential flow description | 24 |
| 2.2 Exact problem formulation | 26 |
| 2.3 Linear Neumann-Kelvin theory | 29 |
| 2.4 Wave resistance, sinkage and trim | 33 |
| <i>Tables and figures</i> | 37 |
| 3. THE KELVIN WAVE SOURCE POTENTIAL | 42 |
| 3.1 Definition and fundamental properties | 42 |
| 3.2 Survey of alternative expressions | 45 |
| 3.3 Analysis of the nearfield disturbance | 49 |
| 3.4 Analysis of the wavelike disturbance | 53 |
| <i>Tables and figures</i> | 60 |
| 4. INTEGRAL IDENTITIES FOR THE DISTURBANCE POTENTIAL | 67 |
| 4.1 Basic integral identity | 67 |
| 4.2 Auxiliary singularity distributions | 72 |
| 4.3 Explicit slender ship approximation | 77 |
| 4.4 Kochin's function and Havelock's formula | 80 |
| <i>Tables and figures</i> | 86 |

| | <i>page</i> |
|---|-------------|
| 5. COMPUTATIONAL ASPECTS | 92 |
| 5.1 Approximation of integral identities | 92 |
| 5.2 Evaluation of the nearfield disturbance | 99 |
| 5.3 Evaluation of the wavelike disturbance | 104 |
| <i>Tables and figures</i> | 110 |
| 6. APPLICATIONS OF THE THEORY | 119 |
| 6.1 Hull data | 119 |
| 6.2 Mathematically defined hull forms | 121 |
| 6.2.1 Submerged prolate spheroid | 121 |
| 6.2.2 Wigley's parabolic hull | 122 |
| 6.3 Realistic hull forms | 126 |
| 6.3.1 HSVA tanker | 126 |
| 6.3.2 'Friesland' class destroyer | 128 |
| 6.3.3 Cruiser hull form | 130 |
| <i>Tables and figures</i> | 132 |
| 7. CONCLUSIONS | 152 |
| APPENDIX Evaluation of special functions | 155 |
| REFERENCES | 161 |
| NOMENCLATURE | 180 |
| ACKNOWLEDGEMENT | 182 |

1. INTRODUCTION

1.1 SHIP WAVES AND WAVE RESISTANCE

The investigation of a ship in steady rectilinear motion at the free surface of a calm sea is a classic problem in ship hydrodynamics. The satisfactory solution of this problem is of great importance to naval architects and engineers. The ship designer has to ensure that a proposed ship achieves the desired speed with a minimum of required power, see Saunders (1957). This difficult task requires an adequate estimate of the resistance to ship motion as well as a thorough understanding of the steady flow properties in order to obtain a good matching between the ship's hull and the propeller. Civil and coastal engineers are more interested in the wave pattern generated by the moving ship, see Sorensen (1973). Ship waves may have important effects on other ships moored or manoeuvring in harbours and navigation channels and on the erosion of shore lines and channel and river banks, see Massie (1978). A recent application of steady ship motion theory concerns the possibility of identifying naval ships and submarines by means of the accurate observation of ship generated waves and water pressures, see Swanson (1984).

The experimental and theoretical investigation of steady ship motion is complicated considerably by the dependence of the ship resistance on both the viscosity of the sea water and the

presence of the gravitational field. The total ship resistance R_t consists of two components, the viscous resistance R_v and the wave resistance R_w . The viscous resistance is due to the viscous stresses acting tangentially to the ship's hull surface and the formation, growth and separation (if this occurs) of the ship's boundary layer, see Todd (1966). The moving ship also generates a characteristic pattern of surface waves trailing downstream in its wake. The work done by the wave resistance equals the energy required for the formation of ship waves, see Wehausen (1973).

If the sea water is regarded as homogeneous and incompressible the resistance is dependent on the density ρ and kinematic viscosity ν of the seawater, the acceleration of gravity g , and the speed V and a characteristic dimension L of the ship. In nondimensional form the decomposition of the total resistance into viscous and wave resistance may then be expressed as:

$$C_t(R_n, F_n) = C_v(R_n, F_n) + C_w(R_n, F_n) \quad , \quad (1.1)$$

where the resistance coefficient $C = R/\rho V^2 L^2$, the subscripts t , v and w refer to the total, viscous and wave resistance respectively, the Reynolds number $R_n = VL/\nu$ and the Froude number $F_n = V/\sqrt{gL}$. The viscous and wave resistance are dependent on both the Reynolds and Froude number and cannot be clearly separated, see Sharma (1965). The frictional resistance, that is, the part due to the viscous tangential stresses, depends on the wave profile along the ship's hull, whereas the formation of ship waves is influenced by the ship's boundary layer and wake. The complete solution of the Navier-Stokes

equations describing the viscous gravitational flow about a moving ship is beyond the present state of computing art (see Miyata et al (1983) for some recent developments).

The difficulties posed by the interaction between viscous and gravitational effects are overcome effectively if it is assumed that equation (1.1) may be approximated by:

$$C_t(R_n, F_n) \approx C_v(R_n) + C_w(F_n) \quad (1.2)$$

This expression is commonly referred to as Froude's (1868) hypothesis concerning the separation of viscous and wave resistance. Froude's method for the experimental determination of ship resistance is based on the assumption that the Froude number alone controls the geometrical similarity of the wave patterns generated by geometrically similar ships (i.e. a small scale model and a full scale ship).

In this study the attention is focussed on an idealised version of the steady ship motion problem. Specifically, the sea water is regarded as homogeneous, incompressible and inviscid (i.e. ideal) and irrotational flow is assumed. In other words, it is supposed that the effects of viscosity on the formation of ship waves are negligible and the wave resistance is a function of the Froude number alone, in agreement with Froude's hypothesis. The usefulness of the investigation of this simplified problem may be seen as follows. For most ships the viscous resistance cannot be significantly reduced by changing the hull form and this leaves

the ship designer more or less free to choose a suitable hull form (from a resistance point of view). Optimal ship forms are those which generate the smallest waves and it is therefore highly desirable to develop a theoretical tool to analyse the relationship between wave resistance and the geometry of the ship's hull.

It should be noticed that the physical interpretation of the 'inviscid' wave resistance is by no means clear and due care is therefore required when comparing experimental data with theoretical predictions. Because of the approximate nature of equation (2.1) measured wave resistance is always endowed with viscous effects. Eggers et al (1967) and Wehausen (1973) discuss a variety of techniques employed in the definition and subsequent measurement of wave resistance.

1.2 HISTORICAL REMARKS

For many years physicists, mathematicians, engineers and naval architects have expended considerable effort in developing an adequate solution of the steady ship motion problem. The experimental and analytical developments are reviewed comprehensively by Wigley (1949), Lunde (1951), Inui (1962), Weinblum (1963), Guilloton (1964), Kostyukov (1968), Gadd (1968), Wehausen (1973) and Newman (1976). Figure 1.1 illustrates the considerable activity in this field. The histograms refer to the number of publications on the experimental and/or theoretical study of ship waves and wave resistance. The data were compiled using the extensive

bibliographies given by Kostyukov (1968), Wehausen (1973, 1976) and Inui (1976). The following remarks may serve to explain some of the features of the frequency curve shown in Figure 1.1.

Because ships are large structures accurate full-scale measurements of ship resistance are difficult, time consuming and expensive. At a very early stage resort was taken to experiments with scale models of ships. Leonardo da Vinci (1452-1519) was among the first to measure model resistance and wave patterns (see Tursini (1953)). Over the next three centuries scientists such as Newton, Lagrange, Euler (1749), Bernoulli (1757) and naval architects in Holland, France, Scandinavia and Great Britain devoted their attention to the problem and carried out model tests.

William Froude (1810-1879) is nowadays generally recognised as the first person to have examined ship resistance in a systematic manner. Froude (1868) pointed out the advantages of model tests and proposed to build a towing tank. The first towing tank of the type commonly used nowadays was built in Torquay in 1871 (see Gawn (1955)). Froude (1876) had also a remarkable insight into the different roles played by viscosity and gravity in the ship resistance problem. The first detailed discussions of the observed characteristics of ship generated waves were presented by W. Froude (1877) and R.E. Froude (1889).

At about the same time Lord Kelvin (see Thomson (1887, 1904)) established the theoretical mechanism of ship wave generation. A moving ship generates a 'Kelvin' wave pattern consisting of two wave systems: a diverging wave system spreading out downstream on either side of the ship and a transverse wave system contained within the wedge shaped area between the diverging waves. Kelvin's theory is generally correct but some theoretical shortcomings and difficulties were later solved by Havelock (1908), Hogner (1922), Peters (1949), Ursell (1960) and others.

J.H. Michell (1863-1940) was the first to establish an analytical relationship between the wave resistance and the geometry of the ship's hull. Michell (1898) presented a theory to describe the steady potential flow about an idealised thin ship hull and arrived at the wave resistance by integrating the water pressure distribution over the ship's hull surface. Theoretical work in the first half of the twentieth century was largely dominated by the efforts of Sir Thomas Havelock (1877-1968) who published a long series of papers. Havelock (1925) gave a new derivation of the thin ship wave resistance formula based upon the use of a Green's function method rather than the Fourier integral method originally used by Michell (1898). Later Havelock (1934) showed that the wave resistance may alternatively be obtained by evaluating the energy contained in the Kelvin wave pattern behind a moving ship (see also Eggers et al (1967) and Newman (1977)). The nature of the thin ship approximation was clarified by Peters and Stoker (1957) who established that Michell's formula is the

first order approximation in a thin ship perturbation expansion.

W.C.S. Wigley (1890-1970) appears to have been the first to have evaluated Michell's formula in a systematic manner (see Wigley (1949) for a review of his works). Due to interference effects between the ship's bow and stern wave systems (see Saunders (1957)) the curve of wave resistance versus ship speed is of a rather oscillatory nature. The humps (maxima) and hollows (minima) occur at Froude numbers where the stern wave system is amplified or cancelled respectively by the bow wave train. Comparison between experimental data and theoretical predictions shows that Michell's wave resistance formula tends to exaggerate the humps and hollows. Moreover, the predicted humps and hollows occur in general at lower Froude numbers than the experimental data.

The wave resistance of an idealised flat ship was investigated by Hogner (1932), who also proposed a remarkable interpolation formula to interpolate between the flat and thin ship wave resistance approximations. Encouraged by the success of slender body theory in aerodynamics and seakeeping theory, Vossers (1962), Maruo (1962) and Tuck (1964) developed a simple approximation formula for the wave resistance of a slender ship. Unfortunately the slender ship formula appears to be a natural limit of the thin and flat ship wave resistance formulas and this approach has been unsuccessful, see Ogilvie (1970) and Noblesse (1983). Recently Maruo (1982) and Yeung and Kim (1984) have proposed new formulations of the slender ship theory of wave resistance, but very few numerical results have been published thusfar, see Maruo and Ikehata (1983).

Various authors have investigated the wavemaking of fully submerged bodies, see Havelock (1931a,b), Kochin (1951), Bessho (1961), Farell (1973) and Guttman (1983). Most surface ships operate at fairly low Froude number and the concept of long, slow ships is utilised in the low Froude number wave resistance theories of Guevel et al (1974), Newman (1976), Baba (1976, 1977), Maruo (1977) and Kayo (1978). Chen and Noblesse (1983b) have made an extensive comparison of experimental data and theoretical wave resistance predictions for the Wigley hull*. They conclude tentatively that the slow ship predictions are in poor agreement with the experimental data except possibly at very low Froude numbers (at which however both the experimental and numerical data show a considerable variation). Certain questions concerning the true asymptotic nature of the low speed limit have recently been investigated by means of the ray theory, see Keller (1974, 1979), Inui and Kajitani (1977), Yim (1981), Chung (1984) and Tulin (1984). A ray theory for slow ships is similar to the theory of geometrical optics and presents two separate relations. One is the dispersion relation for the local wave phase and the other is the transport equation for the local wave amplitude. The ray theory tries to explain the mechanism of ship wave generation but Tulin (1984) concludes that the present knowledge is still inadequate.

* Since first introduced by Wigley (1942) this mathematically defined hull form has been used extensively for both experimental and theoretical studies. This hull form with parabolic frames and waterlines has a beam/length ratio of 0.1 and a (constant) draft/length ratio of 0.0625.

In recent years much attention has been focussed on the so-called Neumann-Kelvin theory which was originally proposed by Brard (1971). In this three-dimensional linearised potential flow theory the nonlinear effects stemming from the presence of the free surface are neglected, while the three-dimensional features of the fluid flow and the hull geometry are fully retained. From a formal mathematical point of view this approach is inconsistent, but in practice it may be argued that most surface ships are somewhat slender and operate at fairly low Froude numbers and therefore the free surface disturbance is relatively small (except possibly in the bow regime). The numerical solution of the Neumann-Kelvin problem for the steady disturbance potential of a moving surface ship is a difficult task and theoretical predictions of the wave resistance have only recently become available, see Kusaka (1976), Guevel et al (1977), Tsutsumi (1979) and Tsai et al (1983). Further aspects of the Neumann-Kelvin theory are discussed in the next section.

Omitted from the previous discussion are the nonlinear wave resistance theories which go beyond the first order linear approximations as used in the consistent thin, flat, slender and slow ship theories and in the inconsistent Neumann-Kelvin theory. The major difficulty in the higher-order wave theories stems from the unknown position of the disturbed free surface and the need to use Taylor series expansions to obtain the boundary conditions on the mean position of the free surface, see Peters and Stoker (1957) for an outline of this procedure. Wehausen (1963),

Maruo (1966) and Eggers (1966) have investigated the second order thin ship theory. The use of Taylor series expansions has led to some criticism with regard to the continuation of the potential flow solution outside the mean flow domain and the occurrence of non-uniformities at the ship's bow and stern. These difficulties can be partially avoided by adopting a Lagrangian description of the fluid flow whereby the physical space is mapped into a reference domain where the disturbed free surface and the hull surface are known coordinate surfaces, see Yim (1968), Wehausen (1969) and Noblesse and Dagan (1976). A particularly interesting albeit formally inconsistent variant of this approach is Guilloton's (1964, 1965) method. This procedure starts with the flow velocity field as predicted by the linear Michell theory and then maps it into a better approximation by means of a kind of inverse streamline tracing method where the hull surface is however forced to be a stream surface. The method has been applied by Emerson (1967, 1971), Gadd (1973,1979) and Guevel et al (1979). At low to moderate Froude numbers there is good agreement between Guilloton's method and measured data. Finally mention is made of some recent attempts to solve numerically the exact nonlinear potential flow problem by means of Rankine source, finite element or finite difference methods, see Korving and Hermans (1977), Oomen (1979, 1981), Daube (1980), Daube and Dulieu (1981), Chan and Chan (1979), Yen and Chamberlain (1983), Chamberlain and Yen (1985) and Maruo and Ogiwara (1985).

1.3 THE PRESENT INVESTIGATION

The present study is concerned with the investigation of the steady flow disturbance caused by a moving surface ship. In this thesis the Neumann-Kelvin theory is adopted, that is, the flow disturbance is described by means of a three-dimensional linearised potential flow theory. Specifically, the free surface condition is linearised about the mean sea plane, but the boundary condition at the ship's wetted hull surface is retained in its exact form. The formal inconsistency of the Neumann-Kelvin theory warrants some clarification of the reasons for its use in this thesis.

The irrotational flow disturbance caused by a ship in steady rectilinear motion at the free surface of a calm ideal sea may be described by means of potential flow theory. The wave resistance and other flow parameters may be derived from the knowledge of the velocity potential function, see for example Wehausen (1973) and Newman (1976). The velocity potential must satisfy appropriate conditions in the flow domain and on its boundaries. The position of the disturbed free surface is of course not known beforehand and the resulting nonlinearity of the free surface condition effectively prohibits the development of the complete solution of the exact potential flow problem. Systematic perturbation schemes may be used to overcome this difficulty and the free surface condition is then linearised about

the undisturbed mean sea plane by means of a Taylor series expansion. However, the consistent application of such techniques requires that one is able to designate a small perturbation parameter connected with the problem in such a manner that the free surface disturbance gradually vanishes as the magnitude of the perturbation parameter is decreased. For example, in the thin and slow ship theories the small perturbation parameter corresponds to the ship's thickness and the Froude number respectively (see Newman (1976)). Mathematically such procedures are consistent and justified, but they do not necessarily imply any better correlation between experiment and theory.

In the Neumann-Kelvin theory the perturbation parameter is not explicitly specified but it is assumed (sic) that the disturbance of the free surface caused by the moving ship is small, without formally identifying the reasons for its smallness. Clearly this procedure cannot be justified from a formal mathematical point of view. However, most surface ships are somewhat slender (elongated) and operate at fairly low values of the Froude number. In practice it may therefore be argued that the ship generated free surface disturbance is relatively small over a wide portion of the sea surface^{*}. Noblesse (1976) shows that the linear Neumann-Kelvin problem for the disturbance

* A possible exception occurs near the ship's bow, where the flow has a stagnation point and the wave amplitude attains a theoretical maximum value.

potential is in fact the consistent first order approximation in a regular perturbation scheme, where the perturbation parameter is chosen as some measure of the ship generated wave pattern; he also points out that the transfer of the exact hull surface condition to the ship's centreplane in the Michell (1898) thin ship theory may be more restrictive in practice than the linearisation of the free surface condition. The foregoing observations then suggest that in a first approximation the linearised free surface condition is adequate, but the three-dimensional features of the hull form should be fully retained. Moreover, the inconsistency of the Neumann-Kelvin approximation should not prevent the practical comparison of experimental and theoretical predictions.

The main problem arising in the application of the Neumann-Kelvin theory is the determination of the solution of the linear boundary value problem for the disturbance potential. Numerical methods to achieve this purpose can be classified into two categories. The first category of so-called boundary integral methods is based on integral identities for the velocity potential obtained by applying Green's second formula to the potential and an appropriate Green's function. The Green's function may be chosen as either a fundamental Rankine source or the potential of a translating submerged source (the Kelvin wave source potential). In the first approach the Rankine sources are distributed over both the mean sea plane and the wetted hull surface, see for example Adachi and Takeshi (1983). The second approach involves the distribution of Kelvin wave sources over both the hull surface

and the water line contour, see Brard (1972). Earlier calculations without the water line integral were carried out by Gadd (1970) and Kobayashi and Ikehata (1970). Calculations including the water line integral have been carried out by Chang (1979), Suzuki (1979), Tsutsumi (1979) and Tsai et al (1983). The second category of numerical methods is that of the finite element methods where the equivalent variational formulation of the Neumann-Kelvin problem is solved by subdividing the flow domain into finite elements. The downstream radiation condition can be satisfied by using appropriate eigenfunction expansions (Bai (1977, 1979)) or boundary integral representations (Lenoir (1982), Guttman (1983)) of the potential.

Table 1.1 compares the experimental data and theoretical wave resistance predictions for the Wigley parabolic hull at four different Froude numbers. The experimental data were taken from a survey of eleven sets of experiments, see Chen and Noblesse (1983b). All theoretical predictions were obtained by numerical solution of the Neumann-Kelvin problem. Bai (1979) used a finite element method, Adachi and Takeshi (1983) used a Rankine source method, while Chang (1979), Suzuki (1979), Tsutsumi (1979) and Tsai et al (1983) all used Kelvin wave source distribution methods. Although the differences between the average experimental data and the average theoretical predictions are fairly small, the large scatter in the theoretical data is clearly unacceptable and must be ascribed to the use of inaccurate numerical procedures. For example, at Froude number $F_n = 0.350$

the variation in the theoretical data is 63%. At the same Froude number the scatter in the four results obtained by means of a Kelvin wave source distribution method is 48%. This discrepancy must be mainly ascribed to the errors occurring in the evaluation of the Kelvin wave source potential. The Kelvin wave pattern generated by a moving submerged source is mathematically expressed as a single integral with a rapidly oscillatory integrand, see Noblesse (1981). Numerical calculation of such integrals is difficult and time consuming. In this study Kelvin wave source distribution methods are used to solve the Neumann-Kelvin problem. A major novelty is the successful development and employment of both accurate and fast algorithms for the evaluation of the Kelvin wave source potential.

1.4 OUTLINE OF THESIS.

In chapter 2 the hydrodynamic theory of steady ship motion is developed. Throughout the present analysis nondimensional flow variables are used in terms of the fluid density, the ship speed and the ship length, as discussed in section 2.1. The exact potential flow problem is formulated in section 2.2. The difficulties associated with the nonlinear free surface condition are discussed in section 2.3, where the linear Neumann-Kelvin formulation is introduced into the analysis. Expressions relating the relevant flow parameters to the disturbance potential are presented in section 2.4. Simplified equations are proposed for the calculation of the sinkage and trim.

Chapter 3 is concerned with the theoretical investigation of the Kelvin wave source potential, that is, the Green's function associated with the Neumann-Kelvin problem. This fundamental function plays an important role in the linear wave resistance theory. Physically it represents the potential of a translating, submerged source. The definition, fundamental properties and physical interpretation of the Kelvin wave source potential are discussed in section 3.1. A variety of alternative expressions are compared in section 3.2. It appears that the most convenient expression from both physical, mathematical and numerical points of view is an expression originally due to Peters (1949). In this formulation the Kelvin wave source potential is expressed as the sum of three components: (i) the potential of a fundamental Rankine source; (ii) the potential of a nonoscillatory nearfield disturbance symmetric upstream and downstream from the source; and (iii) the potential of a wavelike disturbance trailing downstream from the source (and zero upstream). The properties of the nearfield and wavelike disturbance are investigated in sections 3.3 and 3.4 respectively.

In chapter 4 it is discussed how the Kelvin wave source potential can be used to derive integral identities for the disturbance potential of the steady flow about a moving ship. A basic integral identity is obtained in section 4.1 by applying Green's second formula to the disturbance potential and the Kelvin wave source potential. Two alternative strategies are proposed

to obtain the solution of the disturbance potential. The first and classic approach due to Brard (1972) is discussed in section 4.2. The exact solution of the disturbance potential is obtained by relating it to an auxiliary distribution of Kelvin wave sources over the ship's hull surface and water line. The unknown source strength must be solved from a Fredholm integral equation of the second kind obtained by imposing the boundary condition at the hull surface. An alternative strategy to obtain the disturbance potential proposed by Noblesse (1983) is discussed in section 4.3. It is based on an explicit integro-differential equation for the potential itself. This equation can only be solved iteratively and it is shown that the first term in the iterative sequence of potential approximations provides a useful explicit numerical approximation to the exact source strength for sufficiently slender ship forms. The concept of the Kochin (1951) wave amplitude function and the related Havelock (1934) wave resistance formula is briefly discussed in section 4.4 and it is used to demonstrate the importance of the additional water line distribution of Kelvin wave sources.

In chapter 5 the computational procedures are presented which were developed to obtain the solution of the disturbance potential. A standard point-collocation procedure, similar to the one earlier used by Inglis (1980), is used in section 5.1 to discretise the integral identities. A simple Gaussian quadrature method is proposed to evaluate the influence coefficients. The errors associated with the approximation procedure, as well as the exploitation of the ship's lateral

symmetry plane, are discussed. The application of the proposed method relies heavily on the use of accurate and efficient algorithms for the evaluation of the Kelvin wave source potential and its gradient. The methods used to evaluate the nearfield and wavelike disturbance are discussed in sections 5.2 and 5.3 respectively. The algorithm for the nearfield disturbance is based on Chebyshev approximations derived by Newman (1986a). The algorithm for the wavelike disturbance is based on two complementary Neumann series expansions originally obtained by Bessho (1964). Accurate and efficient methods have been developed to evaluate the two series expressions.

In chapter 6 the developed theory is applied to five different hull forms. These are: a submerged prolate spheroid, the Wigley parabolic hull form, a tanker, a cruiser and a destroyer. Extensive comparisons are made between experimental data and theoretical predictions of a wide variety of flow parameters such as wave resistance, sinkage, trim, pressure signatures, wave profiles and vertical force distributions. In most cases the calculations have been carried out for a large number of Froude numbers, thus allowing a detailed assessment of the ability of the Neumann-Kelvin theory to model the steady ship motion problem. In chapter 7 it is concluded that the developed computational tools provide an accurate and efficient tool to analyse the steady flow disturbance phenomena caused by a moving surface ship.

| designation | $F_n = 0.266$ | $F_n = 0.313$ | $F_n = 0.350$ | $F_n = 0.402$ |
|---------------------------|---------------|---------------|---------------|---------------|
| experimental data: | | | | |
| - average | 0.69 | 1.26 | 1.24 | 1.84 |
| - range | 0.19 | 0.39 | 0.36 | 0.74 |
| - scatter (%) | 27 | 31 | 29 | 40 |
| theoretical predictions: | | | | |
| Bai (1979) | - | - | 1.35 | 1.81 |
| Chang (1979) | 0.83 | 1.43 | 1.03 | 2.18 |
| Suzuki (1979) | 1.08 | 0.52 | 1.00 | 2.08 |
| Tsutsumi (1979) | 0.90 | 1.64 | 1.56 | 2.42 |
| Adachi and Takeshi (1983) | 0.47 | 0.80 | 0.84 | 1.24 |
| Tsai et al (1983) | 0.74 | 1.32 | 1.03 | 1.36 |
| ----- | | | | |
| - average | 0.80 | 1.14 | 1.14 | 1.85 |
| - range | 0.61 | 1.12 | 0.72 | 1.18 |
| - scatter (%) | 76 | 98 | 63 | 64 |

Table 1.1 Comparison of experimental data and Neumann-Kelvin theoretical predictions of the wave resistance ($10^4 C_w = 10^4 R_w / \rho V^2 L^2$) for the Wigley parabolic hull form.

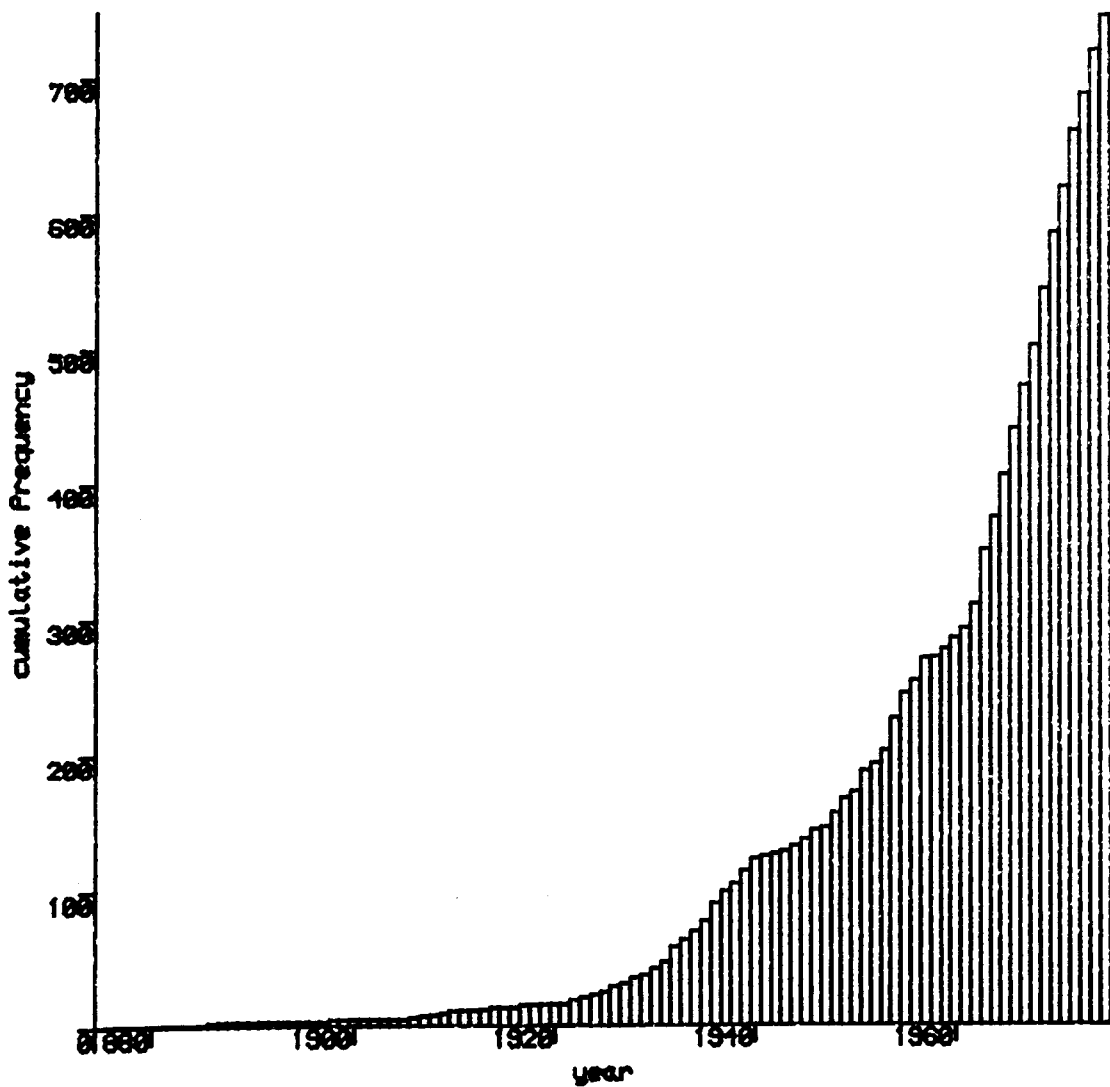
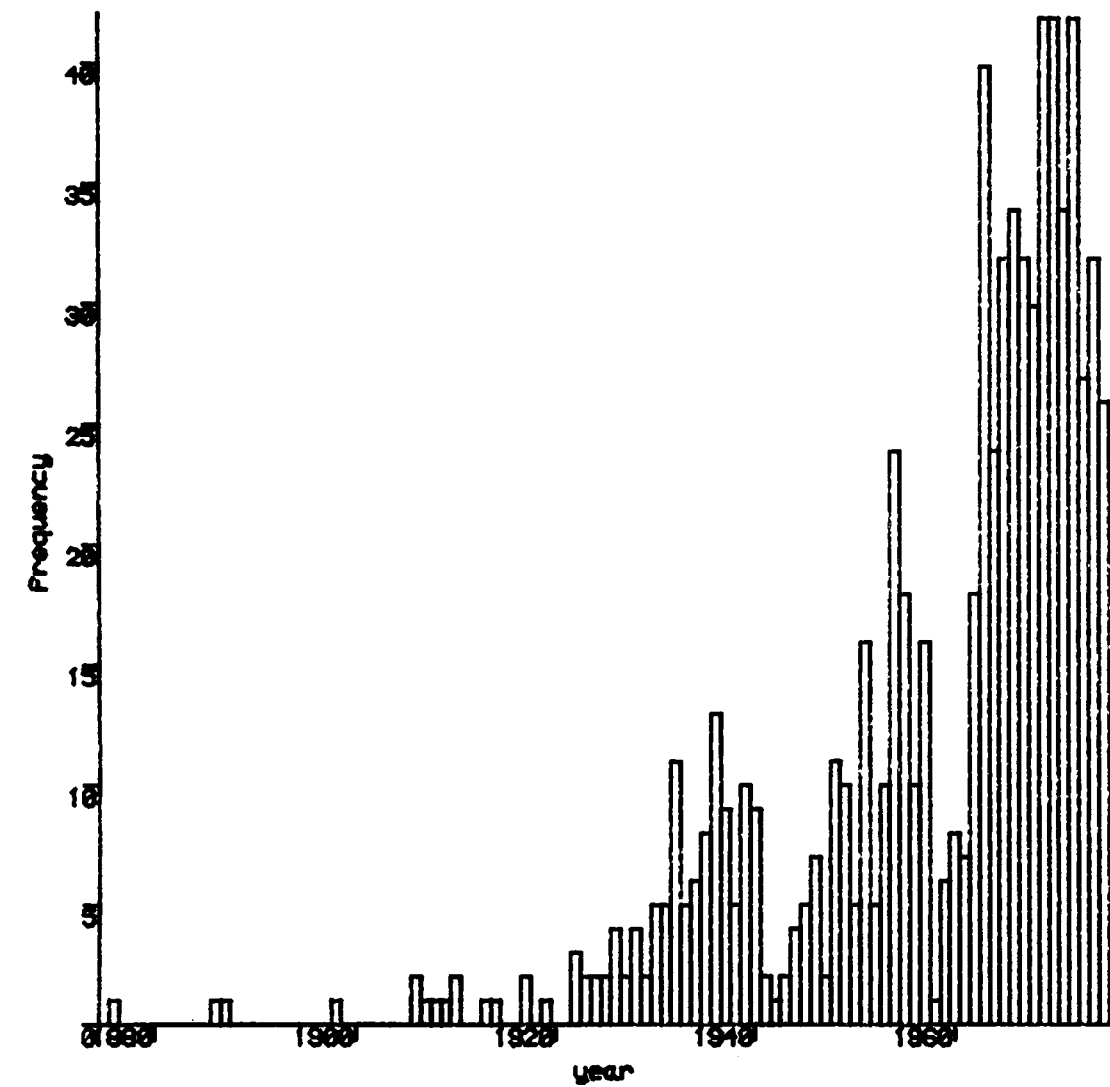


Figure 1.1 Publications on wave resistance and related topics during 1875-1975

2. HYDRODYNAMIC THEORY OF STEADY SHIP MOTION

2.1 POTENTIAL FLOW DESCRIPTION

The present analysis is concerned with the investigation of the flow about a rigid ship in steady rectilinear motion at the free surface of a previously undisturbed sea of infinite depth and width. The sea water is regarded as ideal, that is, homogeneous, incompressible and inviscid, and irrotational flow is assumed. The effects of surface tension, wave breaking and spray formation at the bow are neglected. The external forces acting on the ship are assumed to stem from the presence of a uniform gravitational field.

Nondimensional variables are defined in terms of ρL^3 as reference mass, L as reference length and L/V as reference time, where ρ , L and V denote the density of the fluid, the water line length of the ship and the speed of the ship respectively. Table 2.1 gives the definitions of the thus obtained nondimensional flow variables. Notice in particular the definition of the nondimensional acceleration of gravity as $gL/V^2 = 1/F_n^2$, where g is dimensional and the Froude number $F_n = V/\sqrt{gL}$. In this study the dimensionless variables in terms of ρ , L and V are used exclusively.

Figure 2.1 illustrates the Cartesian reference frame $Oxyz$ attached to the moving ship. The fluid flow is independent

of time with respect to Oxyz. The origin O is located at amidships and the positive Ox axis points towards the bow (i.e. $x \gg 0$ and $x \ll 0$ correspond to the upstream and downstream flow regimes respectively). The positive Oz axis points vertically upward and the mean free surface coincides with the plane $z=0$.

In potential flow theory the irrotational flow of an ideal fluid is uniquely determined by the velocity potential function, as explained for example by Lamb (1932) and Milne-Thomson (1968). Let $\Phi(\underline{x})$ denote the nondimensional potential at position \underline{x} in the fluid. The potential has a steady state characteristic with respect to the moving axis system Oxyz consisting of contributions from both the uniform free stream flow and the steady flow disturbance caused by the moving ship. That is:

$$\Phi(\underline{x}) = -x + \phi(\underline{x}) \quad , \quad (2.1)$$

where $-x$ is the potential of the uniform free stream flow and $\phi(\underline{x})$ denotes the disturbance potential. By definition, the flow velocity vector $\underline{U}(\underline{x})$ is given by:

$$\underline{U} = \nabla\Phi = -\underline{i} + \nabla\phi = -\underline{i} + \underline{u} \quad , \quad (2.2)$$

where $\nabla\Phi = (\frac{\partial\Phi}{\partial x}, \frac{\partial\Phi}{\partial y}, \frac{\partial\Phi}{\partial z}) = (\frac{\partial\Phi}{\partial x}, \frac{\partial\Phi}{\partial y}, \frac{\partial\Phi}{\partial z})$ denotes the gradient of Φ , $\underline{i} = (1,0,0)$ denotes the unit vector along the Ox axis, and the perturbed flow velocity $\underline{u} = \nabla\phi$. The fluid pressure $p(\underline{x})$ is given by the nondimensional Bernoulli equation as:

$$p = \frac{1}{2} - \frac{1}{2} |\nabla\phi|^2 - z/F_n^2 = \phi_x - \frac{1}{2} |\nabla\phi|^2 - z/F_n^2, \quad (2.3)$$

where $|\nabla\phi|^2 = \nabla\phi \cdot \nabla\phi = \phi_x^2 + \phi_y^2 + \phi_z^2$ is the square of the magnitude of the flow velocity vector $\underline{U} = \nabla\phi$ and F_n denotes the Froude number. From this expression it is seen that the total pressure consists of contributions from the uniform free stream flow, the steady perturbed flow and the hydrostatic pressure.

2.2 EXACT PROBLEM FORMULATION

The velocity potential ϕ of the steady flow about a moving ship must satisfy the following conditions (see Wehausen (1973), Newman (1976) and Noblesse and Dagan (1976)):

- (i) The continuity equation (or conservation of fluid mass) requires that the divergence of the flow velocity is identical to zero, that is, $\nabla \cdot \underline{U} = 0$, throughout the flow domain D . Using equation (2.2) this condition may be written as:

$$\nabla^2 \phi = 0 \quad \text{in } D, \quad (2.4)$$

where $\nabla^2 \phi = \phi_{xx} + \phi_{yy} + \phi_{zz}$ denotes the Laplacian of ϕ .

- (ii) If $z = \zeta_w(x,y)$ denotes the unknown elevation of the disturbed free surface S , then the resulting kinematic

condition may be expressed as:

$$\phi_z = \nabla\phi \cdot \nabla\zeta_w \quad \text{on } S .$$

This condition ensures that the fluid particles cannot pass through the free surface. Furthermore, the free surface is a surface of constant atmospheric pressure and it follows from the Bernoulli equation (2.3) that:

$$\zeta_w = \frac{1}{2}F_n^2 (1 - |\nabla\phi|^2) \quad \text{on } S . \quad (2.5)$$

Substituting this dynamic condition into the kinematic condition given in the previous equation, the free surface condition to be satisfied by ϕ becomes:

$$\phi_z = -\frac{1}{2}F_n^2 \nabla\phi \cdot \nabla|\nabla\phi|^2 \quad \text{on } S . \quad (2.6)$$

The actual position of the disturbed free surface is not known beforehand and this implies a major complication in the implicit forms of equations (2.5-6).

(iii) Since fluid particles cannot permeate the wetted hull surface H of the ship, it follows that:

$$\phi_n = 0 \quad \text{on } H , \quad (2.7)$$

where $\phi_n = \partial\phi/\partial n = \nabla\phi \cdot \underline{n}$ and $\underline{n} = (n_x, n_y, n_z)$ is the unit vector normal to the hull and pointing into the fluid.

This kinematic condition ensures that the normal components of the hull velocity and the flow velocity are identical. In general, the moving ship will sink and trim about its position at rest and therefore the actual position of the ship's hull surface is not known beforehand.

(iv) Finally a radiation condition must be imposed to ensure the existence and uniqueness of the potential, see Dern (1977) for a comprehensive discussion of this topic. This condition states that the energy flux of the waves radiated by the moving ship is directed outward at infinity, see Newman (1978). In the present context it is seen that the waves are following the ship and there are no upstream waves. This feature can be expressed by defining:

$$\phi = -x + \begin{cases} O(1/|\underline{x}|) \\ o(1) \end{cases} \text{ as } |\underline{x}| \rightarrow \infty \text{ if } \begin{cases} x > 0 \\ x < 0 \end{cases} \quad (2.8)$$

where $O(x)$ and $o(x)$ denote the Landau order symbols of x as defined by Erdelyi (1956).

Substitution of equation (2.1) into equations (2.4-8) results in the following set of conditions to be satisfied by the disturbance potential ϕ :

(i) continuity:

$$\nabla^2 \phi = 0 \quad \text{in } D \quad ; \quad (2.9)$$

(ii) free surface conditions:

$$\zeta_w = F_n^2 (\phi_x - \frac{1}{2} |\nabla\phi|^2) \text{ on } S, \quad (2.10)$$

$$F_n^2 \phi_{xx} + \phi_z = F_n^2 (2\nabla\phi \cdot \nabla\phi_x - \frac{1}{2} \nabla\phi \cdot \nabla |\nabla\phi|^2) \text{ on } S; \quad (2.11)$$

(iii) hull surface condition:

$$\phi_n = n_x \text{ on } H; \quad (2.12)$$

(iv) radiation condition:

$$\phi = \begin{cases} 0(1/|\tilde{x}|) \\ o(1) \end{cases} \text{ as } |\tilde{x}| \rightarrow \infty \text{ if } \begin{cases} x > 0 \\ x < 0 \end{cases}. \quad (2.13)$$

Equations (2.9-13) are exact within the assumptions stated at the beginning of section 2.1 and together they constitute a nonlinear elliptic boundary value problem from which the disturbance potential must be solved.

2.3 LINEAR NEUMANN-KELVIN THEORY

Unfortunately the complicated nonlinear nature of the free surface conditions given in equations (2.10-11) prohibits the development of an exact solution of the disturbance potential, see however Dawson (1977) and Daube (1980) for some recent

developments. Therefore some method of approximation is required and this may be achieved by means of regular or singular perturbation expansions, as discussed by Wehausen (1973). Such procedures rely on one's ability to choose a small parameter ϵ which is connected with the problem such that as ϵ is decreased the disturbance near the free surface is gradually reduced. Ultimately this results in a linear formulation where the free surface elevation is small and the free surface conditions may be linearised about the mean sea plane.

Three ideas lie behind the choice of a convenient perturbation parameter ϵ , see Table 2.2. Specifically, ϵ may be related to the assumed smallness of:

- (i) the beam/length and/or draft length ratio of the ship (this choice results in the classic thin, flat and slender ship approximations);
- (ii) the Froude number (this choice results in the slow ship approximation);
- (iii) the Froude number based on the immersion depth of a deeply submerged body.

Any of these approaches results in small disturbance of the free surface as ϵ is made smaller, but they also destroy the general three-dimensional character of the present analysis.

An alternative scheme may be based on linearising only the free surface condition while the other conditions are

retained in their exact forms. The resulting approximation is formally inconsistent for surface ships. The free surface conditions valid on the disturbed free surface S may be expanded about the mean free surface s (i.e. the plane $z = 0$) using a Taylor series expansion of the form:

$$\phi(x, y, \zeta_w) = \phi(x, y, 0) + \zeta_w \phi_z(x, y, 0) + \dots$$

The application of this expansion to the free surface conditions given in equations (2.10-11) results in:

$$\zeta_w = F_n^2 (\phi_x - \frac{1}{2} |\nabla\phi|^2) + F_n^4 \phi_x \phi_{xz} + O(F_n^4 \phi^3), \quad (2.14)$$

$$F_n^2 \phi_{xx} + \phi_z = F_n^2 \left\{ 2\nabla\phi \cdot \nabla\phi_x - \frac{1}{2} \nabla\phi \cdot \nabla |\nabla\phi|^2 - (\phi_x - \frac{1}{2} |\nabla\phi|^2) \phi_{zz} - F_n^2 \phi_x \phi_{xxz} \right\} + O(F_n^4 \phi^3) \quad (2.15)$$

valid on s , where $O(F_n^4 \phi^3)$ denotes that the neglected terms are at least of the fourth order in the Froude number and of the third order in derivatives of the disturbance potential, see Newman (1976).

The nonlinear term on the right side of equation (2.15) is of order $F_n^2 \phi^2$ and is assumed to be small in comparison with the linear term $F_n^2 \phi_{xx} + \phi_z$. If terms of $O(F_n^2 \phi^2)$ are neglected in equation (2.15) it follows that the nonlinear boundary value problem given previously in equations (2.9-13) is transformed into the set of linear conditions given by:

(i) continuity:

$$\nabla^2 \phi = 0 \quad \text{in } d ; \quad (2.16)$$

(ii) free surface condition:

$$F_n^2 \phi_{xx} + \phi_z = 0 \quad \text{on } s ; \quad (2.17)$$

(iii) hull surface condition:

$$\phi_n = n_x \quad \text{on } h ; \quad (2.18)$$

(iv) radiation condition:

$$\phi = \begin{cases} 0(1/|\underline{x}|) \\ 0(1) \end{cases} \quad \text{as } |\underline{x}| \rightarrow \infty \quad \text{if } \begin{cases} x > 0 \\ x < 0 \end{cases} . \quad (2.19)$$

In equations (2.16-18) the actual flow domain D , the free surface S and the hull surface H have been replaced by the mean flow domain d , the mean free surface s and the mean hull surface h respectively.

The disturbance potential may now be solved from the linear 'Neumann-Kelvin' problem defined by equations (2.16-19); the hull surface condition given by equation (2.18) is of the Neumann-type, while the linear free surface condition given by equation (2.17) was first investigated by Lord Kelvin, see Thomson (1887). By definition of the Neumann-Kelvin problem, the free surface condition is linearised but no restrictions are

imposed on the shape of the hull surface, see Brard (1971, 1974a,b). In the remainder of this work the linear Neumann-Kelvin approximation is used as the theoretical model for the description of the flow about a moving ship.

Some justification for adopting the linear free surface condition may be derived from experimental evidence which suggests that the disturbance of the free surface is relatively small, except near the bow of surface ships. More precisely, the dimensionless wave elevation $\zeta_w/F_n^2 = \frac{1}{2}(1 - |\nabla\phi|^2)$ given in equation (2.5) is small for most slender ship forms (notice however that $\zeta_w/F_n^2 = \frac{1}{2}$, i.e. not small, at a stagnation point where the flow velocity is zero, e.g. near the pointed bow of a surface ship). Kajitani et al (1983) have measured the wave profiles along the hull of an unrestrained Wigley model. Figure 2.2 shows a typical result and clearly illustrates that ζ_w/F_n^2 is small if the bow wave crest is discarded. The formal inconsistency of the Neumann-Kelvin approximation seems therefore of little practical importance and certainly should not invalidate a direct comparison between experimental and theoretical predictions.

2.4 WAVE RESISTANCE, SINKAGE AND TRIM

Assuming that the disturbance potential is evaluated by solving the Neumann-Kelvin problem, the task is reduced to the derivation of the relevant flow parameters. These are the flow

velocity, the fluid pressure, the wave elevation and the hydrodynamic forces which determine the wave resistance and the induced sinkage and trim angle.

The perturbed flow velocity $\underline{u}(\underline{x})$ and the hydrodynamic pressure $p(\underline{x})$ may readily be obtained from equations (2.2) and (2.3) respectively. Discarding terms of $O(F_n^2 \phi^2)$ in equation (2.14) it follows that the wave elevation $\zeta_w(x,y)$ of the disturbed free surface is given by:

$$\zeta_w(x,y) = F_n^2 \phi_x(x,y,0) \quad . \quad (2.20)$$

The hydrodynamic forces can be obtained either by directly integrating the hydrodynamic pressure on the hull surface or by evaluating the energy contained in the downstream wave pattern of the ship, see Wehausen (1973). Here the first approach is used, while the latter is discussed in section 4.4.

Most ships have a lateral plane of symmetry coinciding with the plane $y=0$ in figure 2.1. For such vessels the only nonzero components of the hydrodynamic force and moment are the drag force d_w , the lift force l_w and the trimming moment m_w , where d_w , l_w and m_w are nondimensional in the manner indicated in Table 2.1. These components may readily be determined by integrating the hydrodynamic pressure over the hull surface and it follows that:

$$d_w = \iint_h (\phi_x - \frac{1}{2} |\nabla\phi|^2) n_x da \quad (2.21a)$$

$$l_w = \iint_h (\phi_x - \frac{1}{2} |\nabla\phi|^2) n_z da \quad (2.21b)$$

$$m_w = \iint_h (\phi_x - \frac{1}{2} |\nabla\phi|^2) (zn_x - xn_z) da \quad (2.21c)$$

where (n_x, n_y, n_z) are the components of the outward unit normal vector on the hull surface.

Associated with the drag, lift and moment acting on the moving ship are the wave resistance C_w , the sinkage s_w and the trimming angle θ_w . However, the hull surface h in equations (2.21a-c) refers to the unknown position of the hull surface after the sinkage and trim have been applied. It follows that the quantities C_w , s_w and θ_w are interrelated and an iterative procedure is required in order to determine them. This procedure can be initialised by considering the hull surface corresponding to the known hydrostatic equilibrium position of the ship at rest, see Wehausen (1969), Yeung (1972), Gadd (1973) and Noblesse and Dagan (1976). In towing tanks a ship model can be restrained (i.e. $s_w=0$ and/or $\theta_w=0$) and the theoretical simulation of this situation is considerably simplified.

In practical calculations the cumbersome iterative procedure for the determination of the wave resistance, sinkage and trim can easily be avoided by assuming that the sinkage and trim are small (this assumption is not tenable at very high ship speeds).

Figure 2.3 illustrates the static equilibrium of the moving ship acted upon by the drag force d_w , the lift force ℓ_w and the trimming moment m_w . The wave resistance C_w is formally defined as negative thrust acting along the propeller shaft line; the additional trimming moment induced by the wave resistance is negligible for most sufficiently slender ship forms, see Wehausen (1973) and Noblesse and Dagan (1976). The sinkage s_w and trim angle θ_w are reckoned positive for increasing draft and a bow-up rotation respectively. For small s_w and θ_w the static equilibrium of the moving ship is described by (see Noblesse and Dagan (1976)):

$$C_w = d_w \quad , \quad (2.22a)$$

$$i_0 s_w - i_1 \theta_w + F_n^2 \ell_w = 0 \quad , \quad (2.22b)$$

$$- i_1 s_w + i_2 \theta_w + F_n^2 m_w = 0 \quad , \quad (2.22c)$$

where F_n denotes the Froude number and the k -th moment of area

i_k of the water line plane is defined by:

$$i_k = \int_{-\frac{1}{2}}^{\frac{1}{2}} x^k b(x) dx \quad ,$$

where $b(x)$ is the beam at position x . These moments of area are dimensionless in the manner indicated in Table 2.2 and relate to the position of the water line plane of the ship at rest. The sinkage and trim are coupled and can be obtained by solving the set of linear algebraic equations (2.22b-c).

| variable | dimensional | nondimensional |
|-------------------------|-------------|-----------------------------|
| density of water | ρ | $1 = \rho/\rho$ |
| length of ship | L | $1 = L/L$ |
| speed of ship | V | $1 = V/V$ |
| acceleration of gravity | g | $gL/V^2 = 1/F_n^2$ |
| beam of ship | B | $b = B/L$ |
| draft of ship | D | $d = D/L$ |
| k-th moment of area | I_k | $i_k = I_k/L^{k+2}$ |
| coordinates | (X,Y,Z) | $(x,y,z) = (X,Y,Z)/L$ |
| velocity potential | Φ | $\phi = \Phi/VL$ |
| flow velocity | U | $u = U/V$ |
| water pressure | P | $p = P/\rho V^2$ |
| wave elevation | Z_w | $\zeta_w = Z_w/L$ |
| drag force | D_w | $d_w = D_w/\rho V^2 L^2$ |
| lift force | L_w | $\ell_w = L_w/\rho V^2 L^2$ |
| trimming moment | M_w | $m_w = M_w/\rho V^2 L^3$ |
| wave resistance | R_w | $C_w = R_w/\rho V^2 L^2$ |
| sinkage | S_w | $s_w = S_w/L$ |
| trim by stern | θ_w | θ_w |

Table 2.1 Definitions of nondimensional flow variables.

| assumption | references | b | d | F_n |
|----------------|--|---------------|---------------|-----------------|
| thin ship | Michell (1898) Wehausen (1973) Noblesse (1983) | $O(\epsilon)$ | $O(1)$ | $O(1)$ |
| flat ship | Hogner (1932) Noblesse (1983) | $O(1)$ | $O(\epsilon)$ | $O(1)$ |
| slender ship | Vossers (1962) Maruo (1962) Tuck (1964) Ogilvie (1970) Noblesse (1983) | $O(\epsilon)$ | $O(\epsilon)$ | $O(1)$ |
| slow ship | Guevel et al (1974) Newman (1976) Baba (1976,1977) Maruo (1977) Kayo (1978) Noblesse (1983) | $O(1)$ | $O(1)$ | $O(\epsilon)$ |
| submerged body | Havelock (1931a,b) Kochin (1951) Bessho (1961) Farell (1973) Guttmann (1983) | $O(1)$ | $O(1)$ | $O(\epsilon)$ * |

* Froude number based on immersion depth

Table 2.2 Comparison of some assumptions resulting in small disturbance near the free surface.

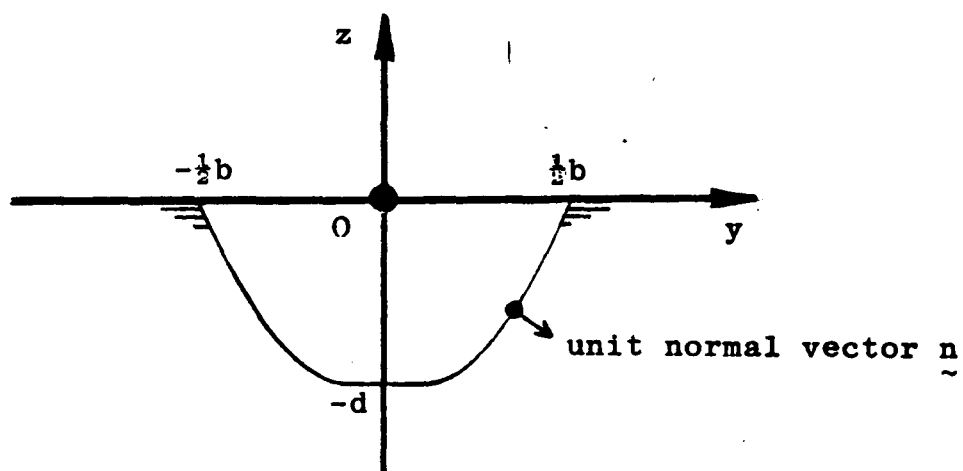
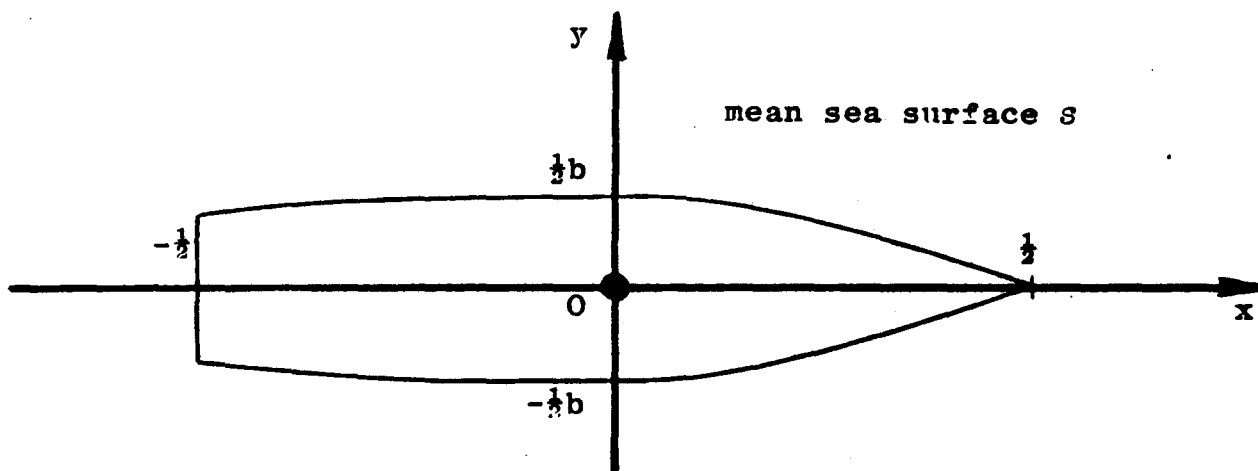
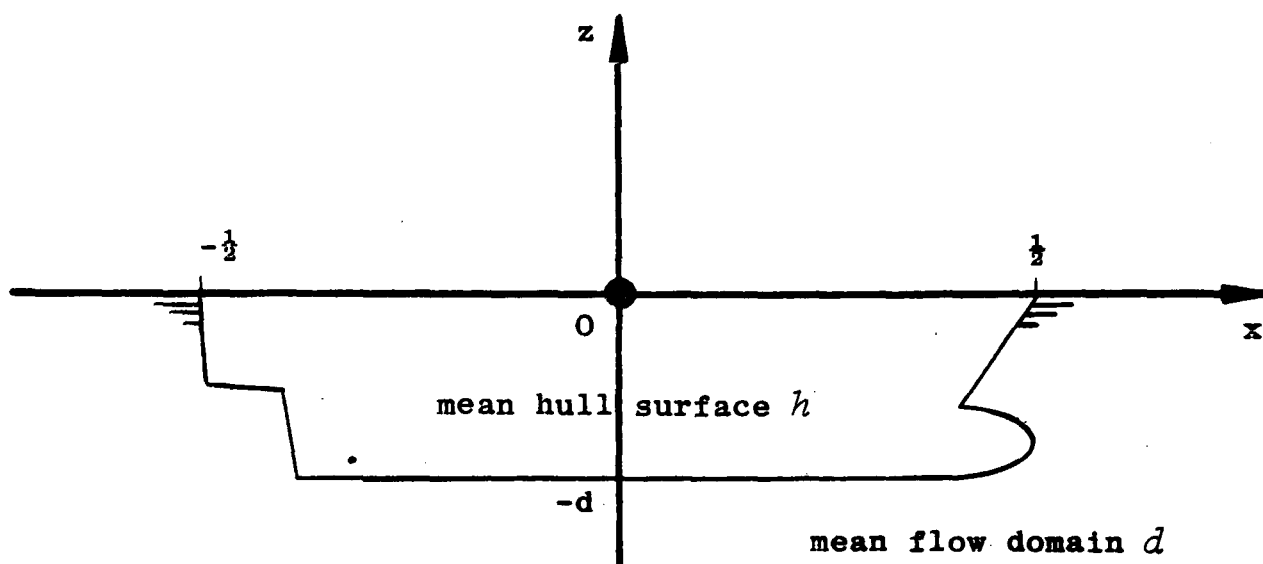


Figure 2.1 Sketch of the coordinate system $Oxyz$ attached to the moving ship. The ship has unit length, beam b and draft d .

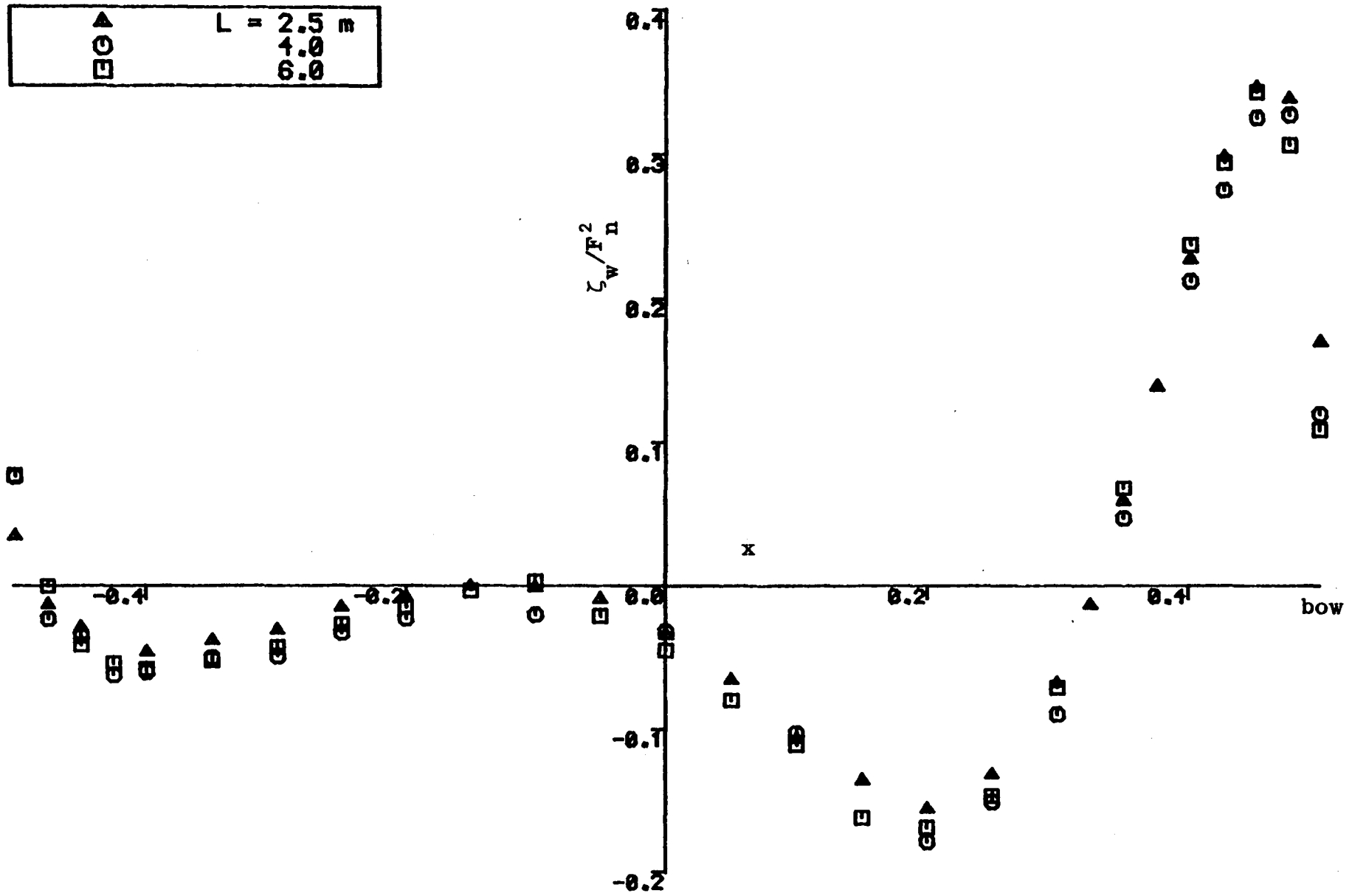


Figure 2.2 Measured wave profiles ζ_w/F_n ($= gZ_w/V^2$) for three different model sizes of the Wigley hull (free-running models at $F_n=0.316$).

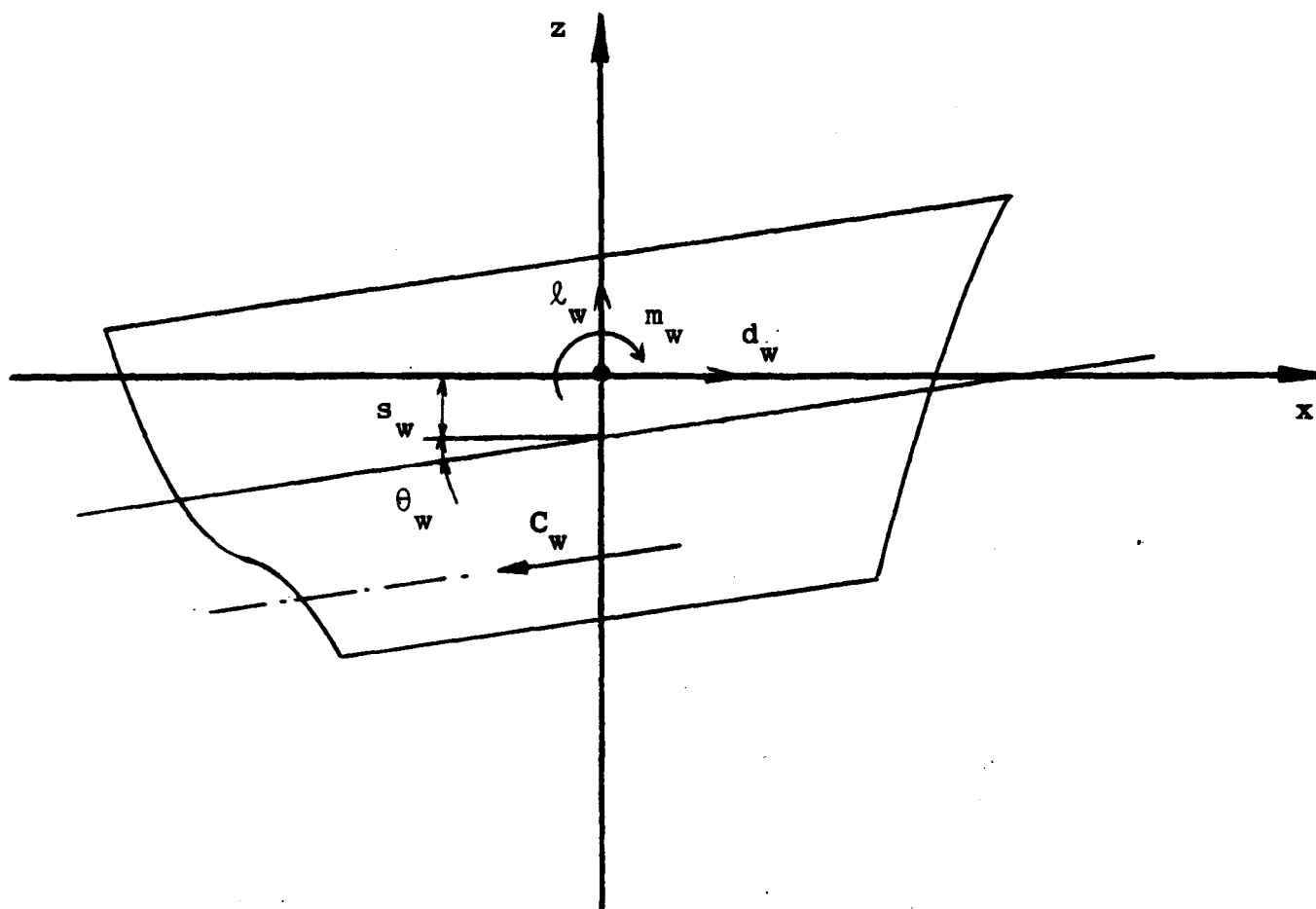


Figure 2.3 Sketch of the moving ship's static equilibrium showing the drag force d_w , the lift force l_w , the trimming moment m_w , the wave resistance C_w , the downward sinkage s_w and the trim by the stern θ_w (ship length $\equiv 1$).

3. THE KELVIN WAVE SOURCE POTENTIAL

3.1 DEFINITION AND FUNDAMENTAL PROPERTIES

The Kelvin wave source potential is defined as the Green's function associated with the Neumann-Kelvin problem and physically this function may be identified with the potential of a translating submerged source. The Kelvin wave source potential plays a significant role in the linear theory of ship waves and wave resistance and this chapter is entirely devoted to its mathematical analysis. For many years mathematicians and hydrodynamicists have expended considerable effort in the development and analysis of the Kelvin wave source potential and their combined efforts have resulted in a vast literature which is reviewed by Wehausen and Laitone (1960), Bessho (1964), Eggers et al (1967), Nakatake (1969), Gamst (1979), Noblesse (1981) and Euvrard (1983).

Let $\underline{\xi}(\xi, \eta, \zeta \leq 0)$ and $\underline{x}(x, y, z \leq 0)$ denote two position vectors referring to the moving axis system Oxyz, as illustrated in Figure 3.1. By definition, the Green's function $G(\underline{\xi}, \underline{x}; F_n^2)$ associated with the Neumann-Kelvin problem given by equations (2.16-19) is the solution to the following boundary value problem (see Noblesse (1981)):

(i) continuity:

$$\nabla^2 G = \begin{cases} \delta(x - \xi)\delta(y - \eta)\delta(z - \zeta) \\ 0 \end{cases} \quad \text{in } z < 0 \text{ if } \begin{cases} \zeta < 0 \\ \zeta = 0 \end{cases} \quad (3.1)$$

(ii) free surface condition:

$$F_n^2 G_{xx} + G_z = \begin{cases} 0 \\ -\delta(x - \xi)\delta(y - \eta) \end{cases} \quad \text{on } z=0 \text{ if } \begin{cases} \zeta < 0 \\ \zeta = 0 \end{cases} \quad (3.2)$$

(iii) radiation condition:

$$G = \begin{cases} 0(1/|\underline{x} - \underline{\xi}|) \\ 0(1) \end{cases} \quad \text{as } |\underline{x} - \underline{\xi}| \rightarrow \infty \text{ if } \begin{cases} \xi > x \\ \xi < x \end{cases} \quad (3.3)$$

In equation (3.1-2) $\delta(x)$ represents the usual Dirac's delta function of x . The Green's function is the singular or fundamental solution to the homogeneous 'Kelvin' problem obtained by discarding the nonhomogeneous Neumann hull surface condition given by equation (2.18) from the Neumann-Kelvin problem.

Physically the Kelvin wave source potential $G(\underline{\xi}, \underline{x}; F_n^2)$ represents the linearised velocity potential at the field point $\underline{\xi}(\xi, \eta, \zeta \leq 0)$ of the unit outflow produced by a source at the source point $\underline{x}(x, y, z < 0)$ in steady rectilinear motion with unit speed at at depth $-z$ below the free surface of an otherwise unbounded fluid. In the limiting case when $z=0$ the source is evidently no longer fully submerged and it may be shown that the unit outflow produced at

($x, y, z=0$) now stems from a flux across the mean free surface, see Ursell (1960), Noblesse (1981) and Euvrard (1983).

From physical considerations it follows that the source flow is symmetric with respect to the centre plane $y=\eta$. That is, the Green's function satisfies the symmetry relationship:

$$G_y = 0 \quad \text{on } y = \eta \quad (3.4)$$

Furthermore, it can be shown that:

$$G(\underline{\xi}, \underline{x}; F_n^2) = G(\underline{x}, \underline{\xi}; F_n^2) \quad ,$$

if and only if the flow direction is reversed, see Brard (1972) and Noblesse (1981).

Noblesse (1981) demonstrates that the Kelvin wave source potential can be expressed in the form:

$$4\pi G(\underline{\xi}, \underline{x}; F_n^2) = -1/|\underline{\xi} - \underline{x}| + \{N(\underline{X}) + W(\underline{X})\}/F_n^2 \quad , \quad (3.5)$$

where $|\underline{\xi} - \underline{x}|$ represents the distance between the field and source points (see figure 3.1) and the dimensionless vector quantity

$\underline{X}(\underline{\xi}, \underline{x}; F_n^2)$ is defined by:

$$\underline{X} = (X, Y, Z \geq 0) = (x - \xi, y - \eta, |z + \zeta|)/F_n^2 \quad . \quad (3.6)$$

The vector $F_n^2 \underline{X}$ joins the field point $\underline{\xi}$ with the free surface mirror image of the source point \underline{x} (notice that $X < 0$ upstream from the source and $X > 0$ downstream from the source).

Equation (3.5) implies that the Kelvin wave source potential is decomposed into three characteristic components:

- (i) the potential $-1/4\pi |\underline{\xi} - \underline{x}|$ of a fundamental Rankine source in infinite fluid (in the absence of the free surface);
- (ii) the potential $N(X)/4\pi F_n^2$ of a localised nonoscillatory near-field disturbance, symmetric upstream and downstream from the source; and
- (iii) the potential $W(X)/4\pi F_n^2$ of a wavelike disturbance which accounts for the waves produced by the source.

The nearfield and wavelike components account for the effects associated with the presence of the free surface and are functions only of the vector quantity \underline{X} defined in equation (3.6).

3.2 SURVEY OF ALTERNATIVE EXPRESSIONS

Equivalent expressions for the Kelvin wave source potential may be obtained by solving the boundary value problem defined by equations (3.1-3), see Noblesse (1981) for a thorough mathematical treatise. It appears that there are five alternative

representations of the Kelvin wave source potential. These are:

- (i) an expression implicitly contained in Michell's (1898) famous paper, rediscovered by Eggers et al (1967) and modified by Noblesse (1981);
- (ii) an expression originally due to Havelock (1932) and subsequently modified by among others Lunde (1951), Kostyukov (1968), Standing (1975) and Shen and Farell (1977);
- (iii) an expression due to Peters (1949) and modified by Noblesse (1977), see also Eggers et al (1967) and Andersson (1975);
- (iv) an expression obtained in a remarkable paper by Bessho (1964), rederived by Ursell (1984) and modified by Simmgen (1968); and
- (v) an expression proposed by Demanche (1981) and rederived by Baar (1984b).

Amongst the foregoing expressions, the second representation due to Havelock (1932) is no doubt the most popular and is also quoted by Wehausen and Laitone (1960). The fourth and fifth expressions are less well known and although they have certain interesting theoretical features they do not appear to offer any practical advantages; here these representations will not be considered further. Instead the attention is focused on the first three representations due to Michell (1898), Havelock (1932) and Peters (1949).

Table 3.1 compares the relevant 'Michell', 'Havelock' and 'Peters' representations of the nearfield and wavelike components as defined by equation (3.5). These equivalent expressions are modifications of the original representations as obtained by Noblesse

(1981). It is seen that the nearfield disturbance $N(X)$ is written as the sum of two terms: firstly, a Rankine sink potential $1/R$, where $R = |\underline{X}|$ and $r = F_n^2 R$ represents the distance between the field point and the free surface mirror image of the source point (see figure 3.1); and, secondly, a single integral term with the integrand expressed in terms of the complex-valued exponential integral function $E_1(A)$, as defined in Abramowitz and Stegun (1972). The integration limits are either finite (Peters) or infinite (Michell and Havelock). It may be verified that in all three representations the nearfield disturbance is symmetric upstream and downstream from the source (i.e. the function N is even with respect to both X and Y).

The differences between the three equivalent expressions in Table 3.1 are clearly recognisable from the respective representations of the wavelike disturbance $W(X)$. This function is expressed as a single integral with at least one infinite integration limit and a rapidly oscillatory integrand (the Michell expression contains an additional integral term with finite integration limits). Both the Michell and the Peters representations have fixed integration limits, while the lower integration limit $-X/|Y|$ of the Havelock expression is variable and depends on the relative position of the field and source points. This feature appears to be a major disadvantage of the Havelock representation, as was pointed out by Eggers et al (1967). The Peters representation of the wavelike disturbance illustrates clearly that the waves follow the source, that is, the waves are only present downstream from the source, in agreement with the radiation condition given by equation (3.3). It is therefore seen that the Peters representation is the most convenient from a physical

point of view; it also appears to be the best suited expression for purposes of mathematical and numerical analysis.

The Kelvin wave source potential $G(\xi, \underline{x}; F_n^2)$ is thus expressed in the form of equation (3.5) in which the nearfield disturbance $N(\underline{X})$ is given by:

$$N(\underline{X}) = 1/R + (2/\pi) \int_{-1}^1 \text{Im}\{\exp(A)E_1(A)\}dt \quad (3.7)$$

where $R = |\underline{X}|$ and the complex argument $A = \{-Z\sqrt{1-t^2} + Yt + i|\underline{X}|\sqrt{1-t^2}\}$; likewise, the wavelike disturbance $W(\underline{X})$ is given by:

$$W(\underline{X}) = -H(\underline{X})4 \int_{-\infty}^{\infty} \sin\{(X+Yt)\sqrt{1+t^2}\} \exp\{-Z(1+t^2)\}dt, \quad (3.8)$$

where the Heaviside unit step function $H(\underline{X})$ is defined by:

$$H(\underline{X}) = \begin{cases} 0 \\ 1 \end{cases} \text{ if } \begin{cases} X < 0 \\ X > 0 \end{cases} \text{ i.e. } \begin{cases} \text{upstream} \\ \text{downstream} \end{cases} \text{ from the source.}$$

The Peters (1949) representation of the Kelvin wave source potential has been neglected for some time, although it was used for instance by Eggers and Choi (1975). In recent years, however, it has been recognised as the most convenient expression from both physical, mathematical and numerical points of view, see for example Noblesse (1981), Euvrard (1983) and Newman (1986a,b). In the remainder of this chapter the properties of the nearfield and wavelike disturbances as defined by equations (3.7) and (3.8) respectively are further investigated.

3.3 ANALYSIS OF THE NEARFIELD DISTURBANCE

The nearfield disturbance may be interpreted as the potential of a localised nonoscillatory disturbance symmetric upstream and downstream from the source. It is convenient to express the function $N(X)$ in the form:

$$N(X) = M(X)/R \quad , \quad (3.9)$$

where $R = |X|$. According to Noblesse (1981) the function $M(X)$ may assume the equivalent forms given by:

$$M = 1 + (2/\pi)R \int_{-1}^1 \text{Im}\{\exp(A)E_1(A)\}dt \quad (3.10)$$

$$= 1 + (2/\pi)R \int_{-\infty}^{\infty} \text{Re}\{\exp(B)E_1(B)\}dt + 4R \int_T^{\infty} \text{Im}\{\exp(B)\}dt \quad (3.11)$$

where $T = |X|/|Y|$ and the complex arguments A and B are defined by:

$$A = \{-Z\sqrt{1-t^2} + Yt + i|X|\sqrt{1-t^2}\} \quad ,$$

$$B = \{-Z\sqrt{1+t^2} + i(|X| - |Y|t)\sqrt{1+t^2}\} \quad .$$

The expression given in equation (3.10) follows immediately from equations (3.7) and (3.9), whereas equation (3.11) may be obtained by considering the equivalence of the Peters and Havelock expressions given in Table 3.1 (i.e. by noting that $N = N_P = N_H + W_H - W_P$, where indices P and H refer to the Peters and Havelock expressions respectively).

The ascending series and the asymptotic expansion of the exponential integral $E_1(z)$ are given by Abramowitz and Stegun (1972) as:

$$E_1(z) = -\{\gamma + \ln(z) + \sum_{n=1}^{\infty} (-1)^n z^n / n n!\} \quad (3.12)$$

$$\sim \exp(-z) \sum_{n \geq 0} (-1)^n n! / z^n \quad (3.13)$$

respectively. The ascending series of the nearfield disturbance may be obtained by substituting equation (3.12) with $z=A$ into the integrand of the integral term in equation (3.10) and evaluating the remaining integrals analytically, see Noblesse (1977, 1978b) and Newman (1985, 1986a). Likewise, the asymptotic expansion of the nearfield disturbance may be obtained by substituting equation (3.13) with $z=B$ into the integrand of the first integral on the right side of equation (3.11), see Noblesse (1975, 1981) and Newman (1986a).

The first few terms of the thus obtained ascending and asymptotic series of the nearfield disturbance are given in Table 3.2, where the function $M(X)$ is expressed in the form;

$$M(X) = M_A(X) + R M_I(X) \quad (3.14)$$

It is seen that the integral terms M_I in the ascending series expressions in Table 3.2 vanish as $R \rightarrow 0$, while the integral terms of the asymptotic expansion vanish as $R \rightarrow \infty$. The algebraic terms M_A of the ascending series have been derived by Noblesse (1977, 1978b). The first algebraic term (i.e. -1) of the asymptotic expansion corresponds to a well-known image source term (i.e. $N \sim -1/R$ as $R \rightarrow \infty$)

which was earlier obtained by Guilloton (1960) and Bessho (1964). Further terms of the ascending and asymptotic series of the nearfield disturbance may in principle be derived, see Newman (1986a).

From the expressions given in Table 3.2 it may be concluded that the function $M(X)$ behaves as:

$$M(X) = \begin{cases} +1 + O(R) \\ -1 + O(1/R) \end{cases} \quad \text{as} \quad \begin{cases} R \rightarrow 0 \\ R \rightarrow \infty \end{cases}, \quad (3.15)$$

and it follows from equation (3.9) that the nearfield disturbance $N(X)$ may alternatively be interpreted as the potential of an image sink, of strength $M(X)$, in the infinite fluid (as if there were no free surface), as discussed by Noblesse (1977). In particular, the nearfield disturbance reduces to a simple image sink as $R \rightarrow 0$ (or $F_n \rightarrow \infty$, as may be seen from equation (3.6)) and an image source as $R \rightarrow \infty$ (or $F_n \rightarrow 0$).

Equation (3.11) clearly illustrates that the nearfield disturbance is symmetric upstream and downstream from the source. That is

$$M(X, Y, Z) = \begin{cases} M(-X, Y, Z) \\ M(X, -Y, Z) \\ M(-X, -Y, Z) \end{cases}. \quad (3.16)$$

When $Y=0$ the additional integral term with lower limit of integration $T=|X|/|Y|$ in equation (3.11) vanishes. The integrands of equations (3.10) and (3.11) then become even functions of the integration variable t , as may be verified by making use of the relationship $E_1(\bar{z}) = \overline{E_1(z)}$, where \bar{z} denotes the complex conjugate of z . The centre

plane nearfield disturbance is thus given by:

$$M(X,0,Z) = 1 + (4/\pi)R \int_0^1 \text{Im}\{\exp(A)E_1(A)\}dt \quad ,$$

$$= 1 + (4/\pi)R \int_0^\infty \text{Re}\{\exp(B)E_1(B)\}dt \quad .$$

It is seen that the Havelock and Peters representations in Table 3.1 become identical when $Y=0$. The centre plane nearfield disturbance $N(X,0,Z)=M(X,0,Z)/\sqrt{X^2+Z^2}$ is of great importance in the thin ship theory of wave resistance and has been investigated extensively by Noblesse (1975) and Newman (1985, 1986a) who have derived the complete ascending and asymptotic series.

A simple picture of the behaviour of the function $M(X)$ may be obtained by considering the two special cases where $Y=0=Z$ and $X=0$ respectively. Bessho (1964) and Noblesse (1977) show that:

$$M(X,0,0) = -1 - 2|X| + \pi|X|\{H_1(|X|) - Y_1(|X|)\}$$

$$M(0,Y,Z) = 1 - 2\sqrt{EF}(\sqrt{E})$$

where the similarity variable $E = \frac{1}{2}(D+Z)$, $D = \sqrt{Y^2 + Z^2}$ and

$H_1(x)$, $Y_1(x)$ and $F(x)$ denote the Struve, Bessel and Dawson's integral*

* Dawson's integral $F(x) = \int_0^x \exp(t^2 - x^2) dt$

functions of x as defined by Abramowitz and Stegun (1972).

Algorithms for these transcendental functions are readily available, see Newman (1984, 1986b). Figure 3.2 shows the functions $M(X,0,0)$, $M(0,Y,0)$ and $M(0,0,Z)$ and clearly illustrates the limiting sink and source behaviour of the nearfield disturbance for small and large values of R respectively, as indicated in equation (3.15).

3.4 ANALYSIS OF THE WAVELIKE DISTURBANCE

The wavelike disturbance defined by equation (3.8) represents the potential of a Kelvin wavelike disturbance trailing downstream from the source (and zero upstream). This fact can be verified by investigating the asymptotic behaviour of the function $W(X)$ for large values of $\rho = \sqrt{X^2 + Y^2}$, using the method of steepest descents (see Erdelyi (1956)). This classic investigation is reported in detail by Wehausen and Laitone (1960), Ursell (1960), Newman (1977), Lighthill (1978) and Euvrard (1983), who show that the function W behaves as:

$$W \sim \begin{cases} O(\rho^{-1}) \\ O(\rho^{-1/3}) \\ O(\rho^{-1/2}) \end{cases} \text{ as } \rho = \sqrt{X^2 + Y^2} \rightarrow \infty \text{ if } \begin{cases} X < 2\sqrt{2}|Y| \\ X \approx 2\sqrt{2}|Y| \\ X > 2\sqrt{2}|Y| \end{cases} \quad (3.17)$$

This expression is a more precise formulation of the radiation condition given in equation (3.3). It is seen that the dominant waves generated by the moving source are confined to a sector making

an angle of $\text{arccot}(2\sqrt{2}) \approx 19^{\circ}28'$ with the downstream sailing line of the source, as illustrated in Figure 3.3. According to equation (3.17) the energy flux is the smallest near the border lines of this sector. A more detailed analysis shows that within the sector two distinct systems of transverse and diverging waves exist; these two systems meet near the border lines with a common angle of $\text{arctan}(\sqrt{2}) \approx 54^{\circ}44'$ with the sailing line (see Figure 3.3).

The wavelike disturbance defined in equation (3.8) may be written in the form:

$$\tilde{W}(X) = - H(X) \tilde{8P}(X) \quad , \quad (3.18)$$

where the function $\tilde{P}(X)$ is defined by

$$\tilde{P}(X) = \frac{1}{2} \int_{-\infty}^{\infty} \sin\{(X+Yt)\sqrt{1+t^2}\} \exp\{-Z(1+t^2)\} dt \quad (3.19)$$

for $X \geq 0$. This function is a special case of the P_n -functions studied by Havelock (1923, 1925) and Bessho (1964).

Table 3.3 gives seven alternative expressions for the function $\tilde{P}(X)$. The first expression in this table may readily be obtained by expanding the trigonometric term in the integrand of equation (3.19). The last expression has been derived by Bessho (1964) and may also be obtained by noting that the function \tilde{P} satisfies the parabolic differential equation $\tilde{P}_{XX} = \tilde{P}_Z$ in the upper half-space $Z > 0$; according to Sneddon (1972) the solution of this heat conduction problem is given by:

$$P(X,Y,Z) = (1/\sqrt{\pi}) \int_{-\infty}^{\infty} \exp(-s^2) P(X - 2s\sqrt{Z}, Y, 0) ds .$$

The remaining expressions in Table 3.3 may be obtained by performing the indicated change of integration variable. The second and third expressions are Fourier transform representations and have been used by Yeung (1972) and Guttman (1983) respectively. The fourth expression is identical to the expression given by Peters (1949). The fifth expression is no doubt the most popular and similar in form to the expression quoted by Wehausen and Laitone (1960).

A simple upper bound on the magnitude of the wavelike disturbance can be obtained from the sixth expression in Table 3.3. Using this expression it may be shown that:

$$|P| < \frac{1}{2} \exp(-Z) \sqrt{\pi/Z}$$

provided that $Z > 0$, and it is seen that the wavelike disturbance decreases exponentially with increasing Z . The sixth expression in Table 3.3 is also useful to obtain an asymptotic expansion of the function P as $Z \rightarrow \infty$ by means of Laplace's method, see Erdelyi (1956) and Guttman (1983).

The wavelike disturbance is symmetric with respect to the centre plane $Y=0$. That is:

$$P(X,Y,Z) = P(X,-Y,Z) ,$$

as may readily be seen from the expressions given in Table 3.3.

In particular, when $Y=0$, it follows that:

$$\begin{aligned}
 P(X,0,Z) &= \int_0^{\infty} \sin(X\sqrt{1+t^2}) \exp\{-Z(1+t^2)\} dt \\
 &= \frac{1}{2}\sqrt{\pi} \int_{-\infty}^{\infty} \exp(-s^2) \text{sign}(2s\sqrt{Z}-X) Y_1(|2s\sqrt{Z}-X|) ds \quad (3.20)
 \end{aligned}$$

where $\text{sign}(x)=x/|x|$ denotes the usual sign-function. The latter expression may be obtained from the last expression in Table 3.3 and was originally derived by Goodwin (1956) and also given in slightly modified form by Noblesse (1978a). The centre plane wavelike disturbance $P(X,0,Z)$ has been further analysed by Noblesse (1978a) and Newman (1986b) who have derived the complete asymptotic expansion which is uniformly valid as $\sqrt{X^2+Z^2} \rightarrow \infty$.

Bessho (1964) has derived two remarkable series representations of the wavelike disturbance. These series assume the form of Neumann expansions (see Watson (1944)) and may be obtained by expanding terms in the integrand of equation (3.19) into integer order Bessel functions, see Baar and Price (1986b). The series representations are given by:

$$P = -\exp(\frac{1}{2}Z) \sum_{n=0}^{\infty} (-1)^n J'_{2n}(X) K_n(\frac{1}{2}D) \cos(n\theta) \quad , \quad (3.21)$$

$$- \pi \exp(\frac{1}{2}Z) \sum_{n \geq 0} Y'_{2n}(X) I_n(\frac{1}{2}D) \cos(n\theta) \quad . \quad (3.22)$$

In these expressions the primed summation sign indicates that the first term (with $n=0$) of the series must be halved and the polar coordinates ($D \geq 0, 0 \leq \theta \leq \frac{1}{2}\pi$) are defined by $D = \sqrt{Y^2 + Z^2}$ and $\theta = \arctan(|Y|/Z)$. The functions $J_n(x)$, $Y_n(x)$, $I_n(x)$ and $K_n(x)$ denote the usual Bessel functions of x of integer order n , as defined in Abramowitz and Stegun (1972); the prime on the functions $J_{2n}'(X)$ and $Y_{2n}'(X)$ denotes the derivative of these functions with respect to X .

The Neumann series representation given in equation (3.21) is convergent everywhere except on the source track $Y=0=Z$ and may be used for both small and moderate values of X^2/D . The complementary series given in equation (3.22) is asymptotic and useful for large values of X^2/D *. In chapter 5 it is shown how the series representations can be used to design a highly effective algorithm for the evaluation of the wavelike disturbance.

A final point of some academic interest concerns the singular behaviour of the wavelike disturbance when the origin is approached, see Ursell (1960), Bessho (1964), Noblesse (1978a), Euvrard (1983), Newman (1986b) and Baar and Price (1986b). When

* In a recent communication Newman (1986c) has pointed out that the asymptotic Neumann expansion given in equation (3.22), as well as the related seventh integral expression in Table 3.3, appear to be too regular to be correct on the free surface $Z=0$, but they are valid if the source track $Y=0=Z$ is approached along an inclined radius beneath the free surface.

$X=0$, it may be seen from equation (3.19) that $P=0$, provided that $Z>0$. However, when $Y=0=Z$, it follows from both equations (3.20) and (3.22) that

$$P(X,0,0) = \frac{1}{2}\pi Y_0'(X) = -\frac{1}{2}\pi Y_1(X) .$$

For small values of X , the Bessel function $Y_1(X)$ behaves as $Y_1(X) = -2/\pi X + O(X \ln X)$ and it is seen that the wavelike disturbance is singular along the source track in the free surface. This singular behaviour may be isolated as follows.

For large values of the integration variable t , the integrand of the first expression in Table 3.3 behaves as $\sin(Xt)\cos(Yt^2)\exp(-Zt^2)$. This behaviour suggests the decomposition of the function P into components $P=P_S+P_R$, where P_R is a regular function and the singular function P_S is defined by Baar and Price (1986b) as:

$$\begin{aligned} P_S &= \int_0^\infty \sin(Xt)\cos(Yt^2)\exp(-Zt^2)dt \\ &= \operatorname{Re}\{F(X/2\Lambda)/\Lambda\} \end{aligned} \tag{3.23}$$

In this expression the complex argument $\Lambda = \sqrt{Z+iY} = \sqrt{D}\exp(\frac{1}{2}i\theta)$ and F denotes the complex-valued Dawson's integral function (see Abramowitz and Stegun (1972), equation 7.4.7). When $Z=0$ the integral in equation (3.23) can be expressed in terms of real-valued Fresnel integral functions (see Gradshteyn and Ryzhik (1980), equation 3.691.6).

When $Y=0=Z$ it may be verified that the singular and regular components become:

$$P_S(X,0,0) = 1/X ,$$

$$P_R(X,0,0) = - \frac{1}{2} Y_1(X) - 1/X ,$$

respectively, so that the singularity along the source track is now entirely accounted for by the singular component function P_S . Physically, the latter function represents the potential of a diverging wave system, as illustrated in Figure 3.4 (an efficient algorithm for the evaluation of the complex Dawson's integral has been prepared by Gautschi (1970)).

Similar decompositions of the wavelike disturbance have been investigated by Bessho (1964) and Euvrard (1983) and, for $Y=0$, by Noblesse (1978a) and Newman (1986b). Bessho (1964) recovers the complex-valued Dawson's integral occurring in equation (3.23) by considering the behaviour of the Bessel functions in equation (3.21) as the origin is approached. It is also noticed that the function P_S arised in two recent new approaches to the slender ship theory of wavemaking, see Maruo (1982) and Yeung and Kim (1984).

| modification of expression by | nearfield disturbance $N(\underline{X}) - 1/R$, $R = \underline{X} $ | wavelike disturbance $W(\underline{X})$ |
|----------------------------------|--|---|
| Michell (1898) | $(2/\pi) \int_{-\infty}^{\infty} (t/\sqrt{1+t^2}) \operatorname{Im}\{\exp(A)E_1(A)\} dt$ $A = \{-X+Zt+i Y \sqrt{1+t^2}\}t$ | $-4 \int_{-\infty}^{\infty} \sin\{(X- Y t)\sqrt{1+t^2}\} \exp\{-Z(1+t^2)\} dt$ $-4 \int_0^1 \cos(X\sqrt{1-t^2}) \exp\{-(Z\sqrt{1-t^2}+ Y t)\sqrt{1-t^2}\} dt$ |
| Havelock (1932) | $(2/\pi) \int_{-\infty}^{\infty} \operatorname{Re}\{\exp(A)E_1(A)\} dt$ $A = \{-Z\sqrt{1+t^2}+i(X+Yt)\}\sqrt{1+t^2}$ | $-4 \int_{\tau}^{\infty} \sin\{(X+ Y t)\sqrt{1+t^2}\} \exp\{-Z(1+t^2)\} dt$ $\tau = -X/ Y $ |
| Peters (1949) | $(2/\pi) \int_{-1}^1 \operatorname{Im}\{\exp(A)E_1(A)\} dt$ $A = \{-Z\sqrt{1-t^2}+Yt+i X \}\sqrt{1-t^2}$ | $-H(X)4 \int_{-\infty}^{\infty} \sin\{X+Yt\}\sqrt{1+t^2}\} \exp\{-Z(1+t^2)\} dt$ $H(X) = (0,1) \text{ if } X (<, >) 0$ |

Table 3.1 Alternative single integral representations of the Kelvin wave source potential (modifications due to Noblesse (1981)).

| term | ascending series |
|------|--|
| 1st | $M_A = 1$ $M_I = (2/\pi) \int_{-1}^1 \text{Im}\{\exp(A)E_1(A)\} dt = (2/\pi) \int_{-\infty}^{\infty} \text{Re}\{\exp(B)E_1(B)\} dt + 4 \int_T^{\infty} \text{Im}\{\exp(B)\} dt$ |
| 2nd | $M_A = 1 - 2R(1+S_Z)$ $M_I = (2/\pi) \int_{-1}^1 \text{Im}\{\exp(A)E_1(A) + \ln(A) + \gamma\} dt$ |
| 3rd | $M_A = 1 - 2R(1+S_Z) - R^2 [R_X \{\ln(S/4) + \gamma - \frac{1}{2} - (1/6)(S_Y^2 - S_Z^2)\} - (2/3)R_Y S_Y - (4/3)R_Z(1+S_Z)]$ $M_I = (2/\pi) \int_{-1}^1 \text{Im}[\exp(A)E_1(A) + \ln(A) + \gamma + \{\ln(A) + \gamma - 1\}A] dt$ |

| term | asymptotic series |
|------|--|
| 1st | $M_A = -1$ $M_I = (2/\pi) \int_{-1}^1 \text{Im}\{\exp(A)E_1(A) - 1/A\} dt = (2/\pi) \int_{-\infty}^{\infty} \text{Re}\{\exp(B)E_1(B) - 1/B\} dt + 4 \int_T^{\infty} \text{Im}\{\exp(B)\} dt$ |
| 2nd | $M_A = -1 - (2/R) \{R_D^2/(1+R_Z) - R_X^2/(1+R_Z)^2\}$ $M_I = (2/\pi) \int_{-\infty}^{\infty} \text{Re}\{\exp(B)E_1(B) - 1/B + 1/B^2\} dt + 4 \int_T^{\infty} \text{Im}\{\exp(B)\} dt$ |

$$(R_X, R_Y, R_Z, R_D) = (|X|, Y, Z, D)/R \quad , \quad (S_X, S_Y, S_Z) = (|X|, Y, Z)/S \quad , \quad D = \sqrt{Y^2 + Z^2} \quad , \quad S = R + |X|$$

Table 3.2 Alternative expressions for the nearfield disturbance.

expression

(i)
$$P = \int_0^{\infty} \sin(X\sqrt{1+t^2}) \cos(Yt\sqrt{1+t^2}) \exp\{-Z(1+t^2)\} dt$$

(ii)
$$P = \int_1^{\infty} (u/\sqrt{u^2-1}) \sin(Xu) \cos(Yu\sqrt{u^2-1}) \exp(-Zu^2) du$$

 ($u = \sqrt{1+t^2}$)

(iii)
$$P = \int_0^{\infty} \{w/(2w^2-1)\} \sin(Xw) \cos(Yv) \exp(-Zw^2) dv$$

 ($v = t\sqrt{t^2+1}$, $2w^2 = 1+\sqrt{1+4v^2}$)

(iv)
$$P = \frac{1}{2} \int_{-\infty}^{\infty} \cosh\tau \sin\{(X+Y\sinh\tau)\cosh\tau\} \exp(-Z\cosh^2\tau) d\tau$$

 ($t = \sinh\tau$)

(v)
$$P = \frac{1}{2} \int_{-\frac{1}{2}\pi}^{\frac{1}{2}\pi} \sec^2\theta \sin\{(X\cos\theta+Y\sin\theta)\sec^2\theta\} \exp(-Z\sec^2\theta) d\theta$$

 ($t = \tan\theta$)

(vi)
$$P = \frac{1}{2} \{ \exp(-Z)/\sqrt{Z} \} \int_{-\infty}^{\infty} \exp(-\lambda^2) \sin\{(X+Y\lambda/\sqrt{Z})\sqrt{1+\lambda^2/Z}\} d\lambda$$

 ($t = \lambda/\sqrt{Z}$)

(vii)
$$P = \frac{1}{2}\sqrt{\pi} \exp\{-\frac{1}{2}(D-Z)\} \int_{-\infty}^{\infty} \exp(-s^2) \{(2s\sqrt{D} - X) Y_1(\omega)/\omega\} ds$$

 ($Y+iZ = D\exp(i\theta)$, $\omega^2 = 4s^2D - 4s\sqrt{D}\cos(\frac{1}{2}\theta) + X^2$)

Table 3.3 Alternative expressions for the wavelike disturbance.

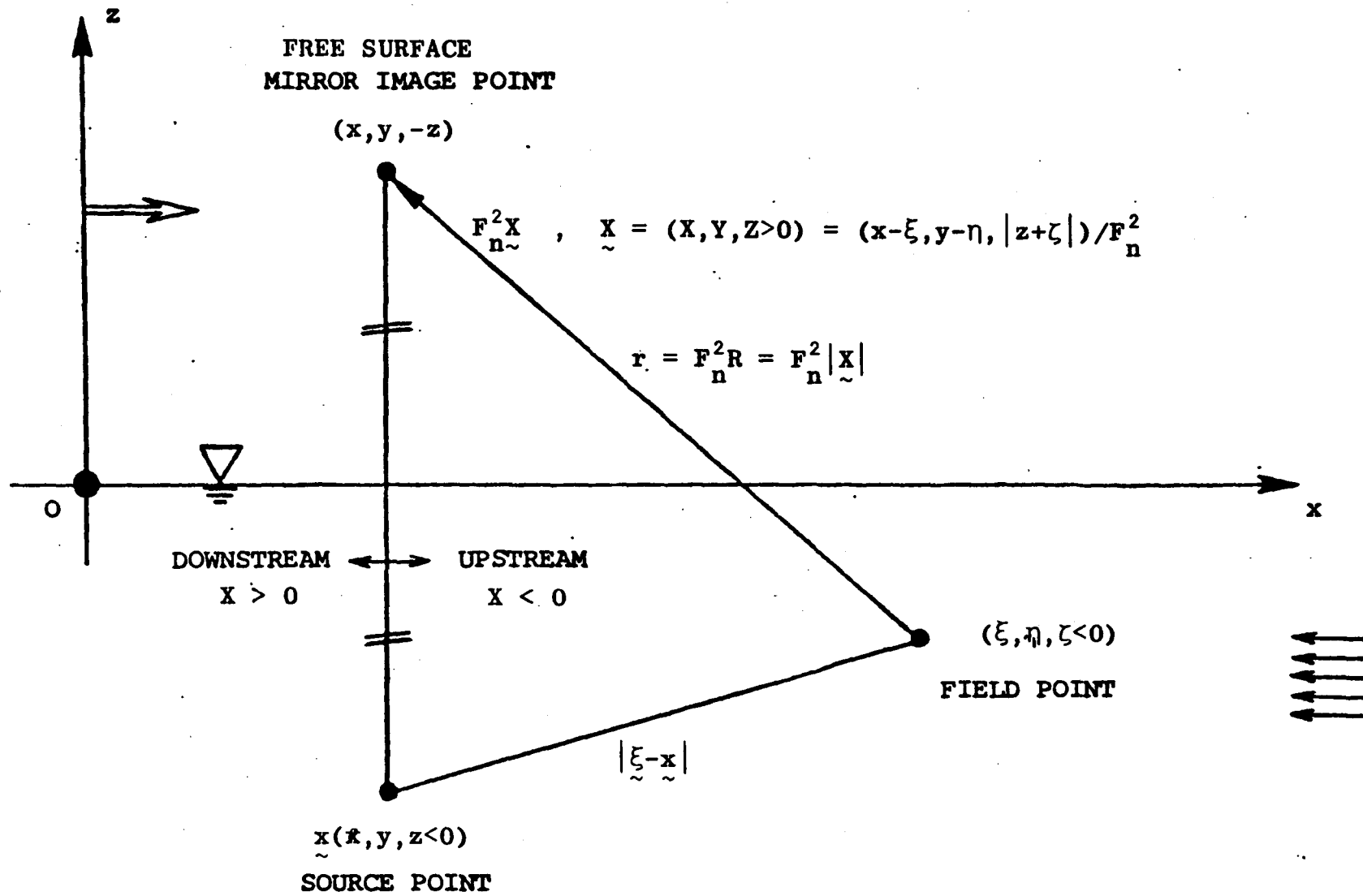


Figure 3.1 Definition sketch for translating source flow.

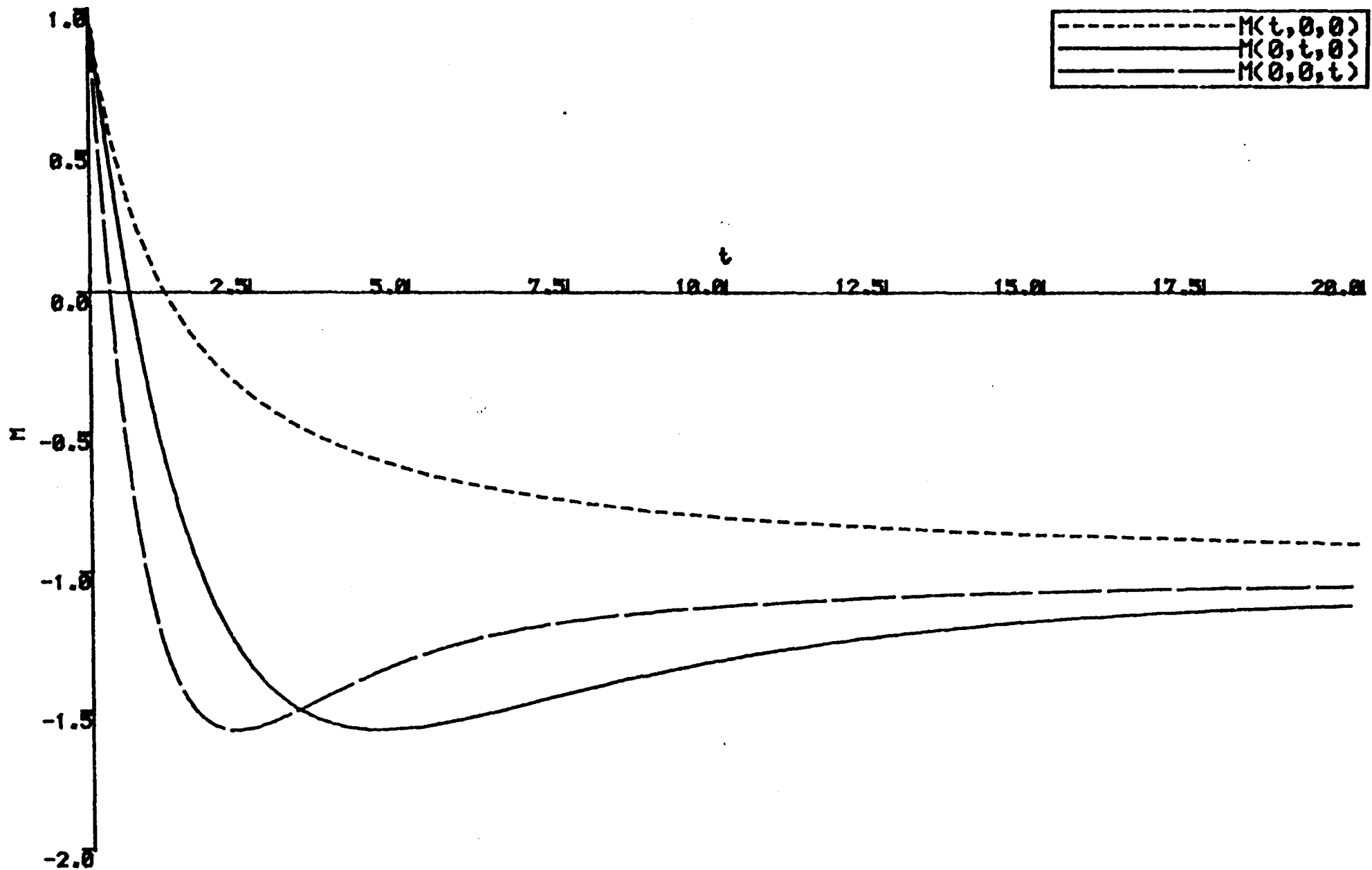


Figure 3.2 Sketch illustrating the typical sink/source behaviour of the nearfield disturbance (shown are the functions $M(X,0,0)$, $M(0,Y,0)$ and $M(0,0,Z)$).

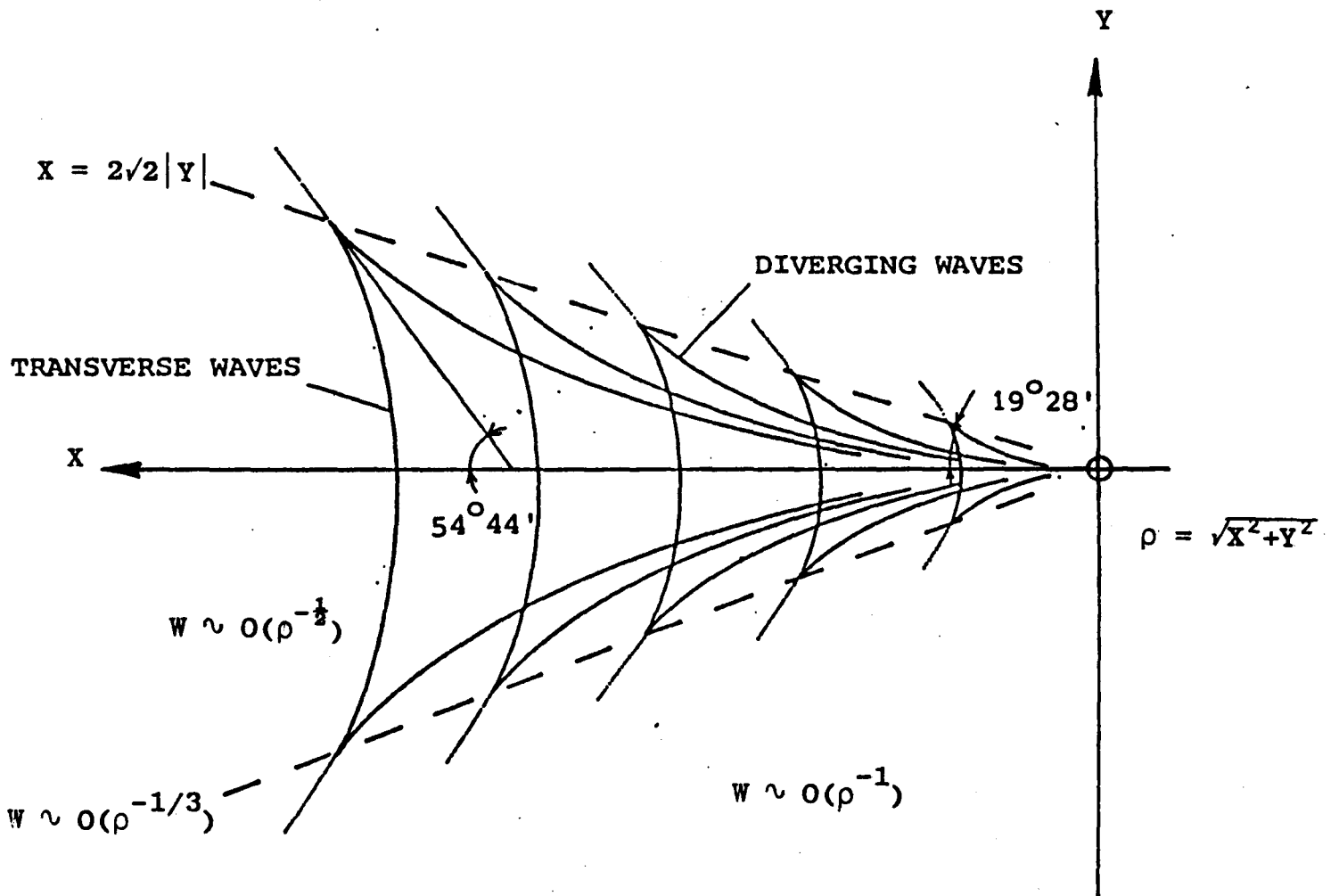


Figure 3.3 Sketch of the Kelvin ship wave pattern.

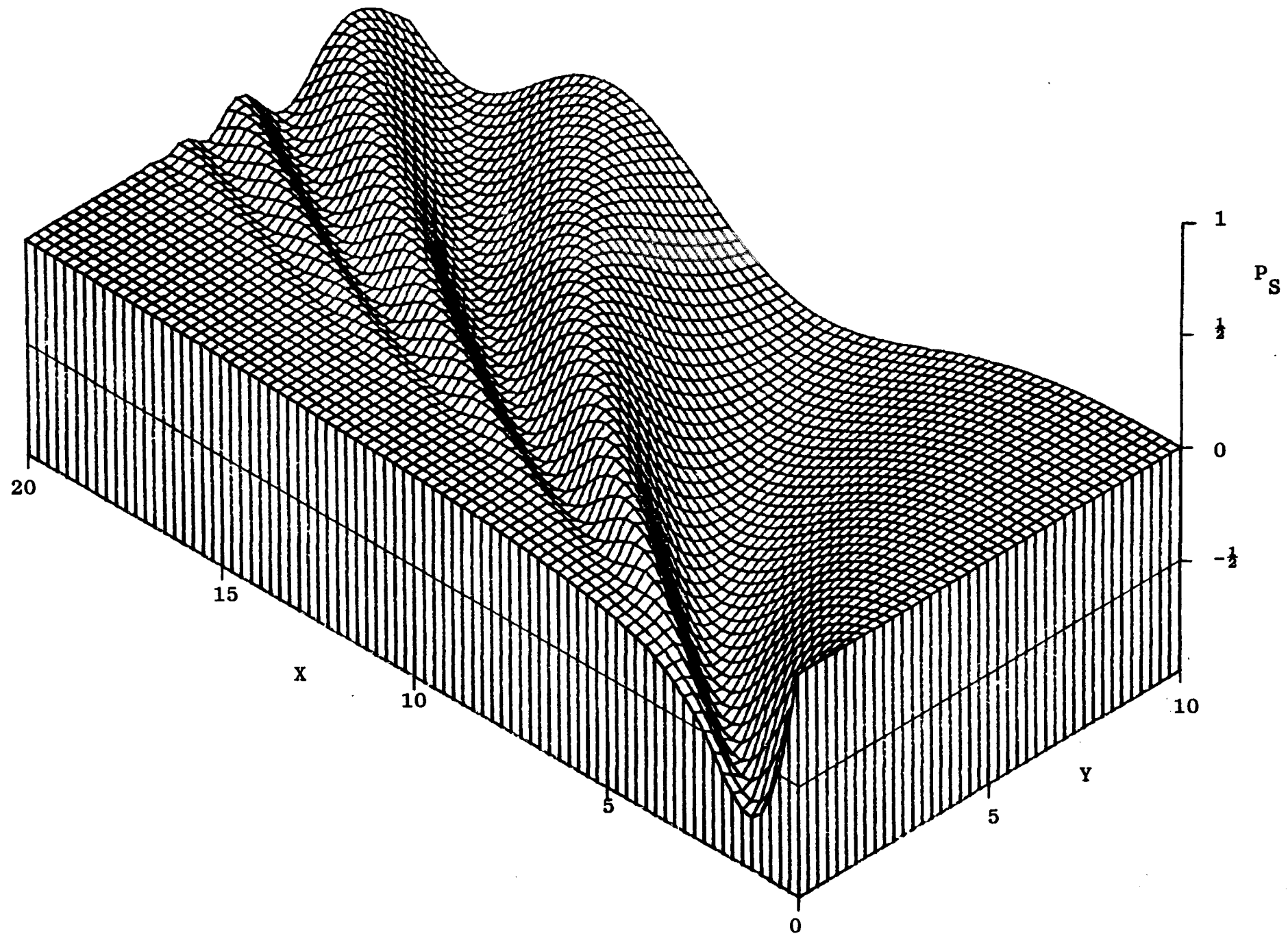


Figure 3.4 Sketch of the singular component $P_S(X, Y, Z)$ of the wavelike disturbance for $0 < X < 20$, $0 < Y < 10$ and $Z = \frac{1}{2}$.

4. INTEGRAL IDENTITIES FOR THE DISTURBANCE POTENTIAL

4.1 BASIC INTEGRAL IDENTITY

Integral identities for the steady disturbance potential may be obtained by applying Green's second formula to the disturbance potential and the Kelvin wave source potential. Recall that the Kelvin wave source potential is defined as the solution to the homogeneous Kelvin problem given in equations (3.1-3). Essentially this Green's function can be identified as the response at the field point due to a unit impulse excitation applied at the source point. The solution of the nonhomogeneous Neumann-Kelvin problem for the disturbance potential (see equations (2.16-2.19)) in terms of an integral distribution of Green's functions (i.e. fundamental Kelvin wave sources) can then be interpreted as the result of superimposing the response of the set of impulses represented by the nonhomogeneous Neumann hull surface condition given by equation (2.18). (Notice the analogy with the impulse response technique often used in ship dynamics, see for example, Price and Bishop (1974) and Bishop and Price (1979)).

Figure 4.1 illustrates the nomenclature used in the present chapter. The finite domain d' is bounded by the hull surface h , the finite mean free surface s' and some exterior surface h_∞ surrounding the hull surface h ; c and c_∞ are the intersection curves of h and h_∞ respectively with the plane $z=0$.

Application of Green's second formula (see Kreyszig (1983)) to the disturbance potential $\phi=\phi(\underline{x})$ and the Kelvin wave source potential $G=G(\underline{\xi},\underline{x};F_n^2)$ gives

$$\iiint_{d'} (\phi \nabla^2 G - G \nabla^2 \phi) dv = \iint_h (G \phi_n - \phi G_n) da + \iint_{s'} (\phi G_z - G \phi_z) dx dy + \iint_{h_\infty} (\phi G_n - G \phi_n) da, \quad (4.1)$$

where $G_n = \partial G / \partial n = \nabla G(\underline{\xi}, \underline{x}; F_n^2) \cdot \underline{n}(\underline{x})$ and \underline{n} is the outward unit normal vector on h as shown in figure 4.1.

Consider the second integral on the right side of equation (4.1). By expressing its integrand as:

$$\phi G_z - G \phi_z = \phi (F_n^2 G_{xx} + G_z) - G (F_n^2 \phi_{xx} + \phi_z) + F_n^2 (G \phi_x - \phi G_x),$$

and by using the Green's identity (see Kreyszig (1983)):

$$\iint_{s'} (G \phi_x - \phi G_x) dx dy = \int_c (G \phi_x - \phi G_x) dy + \int_{c_\infty} (G \phi_x - \phi G_x) dy,$$

equation (4.1) may be rewritten as:

$$I_G = \iint_h (G \phi_n - \phi G_n) da + F_n^2 \int_c (G \phi_x - \phi G_x) dy + I_\phi + I_\infty, \quad (4.2)$$

where I_G , I_ϕ and I_∞ are defined by

$$I_G = \iiint_{d'} \phi \nabla^2 G dv - \iint_{s'} \phi (F_n^2 G_{xx} + G_z) dx dy ,$$

$$I_\phi = \iiint_{d'} G \nabla^2 \phi dv - \iint_{s'} G (F_n^2 \phi_{xx} + \phi_x) dx dy ,$$

$$I_\infty = \iint_{h_\infty} (\phi G_n - G \phi_n) da + F_n^2 \int_{c_\infty} (G \phi_x - \phi G_x) dy ,$$

respectively.

By making use of the radiation conditions given in equations (2.19) and (3.3) it can be shown that I_∞ vanishes as the exterior surface h_∞ is expanded towards infinity and subsequently the finite domain d' and free surface s' may be replaced by the unbounded flow domain d and mean free surface s respectively. Substituting the continuity and free surface conditions given by equations (2.16) and (2.17) respectively it follows that $I_\phi = 0$. Following a suggestion due to Noblesse (1983) the potential is expressed in the form $\phi = \phi_* + (\phi - \phi_*)$ where $\phi = \phi(\underline{x})$ and $\phi_* = \phi(\underline{\xi})$, and I_G becomes

$$I_G = C_e \phi_* + C' \tag{4.3}$$

where,

$$C_e = \iiint_d \nabla^2 G dv - \iint_s (F_n^2 G_{xx} + G_z) dx dy , \tag{4.4a}$$

$$C' = \iiint_d (\phi - \phi_*) \nabla^2 G dv - \iint_s (\phi - \phi_*) (F_n^2 G_{xx} + G_z) dx dy .$$

It is seen from equations (3.1-2) that $C'=0$ provided the disturbance potential is continuous everywhere in the fluid and on the boundaries, that is, if $\phi-\phi_* \rightarrow 0$ as $\underline{x} \rightarrow \underline{\xi}$. This assumption is required to apply Green's second formula (see Kreyszig (1983)).

Substitution of equations (4.3-4a) into equation (4.2) results in the basic integral identity:

$$C_e \phi_* = \iint_h (G\phi_n - \phi G_n) da + F_n^2 \int_c (G\phi_x - \phi G_x) dy, \quad (4.5)$$

where C_e is given by equation (4.4a). Inserting equations (3.1-2) in equation (4.4a) it follows that:

$$C_e = \iiint_d \delta(x-\xi)\delta(y-\eta)\delta(z-\zeta)dv + \iint_s \delta(x-\xi)\delta(y-\eta)dxdy \quad (4.4b)$$

$$= \begin{cases} 1 \\ \frac{1}{2} \\ 0 \end{cases} \text{ for } \underline{\xi} \begin{cases} \text{in } d + s - h - c \\ \text{on } h + c \\ \text{in } d_i + s_i - h - c \end{cases}, \quad (4.4c)$$

where d_i and s_i are the interior domain and mean free surface respectively inside the hull surface h (see Figure 4.1). Equation (4.4c) is a well-known result from the theory of generalised functions and distributions, see Griffel (1981), Kantorovich and Akilov (1982) and Roach (1982). Usually the integral identity (4.5) is obtained in a different manner by applying Green's second formula to the domain $\bar{d} - e$, where e is a small spherical domain surrounding the field point $\underline{\xi}$, see for example Brard (1972, 1974a,b), Inglis (1980) and Baar (1984a); the present derivation is due to Noblesse (1983).

The value of the constant C_e defined in equations (4.4a,b) represents the total amount of fluid created inside the flow domain d (bounded by the hull surface h and the mean free surface s) or stemming from a flux across the mean free surface s (bounded by the waterline c). According to equation (4.4c) $C_e = 1$ if the field point ξ , where the flow is observed, is in d or on s , but strictly outside h and c , while $C_e = 0$ if ξ is strictly inside h or on the mean water line plane s_i . Also $C_e = \frac{1}{2}$ if ξ is exactly on h or on c , provided that the hull is a smooth orientable surface (see Kellogg (1954)); more precisely, the value of $4\pi C_e$ (or $2\pi C_e$) at a point ξ of h (or c) is equal to the angle at which d (or s) is viewed from ξ (this extends the validity of equation (4.5) to piecewise smooth orientable surfaces h , e.g. a ship hull with a transom stern).

In the basic integral identity given by equation (4.5) the disturbance potential is represented as an integral distribution of sources (proportional to G) and dipoles (proportional to G_n and G_x) over the hull surface h and the mean water line c . The discontinuity in the value of the constant C_e across the hull surface can be shown to stem from the corresponding discontinuity in the dipole distributions over h and c , see Kellogg (1954). The presence of the additional water line integral distribution in equation (4.5) was first pointed out by Brard (1972) although earlier the necessity of including this term was also recognised by Peters and Stoker (1957), Wehausen (1963) and Kotik and Morgan (1969). The importance of the water line integral is investigated in Section 4.4.

It is convenient to eliminate the discontinuity in the value of C_e in equation (4.4c). Noblesse and Triantafyllou (1983) have pointed out that there are two strategies for achieving this goal. The first and classical approach is discussed in Section 4.2 and employs auxiliary distributions of singularities over the hull surface, see Kellog (1954) and Hess and Smith (1966). The second approach is discussed in Section 4.3 and employs an integral identity for the potential itself, see Chow et al (1976) and Noblesse (1983). The latter approach is less well-known, but appears to be very useful because it provides an explicit approximation to the disturbance potential of the flow about a sufficiently slender ship moving at fairly low speed.

4.2 AUXILIARY SINGULARITY DISTRIBUTIONS

The basic integral identity given in equation (4.5) relates to the problem of the 'exterior' potential flow about the hull. Recall now that the Kelvin wave source potential is defined throughout the entire lower half-space, see equations (3.1-3). The most well-known technique for eliminating the discontinuity in the value of C_e consists of defining a corresponding 'interior' potential ϕ^i in the interior domain d_i inside the hull h and below the mean water line plane s_i (see Figure 4.1). An integral identity for ϕ^i corresponding to equation (4.5) may readily be obtained in a similar manner as outlined in the previous section and it follows that

$$C_{i\phi_*}^i = - \iint_h (G\phi_n^i - \phi^i G_n) da - F_n^2 \int_c (G\phi_x^i - \phi^i G_x) dy \quad (4.6)$$

where, in analogy with equations (4.4a-c), C_i is given by:

$$C_i = \iiint_{d_i} \nabla^2 G dv - \iint_{s_i} (F_n^2 G_{xx} + G_z) dx dy \quad (4.7a)$$

$$= \iiint_{d_i} \delta(x-\xi)\delta(y-\eta)\delta(z-\zeta) dv + \iint_{s_i} \delta(x-\xi)\delta(y-\eta) dx dy \quad (4.7b)$$

$$= \begin{cases} 0 \\ \frac{1}{2} \\ 1 \end{cases} \text{ for } \xi \sim \begin{cases} \text{in } d + s - h - c \\ \text{on } h + c \\ \text{in } d_i + s_i - h - c \end{cases} \quad (4.7c)$$

The value of C_i represents the total amount of fluid created within the interior domain d_i (bounded by h and s_i) or stemming from a flux across the water line plane s_i (bounded by c).

Addition of equations (4.4a-c) and (4.7a-c) gives:

$$C = C_e + C_i = \iiint_{d+d_i} \nabla^2 G dv - \iint_{s+s_i} (F_n^2 G_{xx} + G_z) dx dy \\ = \iiint_{z<0} \delta(x-\xi)\delta(y-\eta)\delta(z-\zeta) dx dy dz + \iint_{z=0} \delta(x-\xi)\delta(y-\eta) dx dy = 1 \quad (4.8)$$

for all points ξ outside, inside or on the hull surface $h+c$, i.e. for any point ξ in the lower half space $\zeta \leq 0$. The term $C=1$ in equation (4.8) represents the amount of outflow produced by the moving source (for $z<0$) or stemming from a flux across the free surface (for $z=0$). Addition of the corresponding integral identities

given in equations (4.5-6) therefore results in:

$$\phi_* = \iint_h \{G(\phi_n - \phi_n^i) - (\phi - \phi^i)G_n\} da + F_n^2 \int_c \{G(\phi_x - \phi_x^i) - (\phi - \phi^i)G_x\} dy \quad (4.9)$$

where ϕ_* corresponds to $\phi(\xi)$ or $\phi^i(\xi)$ for points ξ outside or inside the hull surface respectively.

It is convenient to modify the form of the waterline integral in equation (4.9). If $\underline{n}=(n_x, n_y, n_z)$ defines the unit normal vector on the hull surface h pointing into the flow domain d , $\underline{t}=(t_x, t_y, 0)$ defines the unit tangent vector to the water line c oriented as shown in Figure 4.1 and $\underline{i}=(1,0,0)$ is the unit vector along the Ox-axis, one obtains the relationship

$$\phi_x = \nabla\phi \cdot \underline{i} = \{n_x \phi_n + t_x \phi_\ell + (n_x t_x) \phi_d\} \cdot \underline{i} = n_x \phi_n + t_x \phi_\ell - n_z t_y \phi_d, \quad (4.10)$$

where ϕ_ℓ and ϕ_d denote the flow velocity components (i.e. derivatives of ϕ) in the direction of \underline{t} and \underline{nxt} respectively (the unit vector \underline{nxt} is tangent to the hull and points downwards). Using a similar expression for ϕ_x^i and replacing dy by $t_y d\ell$, equation (4.10) may be rewritten as:

$$\phi_* = \iint_h (QG + SG_n) da + F_n^2 \int_c \{(Qn_x - S_\ell t_x + S_d n_z t_y)G + SG_x\} t_y d\ell \quad (4.11)$$

where the source strength $Q = \phi_n - \phi_n^i$ and the doublet strength $S = \phi^i - \phi$.

According to equation (4.11), which was first obtained by Brard (1972), the potential is generated by four auxiliary singularity distributions:

- (i) a source distribution over the hull surface h with strength Q per unit area;
- (ii) a doublet (i.e. normal dipole) distribution over h with strength S per unit area;
- (iii) a source distribution along the mean water line c with strength $(Qn_x - S \ell_x + S_d n_z) t_y$ per unit arc length; and
- (iv) a longitudinal doublet distribution along c with strength St_y per unit arc length.

All singularities are of the 'Kelvin' type in agreement with the definition of the Kelvin wave source potential G , that is to say, the singularities satisfy the continuity, free surface and radiation conditions given by equations (3.1-3).

The representation of the potential ϕ_* by means of and auxiliary distribution of singularities over the hull surface and along the water line is not unique. In fact, ϕ_* may be generated by any linear combination of sources and doublets, as explained for example by Brard (1974a,b), Guevel et al (1974, 1977), Chang and Pien (1975) and Baar (1984a). Table 4.1 illustrates four possibilities. Of particular importance is the representation of the disturbance potential by means of a source distribution, as obtained by setting $D=0$, that is, $\phi=\phi^1$, in equation (4.11).

It follows that:

$$\phi(\xi) = \iint_h Q(\underline{x})G(\xi, \underline{x}; F_n^2) da + F_n^2 \int_c Q(\underline{x})G(\xi, \underline{x}; F_n^2) n_x(\underline{x}) dy. \quad (4.12)$$

It is seen that this auxiliary source distribution renders the velocity potential continuous through the hull surface $h+c$, whereas the normal flow velocity is discontinuous. The representation of the disturbance potential by means of a source distribution is no doubt the most popular, see Guevel et al (1977), Tsutsumi (1979), Chang (1979) and Tsai et al (1983).

The unknown source strength $Q(\underline{x})$ in equation (4.12) may be determined by imposing the hull surface condition given in equation (2.18) and it follows that:

$$-\frac{1}{2}Q(\xi) + \iint_h Q(\underline{x})G_n da + F_n^2 \int_c Q(\underline{x})G_n n_x(\underline{x}) dy = n_x(\xi), \quad (4.13)$$

on the hull surface $h+c$, where $G_n = \nabla G(\xi, \underline{x}; F_n^2) \cdot n(\xi)$. The algebraic term $-\frac{1}{2}Q(\xi)$ stems from the normal differentiation of the Rankine source term $-1/4\pi|\xi-\underline{x}|$ in equation (3.5), see Kellog (1954) and Baar (1984a). Equation (4.13) is recognised as a regular Fredholm integral equation of the second kind, see Kantorovich and Akilov (1982).

It is notable that the representation of the disturbance potential by the auxiliary source distribution in agreement with equations (4.12-13) is an alternative and equivalent

formulation of the Neumann-Kelvin problem given by equations (2.16-19), that is to say, by solving the source strength from equation (4.13) and representing the potential by equation (4.12) an exact solution of the Neumann-Kelvin problem is obtained.

4.3 EXPLICIT SLENDER SHIP APPROXIMATION

Returning to equation (4.5) an alternative strategy is now presented for eliminating the discontinuity in the value of the constant C_e . By making use of Gauss' divergence theorem, equation (4.7a) may be rewritten as:

$$\begin{aligned} C_i &= \iint_h G_n da + \iint_{s_i} G_z dx dy - \iint_{s_i} (F_n^2 G_{xx} + G_z) dx dy \\ &= \iint_h G_n da - F_n^2 \iint_{s_i} G_{xx} dx dy = \iint_h G_n da + F_n^2 \int_c G_x dy \quad . \end{aligned}$$

Adding the term $C_i \phi_*$ on both sides of equation (4.5) and using the identity $C_i + C_e = 1$ given in equation (4.8), one finds that:

$$\phi_* = \iint_h \{G \phi_n - (\phi - \phi_*) G_n\} da + F_n^2 \int_c \{G \phi_x - (\phi - \phi_*) G_x\} dy \quad (4.14)$$

for any point ξ inside, outside or on the hull surface $h+c$. This new identity is equivalent to the identity given in equation (4.9) as may easily be verified (see Noblesse (1983)).

Making use of equation (4.10) and substituting the hull surface condition given in equation (2.18), the integral identity given by equation (4.14) may be expressed in the form of the integro-differential equation:

$$\phi(\xi) = \psi(\xi) - L(\xi; \phi) \quad , \quad (4.15)$$

where the potential $\psi(\xi)$ is explicitly defined as:

$$\psi(\xi) = \iint_h G(\xi, \mathbf{x}; F_n^2) n_{\mathbf{x}}(\mathbf{x}) da + F_n^2 \int_c G(\xi, \mathbf{x}; F_n^2) n_{\mathbf{x}}^2(\mathbf{x}) dy \quad (4.16)$$

and the linear transform $L(\xi; \phi)$ is given by:

$$L(\xi; \phi) = \iint_h (\phi - \phi_*) G_n da + F_n^2 \int_c \{ (\phi - \phi_*) G_x - G(t_x \phi_\ell - n_z t_y \phi_d) \} dy \quad . \quad (4.17)$$

The potential $\psi(\xi)$ given in equation (4.16) is explicitly defined in terms of the hull geometry, whereas the linear transform $L(\xi, \phi)$ is not known in advance. Equations (4.15-17) constitute yet another alternative and equivalent formulation of the Neumann-Kelvin problem. The implicit integral identity given in equation (4.15) may be solved iteratively by means of the recurrence relationship:

$$\phi^{(n+1)}(\xi) = \psi(\xi) - L(\xi; \phi^{(n)}) \quad (4.18)$$

for $n=0,1,\dots$, where the initial approximation is simply defined as $\phi^{(0)}=0$, see Noblesse (1983).

Associated with the sequence of potential approximations $\phi^{(0)}=0, \phi^{(1)}=\psi, \phi^{(2)}, \dots$ is a sequence of wave resistance approximations $C_w^{(n)}, n \geq 0$, as discussed by Noblesse (1983). The zeroth order approximation $C_w^{(0)}$ can be related to the classic thin, flat and slender ship wave resistance approximations in the thin, flat and slender ship limits respectively, whilst the first order approximation $C_w^{(1)}$ is closely related to the slow ship wave resistance approximation in the low Froude number limit (see Table 2.2).

In the zero Froude number limit the potential becomes the zero Froude number potential ϕ_0 corresponding to the flow about the hull when the free surface is replaced by a rigid wall, as may be seen from equation (2.17). Alternatively, ϕ_0 may be interpreted as the 'double hull' potential of the waveless flow about the hull and its mirror image with respect to the plane $z=0$ in infinite fluid. Table 4.2 gives the zero Froude number boundary conditions and alternative integral identities, corresponding to equations (2.16-19), (4.12-13) and (4.15-18) respectively. Noblesse and Triantafyllou (1983) show that $L_0 \ll \psi_0 \approx \phi_0$ for slender bodies moving in the direction of their major axis. When the hull surface is the lower half of a slender ellipsoid the potentials ϕ_0 and ψ_0 become proportional, that is, $\psi_0 = k\phi_0$, and the constant k is close to unity, see Havelock (1931a,b). Figure 4.2 shows the relative error $\epsilon_n = (\phi_0 - \phi_0^{(n)}) / \phi_0 = (1-k)^n$ associated with the n th zero Froude number potential approximation for a prolate spheroid of aspect ratio q . It is seen that $0 \leq \epsilon_1 \leq 1/3$; in particular, $\epsilon_1 = 0$ if $q=0$ (i.e. a 'needle') and $\epsilon_1 = 1/3$ if $q=1$. For slender spheroids with low

aspect ratios between 0.1 and 0.2 (the usual range for ships) the relative error ϵ_1 associated with the zero Froude number explicit potential approximation is less than about 5%.

The foregoing remarks suggest that the explicit potential approximation $\phi = \psi$, where ψ is defined by equation (4.16), provides a useful approximation to the disturbance potential of the flow about a slender ship hull moving at low Froude number, as is usually the case in practice. Comparing equations (4.12) and (4.16) it is seen that the explicit potential approximation $\phi = \psi$ is equivalent to the explicit source strength approximation $Q = n_x$. The flow velocity $\nabla\psi$ is continuous everywhere. It can also be shown that in the thin ship limit the potential ψ reduces to the classic Michell (1898) thin ship potential. Further arguments to support that ψ is an acceptable slender ship potential approximation are given in the next section and in Chapter 6.

4.4 KOCHIN'S FUNCTION AND HAVELOCK'S FORMULA

In section 2.4 it was pointed out that the wave resistance may also be obtained by evaluating the amount of radiated energy contained in the free waves far behind the moving ship. Presently this method is outlined and subsequently used to investigate the importance of the water line integral term in equation (4.12), as well as to further assess the usefulness of the explicit slender ship approximation given by equation (4.16).

Consider the Kelvin wave source potential $G(\xi, x; F_n^2)$ defined by equation (3.5). From equations (3.15) and (3.17) it is seen that far downstream from the moving source, as $\xi \rightarrow -\infty$, both the fundamental Rankine source term $-1/4\pi |\xi - x|$ and the nearfield disturbance $N(X)/4\pi F_n^2$ are negligible in comparison with the wavelike disturbance $W(X)/4\pi F_n^2$. That is

$$G \sim (1/\pi F_n^2) \text{Im} \int_{-\infty}^{\infty} \exp\left\{[(\zeta+c)\sqrt{1+t^2} + i((\xi-x)+(\eta-y)t)]\sqrt{1+t^2}/F_n^2\right\} dt$$

as $\xi \rightarrow -\infty$, as may readily be obtained from equations (3.6) and (3.8). Substituting this expression into equation (4.12) and reversing the order of integration it follows that:

$$\phi(\xi) \sim (1/\pi) \text{Im} \int_{-\infty}^{\infty} K(t) \exp\left\{[\zeta\sqrt{1+t^2} + i(\xi+\eta t)\sqrt{1+t^2}/F_n^2]\right\} dt \quad (4.19)$$

as $\xi \rightarrow -\infty$, where the function $K(t)$ is defined by:

$$K(t) = F_n^{-2} \int_h^{\infty} \exp\{z(1+t^2)/F_n^2\} EQ da + \int_c^{\infty} EQn_x dy, \quad (4.20)$$

with the function $E = E(x, y, t, F_n^2)$ given by:

$$E = \exp\{-i(x+yt)\sqrt{1+t^2}/F_n^2\}. \quad (4.21)$$

Substituting equation (4.19) into equation (2.20) it is found that the elevation of the free surface far behind the ship is given by:

$$\zeta_w(\xi, \eta) \sim (1/\pi) \text{Re} \int_{-\infty}^{\infty} \sqrt{1+t^2} K(t) \exp\{i(\xi+\eta t)\sqrt{1+t^2}/F_n^2\} dt \quad (4.22)$$

as $\xi \rightarrow -\infty$.

Equations (4.19) and (4.22) relate the potential and the wave elevation far behind the ship to a superposition of elementary plane waves, see Newman (1977). The function $K(t)$ defined by equation (4.20) is a function of the ship geometry and the Froude number and is known as Kochin's wave amplitude function (see Kochin (1951)); it represents the amplitude of the free wave component at angle $\theta = \arctan(t)$ with the negative Ox-axis (i.e. the limits $t \rightarrow 0$ ($\theta \rightarrow 0$) and $t \rightarrow \infty$ ($\theta \rightarrow \frac{1}{2}\pi$) correspond to the transverse and diverging waves respectively in the spectrum of the free waves following the ship, see Figure 3.3).

The wave resistance may now be determined by evaluating the energy contained in the downstream wave pattern given by equation (4.22), see Eggers et al (1967), Wehausen (1973) and Newman (1977). It follows that C_w is given by the Havelock (1934) formula:

$$C_w = (1/2\pi) \int_{-\infty}^{\infty} \sqrt{1+t^2} |K(t)|^2 dt \quad (4.23)$$

For ships with a lateral plane of symmetry the Kochin's function $K(t)$ becomes an even function of t and the integrals occurring in equations (4.19, 22-23) may be expressed as integrals over the semi-infinite interval $(0, \infty)$.

A variety of alternative expressions and approximations for the Kochin's function may be found in Noblesse (1983). Of particular interest, because of their simplicity, are the thin ship and slow ship approximations. Let the hull surface h be defined by the equation $y=b(x,z)$. In the thin ship limit, equation (4.20)

becomes identical to the Michell (1898) thin ship approximation

$K_M(t)$ given by:

$$K_M(t) = 2 \iint_{h_y} \exp\{ (z\sqrt{1+t^2} - ix)\sqrt{1+t^2}/F_n^2 \} b_x(x, z) dx dz, \quad (4.24)$$

where h_y denotes the projection of h on the ship's centre plane $y=0$ and the source strength $b_x = \partial b / \partial x$. The low Froude number approximation

$K_{\ell F}(t)$ of $K(t)$ is obtained by approximating the source strength Q by the zero Froude number source strength Q_0 defined in Table 4.2.

That is:

$$K_{\ell F}(t) = F_n^{-2} \iint_h \exp\{ z(1+t^2)/F_n^2 \} EQ_0 da + \int_c EQ_0 n_x dy. \quad (4.25a)$$

Guevel et al (1974), Baba (1976, 1977), Maruo (1977) and Kayo (1977) show that this expression is identical to:

$$K_{\ell F}(t) = \iint_s E \phi_{0xx} dx dy \quad (4.25b)$$

where s denotes the mean free surface (excluding the ship's water line plane s_z), E is given by equation (4.21) and the zero Froude number potential ϕ_0 is defined in Table 4.2.

For simple mathematically defined hull forms the slow ship approximation $K_{\ell F}(t)$ may be evaluated analytically using either equation (4.25a) or (4.25b), see for example Baba (1977). Here only the case of a vertical semi-infinite prism with elliptic water line is considered. Taking the length of the major axis as reference

length, the water line contour c is defined by the dimensionless equation $x^2 + y^2/q^2 = 1$, where q denotes the aspect (thickness) ratio. The zero Froude number potential ϕ_0 and source strength Q_0 are given by $\phi_0 = -qx$ and $Q_0 = -(1+q)x/\sqrt{x^2 + y^2/q^4}$, see Milne-Thomson (1968). Brard (1972) has evaluated the corresponding low Froude number Kochin's function given by equation (4.25a). The low Froude number wave resistance $C_w^{\ell F}$ can be computed by means of Havelock's formula given by equation (4.23).

Figure 4.3 shows the low Froude number wave resistance approximation $C_w^{\ell F}$ as function of the Froude number F_n for four different aspect ratios q (see Guevel et al (1974)). The two curves shown correspond to the evaluation of equation (4.25a) with and without the water line integral term respectively. It is clearly seen that the water line integral has an important effect on the wave resistance, in particular at low Froude number and for high aspect ratio. For example, when the water line is circular ($q=1$) it may be shown that $C_w^{\ell F}$ behaves like

$$C_w^{\ell F} = (3328/315)F_n^6 + 16\sqrt{\pi}F_n^7 \sin(1/F_n^2 + \pi/4)$$

as $F_n \rightarrow 0$. If the water line integral is omitted, $C_w^{\ell F}$ behaves like

$$C_w^{\ell F} = (64/15)F_n^2 - 4\sqrt{\pi}F_n^3 \sin(1/F_n^2 + \pi/4)$$

as $F_n \rightarrow 0$. When the aspect ratio decreases the effect of the water line integral becomes less important but certainly not negligible. For values of q between 0.1 and 0.2 (the usual range for ships) the

relative importance of the water line integral increases as F_n decreases. In the zero Froude number limit terms in the hull surface and water line integrals can be shown to partially cancel out each other, see Kusaka (1976), Hirata and Levi da Conceicao (1976) and Bessho (1976).

A simple physical interpretation of the water line integral may be obtained by slightly immersing the hull and closing it on top by means of a horizontal plane. The water line source distribution may then be shown to stem from the zero immersion limit of the surface source distribution over the top surface of the slightly immersed closed hull, see Noblesse (1983). Eggers (1980) has pointed out that the flow velocity field associated with the hull surface source distribution alone is not continuous along the water line, and that the water line source distribution is needed to obtain a continuous flow velocity field.

Associated with the sequence of zero Froude number potentials $\phi_0^{(0)}=0, \phi_0^{(1)}=\psi_0, \phi_0^{(2)}, \dots$, defined in Table 4.2, is a sequence of low Froude number wave resistance approximations $C_w^{(n)}$, $n \geq 0$, which may be evaluated by substituting $\phi_0 = \phi_0^{(n)}$ in equation (4.25b). Noblesse (1984) has proved the convergence of the sequence $C_w^{(n)}$, $n \geq 0$, for the vertical prism with elliptic water line. Figure 4.4 shows the relative error $\epsilon_n = (C_w^{2F} - C_w^{(n)}) / C_w^{2F}$ associated with the n th approximation as function of the aspect ratio q . For $q=0.15$ the relative error ϵ_1 is about 3.4% and it is seen that the explicit potential approximation $\phi_0 \approx \phi_0^{(1)} = \psi_0$ provides an acceptable low Froude number approximation to the wave resistance of a slender vertical prism.

| distribution | sources | doublets | mixed | mixed |
|------------------|----------------|--------------------|-------------|---------------|
| condition | $\phi' = \phi$ | $\phi'_n = \phi_n$ | $\phi' = 0$ | $\phi'_n = 0$ |
| source strength | $Q \neq 0$ | $Q = 0$ | $Q \neq 0$ | $Q = \phi_n$ |
| doublet strength | $S = 0$ | $S \neq 0$ | $S = \phi$ | $S \neq 0$ |
| potential * | + | - | - | - |
| velocity * | - | + | - | - |

* + = continuous through the hull surface

- = discontinuous through the hull surface

Table 4.1 Comparison of singularity distribution methods.

zero Froude number boundary conditions:

$$\begin{aligned} \nabla^2 \phi_0 &= 0 & \text{in } d & & \phi_{0z} &= 0 & \text{on } h \\ \phi_{0n} &= n_x & \text{on } h & & \phi_0 &= O(1/|\tilde{x}|) & \text{as } |\tilde{x}| \rightarrow \infty \end{aligned}$$

zero Froude number Green's function:

$$\begin{aligned} 4\pi G_0(\tilde{\xi}, \tilde{x}) &= -1/|\tilde{\xi}-\tilde{x}| + 1/R \\ R^2 &= (\xi-x)^2 + (\eta-y)^2 + (\zeta+z)^2 \end{aligned}$$

auxiliary source distribution representation:

$$\begin{aligned} \phi_0(\tilde{\xi}) &= \iint_h Q_0(\tilde{x}) G_0(\tilde{\xi}, \tilde{x}) da \\ -\frac{1}{2} Q_0(\tilde{\xi}) + \iint_h Q_0(\tilde{x}) G_{0n} da &= n_x(\tilde{\xi}) \quad \text{on } h \end{aligned}$$

explicit integral identity:

$$\begin{aligned} \phi_0(\tilde{\xi}) &= \psi_0(\tilde{\xi}) - L_0(\tilde{\xi}; \phi_0) \\ \psi_0(\tilde{\xi}) &= \iint_h G_0(\tilde{\xi}, \tilde{x}) n_x(\tilde{x}) da \\ L_0(\tilde{\xi}, \phi_0) &= \iint_h \{ \phi_0(\tilde{x}) - \phi_0(\tilde{\xi}) \} G_{0n} da \\ \phi_0^{(n+1)}(\tilde{\xi}) &= \psi_0(\tilde{\xi}) - L_0(\tilde{\xi}, \phi_0^{(n)}) \quad , \quad n = 0, 1, \dots \\ \phi_0^{(0)} &\equiv 0 \quad , \quad \phi_0^{(1)} \equiv \psi_0 \end{aligned}$$

Table 4.2 Zero Froude number boundary conditions, Green's function and integral identities.

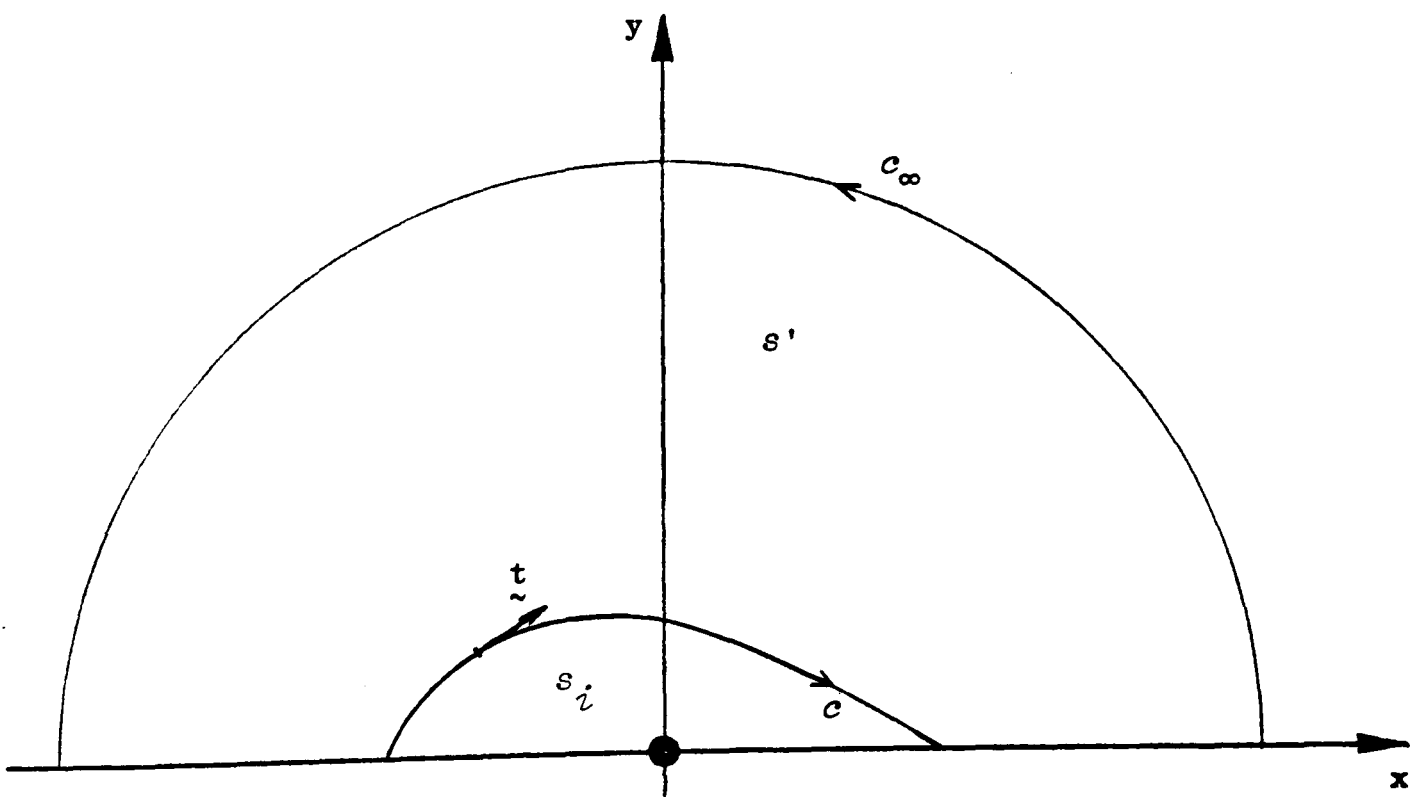
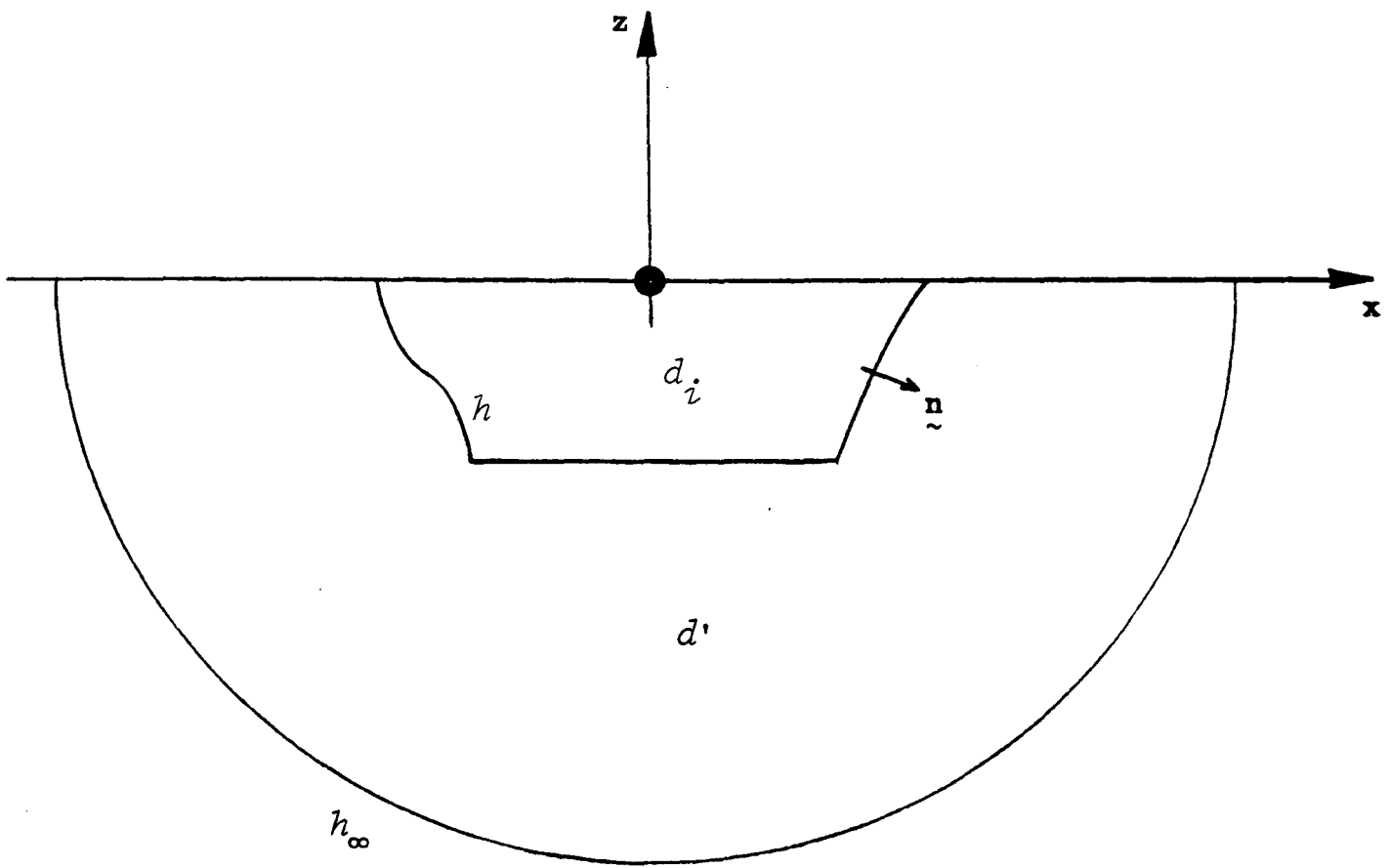


Figure 4.1 Definition sketch for application of Green's theorem (only port half of mean sea surface is drawn).

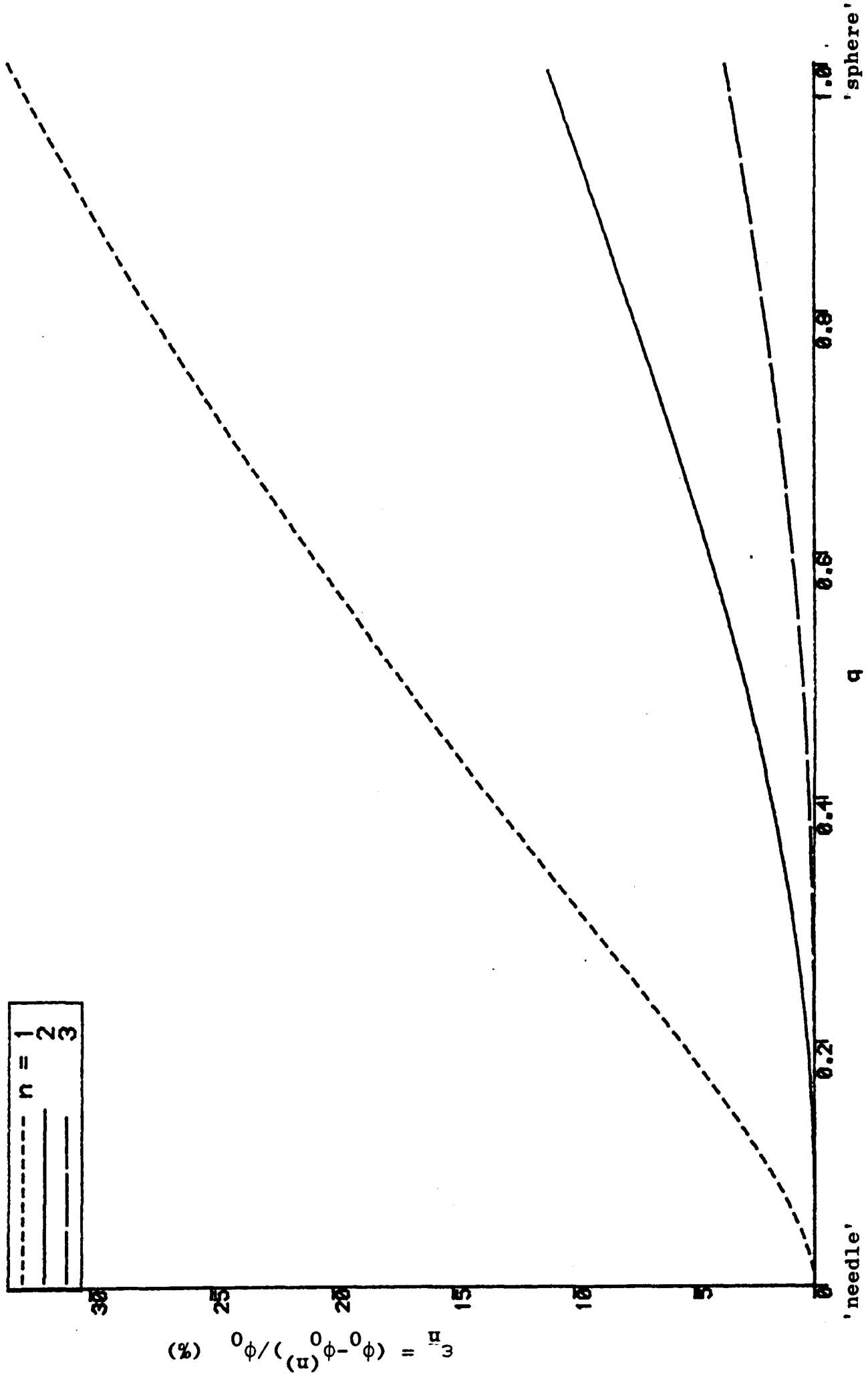


Figure 4.2 Relative error associated with the n-th zero Froude number potential approximation for a prolate spheroid of aspect ratio q.

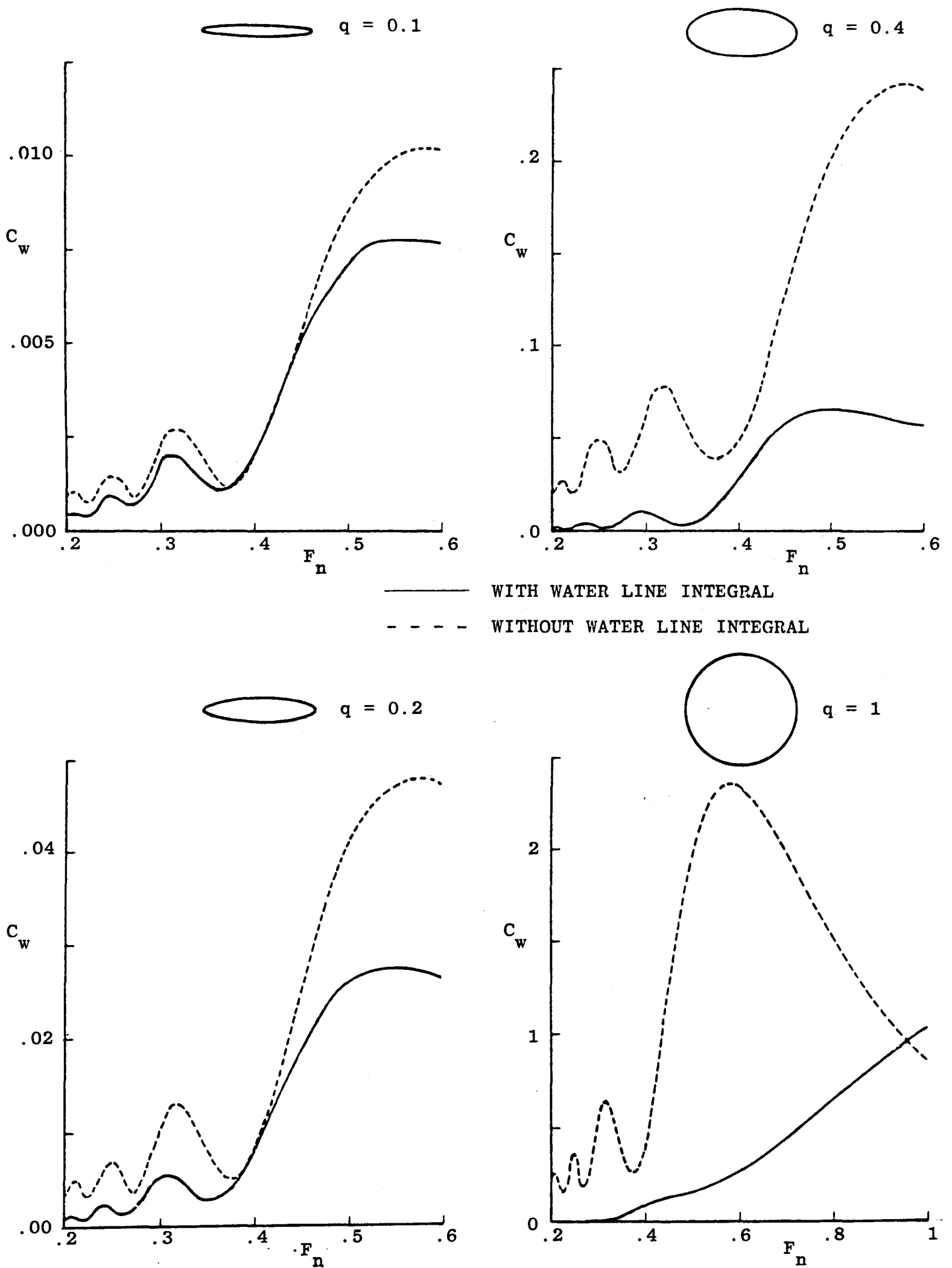


Figure 4.3 Wave resistance of vertical elliptical prisms
(see Guevel et al (1974), notice the different scales!).

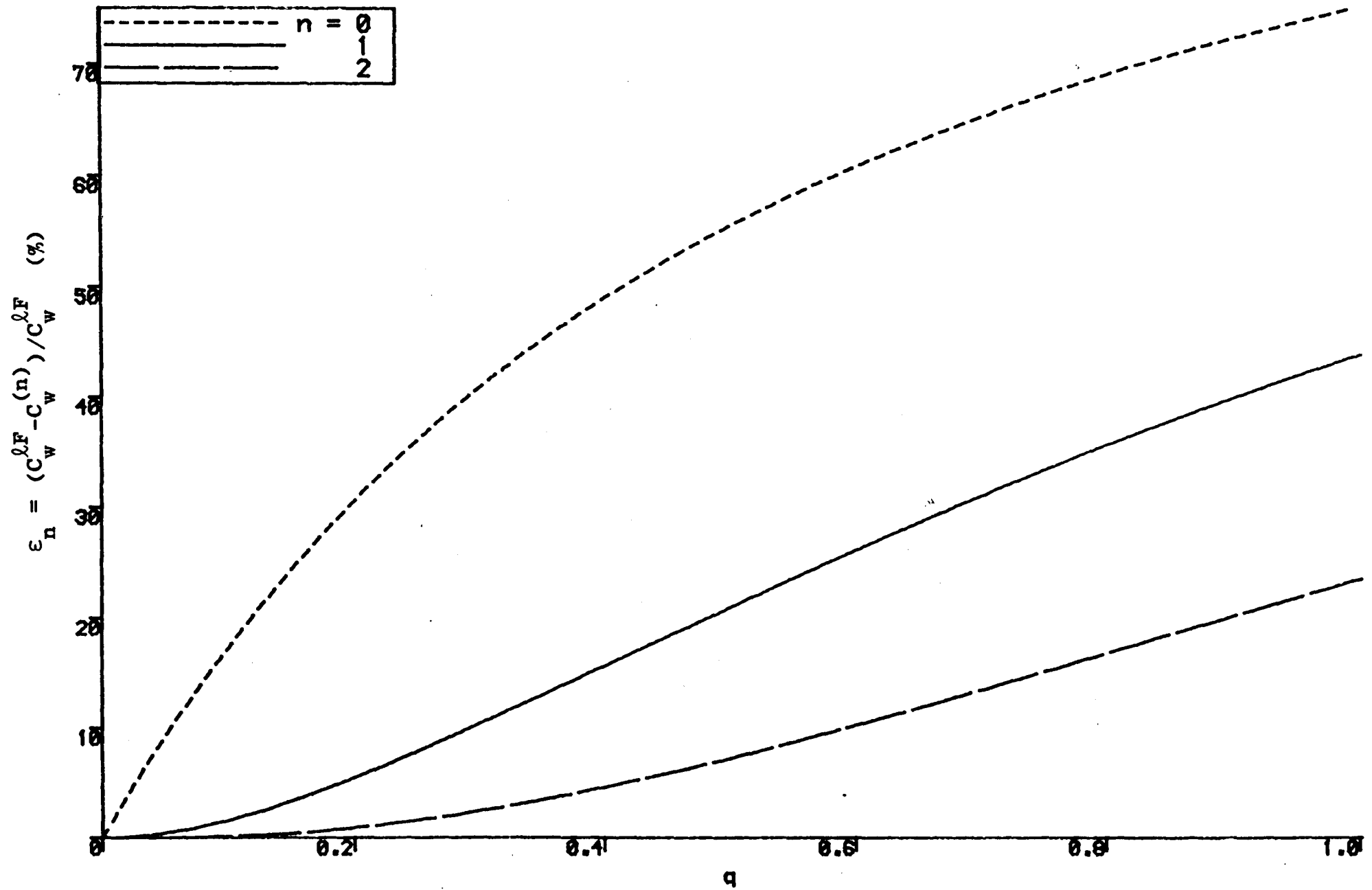


Figure 4.4 Relative error associated with the n-th low Froude number wave resistance approximation for a vertical prism with elliptic water line (aspect ratio q).

5. COMPUTATIONAL ASPECTS

5.1 APPROXIMATION OF INTEGRAL IDENTITIES

The disturbance potential of the flow about a moving ship is expressed in equation (4.12) in terms of a continuous distribution of Kelvin wave sources over the mean hull surface and water line of the ship. The unknown source strength distribution must be determined by solving the Fredholm integral equation of the second kind given by equation (4.13). This may be accomplished by means of a point-collocation method as used for instance by Inglis (1980) and Wu (1984). In the point-collocation procedure the integral equations (4.12-13) are approximated by matrix equations.

The mean hull surface h is subdivided into a large number N of quadrilateral panels. The position vector of the centroid and the area of the j -th panel ($j=1, \dots, N$) are denoted by \tilde{x}_j and Δh_j respectively. The panels are numbered such that the first M panels are adjacent to the mean water line c and Δc_j denotes the arc length of the j -th water line segment ($j=1, \dots, M$). The integral identities given by equations (4.12-13) are satisfied at one control point on each panel, taken at the panel's centroid. The source strength is assumed constant over each small panel and the source strength on a water line segment is taken equal to that of the adjacent hull surface panel. Under these assumptions the

integral identities may be written in discretised form as matrix equations given by:

$$\phi_i = \sum_{j=1}^N \alpha_{ij} Q_j \quad , \quad (5.1)$$

$$\sum_{j=1}^N \beta_{ij} Q_j = n_{xi} \quad , \quad (5.2)$$

for $i=1, \dots, N$, where $\phi_i = \phi(\underline{x}_i)$ and $n_{xi} = n(\underline{x}_i)$ are the values of the disturbance potential and the normal component of the hull velocity at the i -th control point and $Q_j = Q(\underline{x}_j)$ is the source strength on the j -th panel. The influence coefficients α_{ij} and β_{ij} represent the contributions on the i -th panel to the Kelvin wave source potential and its normal derivative in the j -th control point and are given by

$$\alpha_{ij} = \iint_{\Delta h_j} G(\underline{\xi}_i, \underline{x}; F_n^2) da + H_{Mj} F_n^2 \int_{\Delta c_j} G(\underline{\xi}_i, \underline{x}; F_n^2) n_{xy} dl \quad (5.3)$$

$$\beta_{ij} = -\frac{1}{2} \delta_{ij} + \iint_{\Delta h_j} G_n(\underline{\xi}_i, \underline{x}; F_n^2) da + H_{Mj} F_n^2 \int_{\Delta c_j} G_n(\underline{\xi}_i, \underline{x}; F_n^2) n_{xy} dl \quad (5.4)$$

for $i, j=1, \dots, N$, where $H_{Mj} = 1$ if $j=1, \dots, M$ and $H_{Mj} = 0$ if $j=M+1, \dots, N$, and $\delta_{ij} = 1$ if $i=j$ and $\delta_{ij} = 0$ if $i \neq j$.

Equation (5.2) represents a system of N linear algebraic equations in the N unknown source strengths. Having evaluated the influence coefficients β_{ij} from equation (5.4), this system may readily be solved and the values of the potential

at the N control points follow from equations (5.1) and (5.3). In order to compute the influence coefficients it is convenient to express the Kelvin wave source potential in the form:

$$G(\xi, x; F_n^2) = G_1(\xi, x) + G_2(\xi, x; F_n^2) \quad , \quad (5.5a)$$

where the 'infinite Froude number' Green's function $G_1(\xi, x)$ is given by

$$4\pi G_1(\xi, x) = -1/|\xi-x| + 1/r \quad , \quad (5.5b)$$

with $r = \sqrt{(\xi-x)^2 + (\eta-y)^2 + (\zeta+z)^2}$ representing the distance between the field point ξ and the free surface mirror image of the source point x . The function $G_2(\xi, x; F_n^2)$ is given by:

$$4\pi F_n^2 G_2(\xi, x; F_n^2) = \{M(X) - 1\}/R - H(X)8P(X) \quad (5.5c)$$

in agreement with equations (3.5-6), (3.9) and (3.18). The infinite Froude number Green's function $G_1(\xi, x)$ and its normal derivative vanish when $\zeta=0=z$ and this function does not contribute to the water line integral. Substituting equation (5.5a) into equations (5.3-4) gives:

$$\alpha_{ij} = \alpha_{ij}^{(1)} + \alpha_{ij}^{(2)} \quad , \quad \beta_{ij} = -\frac{1}{2}\delta_{ij} + \beta_{ij}^{(1)} + \beta_{ij}^{(2)} \quad ,$$

where

$$\alpha_{ij}^{(1)} = \iint_{\Delta h_j} G_1(\xi_i, \mathbf{x}) da \quad , \quad \beta_{ij}^{(1)} = \iint_{\Delta h_j} G_{1n}(\xi_i, \mathbf{x}) da \quad ,$$

$$\alpha_{ij}^{(2)} = \iint_{\Delta h_j} G_2(\xi_i, \mathbf{x}; F_n^2) da + H_{Mj} F_n^2 \int_{\Delta c_j} G_2(\xi_i, \mathbf{x}; F_n^2) n_x t_y d\ell$$

$$\beta_{ij}^{(2)} = \iint_{\Delta h_j} G_{2n}(\xi_i, \mathbf{x}; F_n^2) da + H_{Mj} F_n^2 \int_{\Delta c_j} G_{2n}(\xi_i, \mathbf{x}; F_n^2) n_x t_y d\ell \quad ,$$

for $i, j=1, \dots, N$. The integrands of the influence coefficients $\alpha_{ij}^{(1)}$ and $\beta_{ij}^{(1)}$ involve fundamental Rankine source terms only and these terms may be integrated analytically using the Hess and Smith (1966) formulas. The integrands of the panel surface and water line segment integrals in the expressions for the influence coefficients $\alpha_{ij}^{(2)}$ and $\beta_{ij}^{(2)}$ are dependent on the Froude number F_n and regular for all values of $i, j=1, \dots, N$ (provided $\zeta_i + z < 0$ as is assumed here). Such integrals may be integrated numerically by means of Gaussian quadrature, as illustrated in Figure 5.1. The procedure is based on a linear isoparametric mapping of the integration domain to the normalised integration domain where the integration variable is less than unity in absolute value. This device is frequently used in the Finite Element Method, see Zienkiewicz (1977).

Five possible sources of error are associated with the approximation procedure outlined above. These are:

- (i) *The approximation of the hull surface.* Guidelines for obtaining a suitable subdivision of the hull surface have been formulated by Inglis (1980). Whenever possible, panels with low aspect ratios should be avoided, variations in size between adjacent panels should be kept small and the panels should be concentrated in areas of large curvature of the hull surface where the flow velocity might change rapidly.
- (ii) *The approximate way in which the integral identities are satisfied.* The point-collocation procedure relies on the assumption that the source strength is constant on each panel. For water wave radiation/diffraction problems it has been suggested by Mei (1978) and Yeung (1982) that the individual panel dimensions should not exceed one eighth of the wave length. In the present context the dimensionless wavelength is proportional to F_n^2 and it follows that the number of panels N is proportional to F_n^{-4} . At low Froude number a very fine discretisation of the hull surface may therefore be required. Numerical experience suggests that the present approximation of the water line integral is reasonable, see for example Tsutsumi (1979) and Tsai et al (1983).
- (iii) *Quadrature errors in the numerical integration of the influence coefficients.* There is some discussion of this topic in Sclavounos and Lee (1985). The integrands of the influence, $\alpha_{ij}^{(2)}$ and $\beta_{ij}^{(2)}$ are in general slowly varying functions except at very low Froude number when the contribution from the

wavelike disturbance component of the Kelvin wave source potential may vary substantially within a panel. In the present approach a two-point Gauss-Legendre quadrature is used with weights $w_j=1$ and abscissae $a_j=(-1)^j/\sqrt{3}$ for $j=1,2$ (see Figure 5.1); this formula integrates a cubic polynomial exactly, see Davis and Rabinowitz (1975).

- (iv) *The evaluation of the Kelvin wave source potential.* In sections 5.2-3 algorithms are discussed for the evaluation of this function with an absolute accuracy of between five and six significant digits. This is considered sufficient for practical applications.
- (v) *Roundoff-errors in the solution of the linear system of equations in the unknown source strength.* (This source of error is not relevant when the explicit slender body approximation discussed in Section 4.3 is used, in which case the source strengths are approximated by the known normal components of the hull velocity on the panel). The present state of the art of linear system solvers is such that this type of error can easily be kept at bay, see Nonweiler (1984). In this study the linear system given by equation (5.2) is solved by means of Crout's factorisation method with partial pivoting and iterative refinement.

Most ships have a lateral plane of symmetry and this feature may be exploited advantageously to halve the required number of evaluations of the Kelvin wave source potential and its gradient, see Inglis (1980) and Wu (1984). This number equals $N^2 + M^2$ if no use is made of ship symmetry and the influence coefficients are evaluated by means of the usual single node centroid integration (i.e. the one-point Gaussian quadrature as used for instance by Inglis (1980)). Use of the two-point Gauss-Legendre rule raises the number of evaluations by about a factor four to $4N^2 + 2M^2$. If the ship symmetry is efficiently exploited, this number may be reduced by a factor two to $2N^2 + M^2$. This may be achieved as follows. In matrix notation equation (5.2) may be written as:

$$\begin{matrix} B & = & N \\ \sim & & \sim \end{matrix} \quad (5.6)$$

where B is the $(N \times N)$ matrix of influence coefficients and Q and N are $(N \times 1)$ column vectors of source strengths and normal hull velocity components respectively. If a ship has a lateral plane of symmetry such that the port side panels 1 to $\frac{1}{2}N$ are the mirror images with respect to the plane $y=0$ of the starboard side panels $\frac{1}{2}N+1$ to N then the matrix equation (5.6) may be partitioned as follows:

$$\begin{vmatrix} B_1 & B_2 \\ \sim_1 & \sim_2 \\ B_3 & B_4 \\ \sim_3 & \sim_4 \end{vmatrix} \begin{vmatrix} Q_p \\ \sim_p \\ Q_s \\ \sim_s \end{vmatrix} = \begin{vmatrix} N_p \\ \sim_p \\ N_s \\ \sim_s \end{vmatrix}$$

where B_1, B_2, B_3 and B_4 are $(\frac{1}{2}N \times \frac{1}{2}N)$ matrices, Q_p, Q_s, N_p and N_s are $(\frac{1}{2}N \times 1)$ column vectors and the indices p and s refer to panels on the port and starboard side respectively. Due to symmetry

$B_{\sim 1} = B_{\sim 3}$, $B_{\sim 2} = B_{\sim 4}$, $Q_{\sim p} = Q_{\sim s}$ and $N_{\sim p} = N_{\sim s}$ and the unknown source strengths on the port half of the ship's hull are found from:

$$B_{\sim p} Q_{\sim p} = N_{\sim p} \quad ,$$

where $B_{\sim p} = B_{\sim 1} + B_{\sim 2}$ is an $(\frac{1}{2}N \times \frac{1}{2}N)$ matrix. In this approach the saving in computing time and storage space is about 50%.

The remainder of this chapter is devoted to the presentation and discussion of accurate and efficient algorithms for the evaluation of the nearfield and wavelike components of the Kelvin wave source potential. From the previous considerations it is evident that the efficiency of these algorithms is very important if an unrealistically large amount of computing time is to be avoided.

5.2 EVALUATION OF THE NEARFIELD DISTURBANCE

By choosing a suitable expression from any of the alternative representations given in Table 3.2 the problem of the numerical evaluation of the nearfield disturbance is reduced to calculating a single integral with a slowly varying integrand which is expressed in terms of the complex-valued exponential integral function. The ascending series representations are best suited for evaluating the function $M(X)$ for small values of $R = |X|$, whereas the asymptotic expansion expressions may be used for large values of R ,

see Noblesse (1978b). Direct numerical integration of the nearfield disturbance is both cumbersome and time-consuming. On the one hand, the evaluation of the exponential integral tends to be rather time-consuming, as discussed by Baar (1985) and Newman (1985); a 'near-optimal' algorithm for the evaluation of this function is presented in the Appendix. On the other hand, the integrands of the integrals in Table 3.2 have discontinuous low order derivatives at the endpoints of the integration interval; this feature prohibits the immediate use of an efficient Gaussian quadrature method without taking special precautions, as discussed by Davis and Rabinowitz (1975) and Baar and Price (1986b).

Newman (1986a) has developed a highly efficient algorithm for the evaluation of the nearfield disturbance which effectively overcomes these problems. The method is based on four complementary trivariate Chebyshev expansions which cover the entire definition domain of the function $M(\underline{X})$. Chebyshev approximation (see Fox and Parker (1968)) has proved to be a very useful tool in numerical ship hydrodynamics (see Newman (1985)) and is based on the following principle. For the function $f(x)$ defined in $-1 \leq x \leq 1$ the Chebyshev series is given by:

$$f(x) = \sum_{n=0}^{\infty} 'a_n T_n(x) ,$$

where the primed summation sign indicates that the first term in the series must be halved and $T_n(x)$ is the Chebyshev polynomial as defined in Abramowitz and Stegun (1972). The Chebyshev coefficients

a_n are given by:

$$a_n = (2/\pi) \int_0^\pi f(\cos\theta) \cos(n\theta) d\theta .$$

The Chebyshev series may be shown to converge if $f(x)$ is sufficiently smooth in $-1 \leq x \leq 1$. For some special functions the Chebyshev coefficients a_n can be evaluated analytically, see for example Luke (1969); in general, however, they are computed by means of a suitable quadrature formula, see Fox and Parker (1968). In computational practice the infinite Chebyshev series expansion is truncated beyond some suitable value $n=N$, giving the polynomial approximation

$$f_N(x) = \sum_{n=0}^N a_n T_n(x) + \epsilon_N(x) .$$

The beauty of Chebyshev approximation is that a simple estimate for the truncation error $\epsilon_N(x)$ is immediately available. The Chebyshev polynomials oscillate between -1 and $+1$ and the contribution from any term in the expansion is bounded by the magnitude of the corresponding coefficient. That is:

$$|\epsilon_N| < \sum_{n=N+1}^{\infty} |a_n| ,$$

and the summation of the Chebyshev series may be terminated once the coefficients become less in absolute value than the desired accuracy of the approximation. The evaluation of the truncated Chebyshev series is facilitated by converting it into an equivalent ordinary polynomial of the form:

$$f_N(x) = \sum_{n=0}^N p_n x^n + \epsilon_n(x) .$$

An algorithm for this conversion is given by Nonweiler (1984); ordinary polynomials are rapidly evaluated by means of Horner's nested multiplication method.

The Chebyshev approximation procedure may be extended to functions of more than one variable, such as the nearfield disturbance $M(X)$ defined by equation (3.10). For this purpose it is convenient to write equation (3.14) as:

$$M(X) = M_A(X) + RM_I(R, \alpha, \beta) ,$$

where the spherical coordinates (R, α, β) are defined by

$(X, Y, Z) = R(\sin\alpha, \cos\alpha\sin\beta, \cos\alpha\cos\beta)$. Because of the symmetry relations given by equation (3.16) only the range $(X \geq 0, Y \geq 0, Z \geq 0)$ or

$(R \geq 0, 0 \leq \alpha \leq \frac{1}{2}\pi, 0 \leq \beta \leq \frac{1}{2}\pi)$ has to be considered. Newman (1986a) defines

$M_A = 1$ if $R > 1$ and

$$M_A = 1 - (2/\pi)R \int_{-1}^1 \text{Im}\left\{ \left(1 + A + \frac{1}{2}A^2 + \frac{1}{6}A^3 \right) \ln(A) \right\} dt$$

if $R < 1$. This expression may be evaluated analytically by means of simple recurrence relationships, see Newman (1986a). The slowly varying integral terms M_I are approximated by means of four complementary Chebyshev expansions of the form:

$$\begin{aligned}
 M_I &= \sum_{i=0}^{\tilde{R}} \sum_{j=0}^{\tilde{\alpha}} \sum_{k=0}^{\tilde{\beta}} a_{ijk} T_i(\tilde{R}) T_j(\tilde{\alpha}) T_k(\tilde{\beta}) \\
 &= \sum_{i=0}^{\tilde{R}} \sum_{j=0}^{\tilde{\alpha}} \sum_{k=0}^{\tilde{\beta}} p_{ijk} R^{\tilde{i}} \alpha^{\tilde{j}} \beta^{\tilde{k}}
 \end{aligned}$$

where $-1 \leq \tilde{R}, \tilde{\alpha}, \tilde{\beta} \leq 1$, $\tilde{\alpha} = 2(\alpha/\frac{1}{2}\pi) - 1$, $\tilde{\beta} = 2(\beta/\frac{1}{2}\pi)^2 - 1$ and

$$\tilde{R} = \begin{cases} 2R-1 & 0 \leq R \leq 1 \\ (2R-5)/3 & 1 \leq R \leq 4 \\ (R-7)/3 & 4 \leq R \leq 10 \\ 1-20/R & R \geq 10 \end{cases}$$

In these four domains the ordinary polynomial representations of M_I are evaluated rapidly with an accuracy of between five and six significant digits if the non zero coefficients p_{ijk} are prestored in four arrays of 187, 206, 198 and 165 elements respectively. Tables of both the Chebyshev coefficients a_{ijk} and the ordinary polynomial coefficients p_{ijk} , as well as a full description of the numerical methods used to obtain these coefficients, may be found in Newman (1986a).

A Fortran 77 subroutine has been prepared which implements Newman's algorithm for the evaluation of the nearfield disturbance. The gradient is computed by analytical differentiation of the polynomial representations (this procedure slightly degrades the accuracy by about one significant digit). The nested multiplication algorithm for the evaluation of an ordinary polynomial is very well suited to vectorisation on a parallel computer, see Schendel (1984), and the computing time on a Cray-1S machine is

only a few microseconds per evaluation of M and ∇M . Figure 5.2 shows surface plots of the function $M(X,Y,Z)$ for $Y=0$ and several values of Z . Figures 5.2a-b clearly illustrate the limiting behaviour of M for small and large values of R as indicated by equation (3.15) (compare with Figure 3.2).

5.3 EVALUATION OF THE WAVELIKE DISTURBANCE

Numerical integration of equation (3.19) presents no particular difficulties except from the possible accumulation of roundoff-errors due to the presence of the rapidly oscillatory integrand (at small values of $D=\sqrt{Y^2+Z^2}$ it may be better to use the seventh integral expression given in Table 3.3). Baar and Price (1986a) have presented an efficient numerical integration procedure based on a sequence of high precision Gaussian quadrature rules with interlacing abscissae (see Patterson (1973)). However, the efficiency of direct numerical integration is somewhat limited by the excessive number of integrand evaluations which is required when the integrand is rapidly oscillatory, see Davis and Rabinowitz (1975). Alternatively, any of the equivalent integral expressions given in Table 3.3 may be used to develop an alternative algorithm for the evaluation of the wavelike disturbance, see for example Guttman (1983) who implemented Weber's (1981) method to evaluate the third Fourier transform integral expression given in Table 3.3.

In practice an ideal algorithm for the evaluation of the wavelike disturbance is a method which avoids numerical integration altogether. Therefore Baar and Price (1986b) have investigated the usefulness of the two series representations given by equations (3.21-22). Due care is required when evaluating Neumann series of this type. The Bessel functions satisfy three-term recurrence relationships with respect to their degree n , as discussed in the Appendix, equations (A.4-5). Table 5.1 gives values of the Bessel functions for different n and x . It is seen that only the functions Y_n and K_n are numerically increasing functions of n and these functions can be evaluated without difficulty by means of forward recursion. The functions J_n and I_n are numerically decreasing functions of n and are so-called 'minimal' solutions of their respective three-term recurrence relationships, see Gautschi (1967); recursion is therefore only stable if applied in the backward sense. Table 5.1 also clearly illustrates that the functions Y_n and K_n increase exponentially in magnitude with increasing n , whereas the functions J_n and I_n vanish in an exponential manner. This feature causes serious cancellation errors and under/overflow problems during the running summation of the Neumann series. Effective algorithms to overcome these problems have been derived by Baar and Price (1986b) who showed that the difficulties associated with the generation of Bessel functions can be avoided by computing ratios of Bessel functions rather than the functions themselves, as suggested by Gautschi (1967). Details of this method are described in the Appendix.

For purposes of numerical evaluation it is convenient to write both series representations given by equation (3.21-22) in the form

$$P = C_N(\theta) + \epsilon_N ,$$

where ϵ_N denotes the truncation error and the finite Fourier cosine series $C_N(\theta)$ is given by:

$$C_N(\theta) = \sum_{n=0}^N a_n \cos(n\theta) .$$

Series of this type may be evaluated rapidly by means of the Goertzel-Clenshaw algorithm (see Nonweiler (1984)), which can be expressed as $C_N(\theta) = \frac{1}{2}(b_0 - b_2)$, where b_0 and b_2 are obtained recursively from:

$$b_n = a_n + 2\cos(\theta)b_{n+1} - b_{n+2}$$

for $n=N, N-1, \dots, 0$, where $\cos(\theta)=Z/D$ and the initial values are given by $b_{N+2}=b_{N+1}=0$.

The Fourier coefficients a_n , $n=0,1,\dots,N$, corresponding to the series representations given by equations (3.21-22) are evaluated in an efficient manner by means of the following two-step procedure:

(i) Compute the sequences of ratios of Bessel functions defined by:

$$j_n(X) = J_{2n+1}(X)/J_{2n-1}(X) \quad (5.7a)$$

$$k_n(\frac{1}{2}D) = K_{n+1}(\frac{1}{2}D)/K_n(\frac{1}{2}D) \quad (5.7b)$$

for $n=0,1,\dots,N$ in the series given by equation (3.21); and

$$y_n(X) = Y_{2n+1}(X)/Y_{2n-1}(X) \quad (5.7c)$$

$$i_n(\frac{1}{2}D) = I_{n+1}(\frac{1}{2}D)/I_n(\frac{1}{2}D) \quad (5.7d)$$

for $n=0,1,\dots,N$ in the series given by equation (3.22).

Notice that $j_0=y_0=-1$. Algorithms for obtaining these sequences are outlined in the Appendix.

(ii) Compute the Fourier coefficients $a_n, n=0,1,\dots,N$ using the recursion relationships:

$$a_{n+1} = -a_n k_n j_n (1 - j_{n+1}) / (1 - j_n) \quad (5.8a)$$

for $n=0,1,\dots,N-1$ in the series given by equation (3.21), the initial value being $a_0 = \exp(-\frac{1}{2}Z) J_1(X) K_0(\frac{1}{2}D)$; and

$$a_{n+1} = a_n i_n y_n (1 - y_{n+1}) / (1 - y_n) \quad (5.8b)$$

for $n=0,1,\dots,N-1$ in the series given by equation (3.22), the initial value being $a_0 = -\pi \exp(-\frac{1}{2}Z) Y_1(X) I_0(\frac{1}{2}D)$. Equations (5.8a-b)

may be verified by making use of the derivative relationships for the Bessel functions given in the Appendix, equations (A.7-8).

Extensive numerical experiments have been performed to assess the range and capability of the present algorithms, as well as to establish the convergence properties of the two series representations. In these experiments no attempt has been made to evaluate the wavelike disturbance at the free surface (i.e. only strictly positive values of Z have been considered). An absolute error tolerance of $\epsilon=10^{-6}$ was specified, giving an accuracy of between five and six significant digits. It appears that the two series are indeed complementary: the series given by equation (3.22) is best suited for small values of D/X^2 with no more than about 20 terms required to achieve full convergence to within the specified accuracy, whereas the series given by equation (3.21) may be used for moderate and large values of D/X^2 with no more than about 70 terms required.

The precise transition value of D/X^2 between the two regimes of convergence depends in a rather complicated fashion on both the coordinate X , the distance $D=\sqrt{Y^2+Z^2}$ from the source track, the angular orientation $\Theta=\arctan(Y/Z)$ and the specified tolerance ϵ (as expected in view of the asymptote nature of the series given by equation (3.22)). The following device to establish which series should be used has proved very effective in computational practice, at little additional cost. Initially the sequences of Bessel function ratios given by equations (5.7a-b) are generated for $n=0,1,\dots,75$

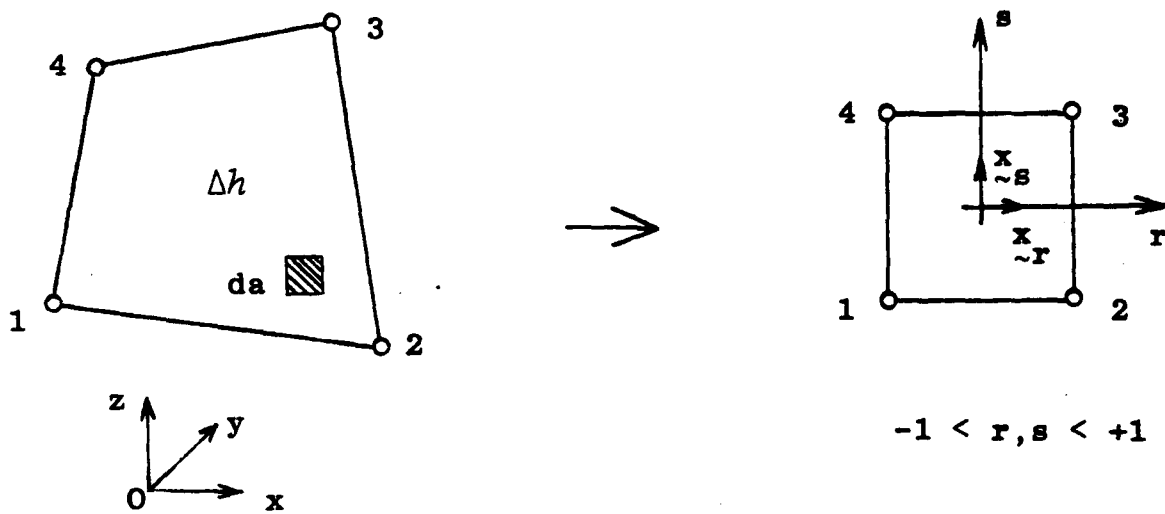
and these sequences are used to generate the a_n 's by means of equation (5.8a). The convergence of the a_n 's may easily be monitored by checking if $|a_N| < \epsilon$ for $N < 75$. If this is not the case the series given by equation (3.21) is too slowly convergent and the asymptotic series given by equation (3.22) is evaluated using equations (5.7c-d) with $N=25$ and equation (5.8b) until $|a_N| < \epsilon$. The wavelike disturbance is subsequently obtained by evaluating the relevant convergent finite Fourier cosine series.

A Fortran 77 subroutine has been prepared which implements the outlined algorithms for the evaluation of the series representations of the wavelike disturbance. Recurrence relationships for the evaluation of the gradient ∇P of P are obtained by analytical differentiation of the series given by equation (3.21-22). The derived recursion schemes are very well suited to vectorisation (see Schendel (1984)) and the average computing time on a Cray-1S machine is about 70 micro-seconds per evaluation of P and ∇P . (This is about 100 times faster than direct numerical integration of equation (3.19) to within the same accuracy). Figure 5.3 shows surface plots of the function $P(X,Y,Z)$ for several values of Z (compare with Figure 3.3).

| x | n | $J_n(x)$ | $Y_n(x)$ | $I_n(x)$ | $K_n(x)$ |
|-----|-------------|-------------|-------------|-------------|-------------|
| 1 | 0 | (- 1) 7.652 | (- 2) 8.826 | (0) 1.266 | (- 1) 4.210 |
| | 1 | (- 1) 4.401 | (- 1)-7.812 | (- 1) 5.652 | (- 1) 6.019 |
| | 2 | (- 1) 1.149 | (0)-1.651 | (- 1) 1.357 | (0) 1.625 |
| | 5 | (- 4) 2.498 | (2)-2.604 | (- 4) 2.715 | (2) 3.610 |
| | 10 | (-10) 2.631 | (8)-1.216 | (-10) 2.753 | (8) 1.807 |
| | 20 | (-25) 3.874 | (22)-4.114 | (-25) 3.967 | (22) 6.294 |
| | 50 | (-80) 2.906 | (77)-2.191 | (-80) 2.935 | (77) 3.407 |
| 2 | 0 | (- 1) 2.239 | (- 1) 5.104 | (0) 2.280 | (- 1) 1.139 |
| | 1 | (- 1) 5.767 | (- 1)-1.070 | (0) 1.591 | (- 1) 1.399 |
| | 2 | (- 1) 3.528 | (- 1)-6.174 | (- 1) 6.889 | (- 1) 2.538 |
| | 5 | (- 3) 7.040 | (0)-9.936 | (- 3) 9.826 | (0) 9.431 |
| | 10 | (- 7) 2.515 | (5)-1.292 | (- 7) 3.017 | (5) 1.625 |
| | 20 | (-19) 3.919 | (16)-4.082 | (-19) 4.311 | (16) 5.771 |
| | 50 | (-65) 3.224 | (62)-1.976 | (-65) 3.353 | (62) 2.980 |
| 5 | 0 | (- 1)-1.776 | (- 1)-3.085 | (1) 2.724 | (- 3) 3.691 |
| | 1 | (- 1)-3.276 | (- 1) 1.479 | (1) 2.434 | (- 3) 4.045 |
| | 2 | (- 2) 4.657 | (- 1) 3.677 | (1) 1.751 | (- 3) 5.309 |
| | 5 | (- 1) 2.611 | (- 1)-4.537 | (0) 2.158 | (- 2) 3.271 |
| | 10 | (- 3) 1.468 | (1)-2.513 | (- 3) 4.580 | (0) 9.759 |
| | 20 | (-11) 2.770 | (8)-5.934 | (-11) 5.024 | (8) 4.827 |
| | 50 | (-45) 2.294 | (42)-2.789 | (-45) 2.931 | (42) 3.394 |
| 10 | 0 | (- 1)-2.459 | (- 2) 5.567 | (3) 2.816 | (- 5) 1.778 |
| | 1 | (- 2) 4.347 | (- 1) 2.490 | (3) 2.671 | (- 5) 1.865 |
| | 2 | (- 1) 2.546 | (- 3)-5.868 | (3) 2.282 | (- 5) 2.151 |
| | 5 | (- 1)-2.341 | (- 1) 1.354 | (2) 7.772 | (- 5) 5.754 |
| | 10 | (- 1) 2.075 | (- 1)-3.598 | (1) 2.189 | (- 3) 1.614 |
| | 20 | (- 5) 1.151 | (3)-1.597 | (- 4) 1.251 | (2) 1.787 |
| | 50 | (-30) 1.785 | (27)-3.641 | (-30) 4.757 | (27) 2.061 |
| 50 | 0 | (- 2) 5.581 | (- 2)-9.806 | (20) 2.933 | (-23) 3.410 |
| | 1 | (- 2)-9.751 | (- 2)-5.680 | (20) 2.903 | (-23) 3.444 |
| | 2 | (- 2)-5.971 | (- 2) 9.579 | (20) 2.816 | (-23) 3.548 |
| | 5 | (- 2)-8.140 | (- 2)-7.855 | (20) 2.279 | (-23) 4.367 |
| | 10 | (- 1)-1.138 | (- 3) 5.724 | (20) 1.072 | (-23) 9.151 |
| | 20 | (- 1)-1.167 | (- 2) 1.644 | (18) 5.442 | (-21) 1.706 |
| | 50 | (- 1) 1.214 | (- 1)-2.103 | (10) 1.765 | (-13) 4.006 |
| 100 | (-21) 1.116 | (18)-3.294 | (-16) 2.728 | (13) 1.639 | |

Example : $J_{10}(50) = (- 1)-1.138 = - 1.138 \cdot 10^{-1} = - 0.1138$.

Table 5.1 Bessel functions of integer order.



→ shape functions $S_i(r,s) = \frac{1}{4}(1+rr_i)(1+ss_i)$ ($i=1,2,3,4$)

→ isoparametric coordinate transformations:

$$\tilde{x}(r,s) = \sum_{i=1}^4 S_i(r,s) \tilde{x}_i$$

$$\tilde{x}_{\tilde{r}} = (\partial x/\partial r, \partial y/\partial r, \partial z/\partial r) \quad \tilde{x}_{\tilde{s}} = (\partial x/\partial s, \partial y/\partial s, \partial z/\partial s)$$

$$\begin{aligned} \rightarrow \iint_{\Delta h} f(\tilde{x}) da &= \int_{-1}^1 \int_{-1}^1 f(\tilde{x}(r,s)) |\tilde{x}_{\tilde{r}} \times \tilde{x}_{\tilde{s}}| dr ds \\ &\equiv \int_{-1}^1 \int_{-1}^1 g(r,s) dr ds \\ &\approx \sum_{j=1}^N \sum_{k=1}^N w_j w_k g(a_j, a_k) \end{aligned}$$

Figure 5.1 Illustration of procedure for evaluating the influence coefficients by means of Gaussian quadrature.

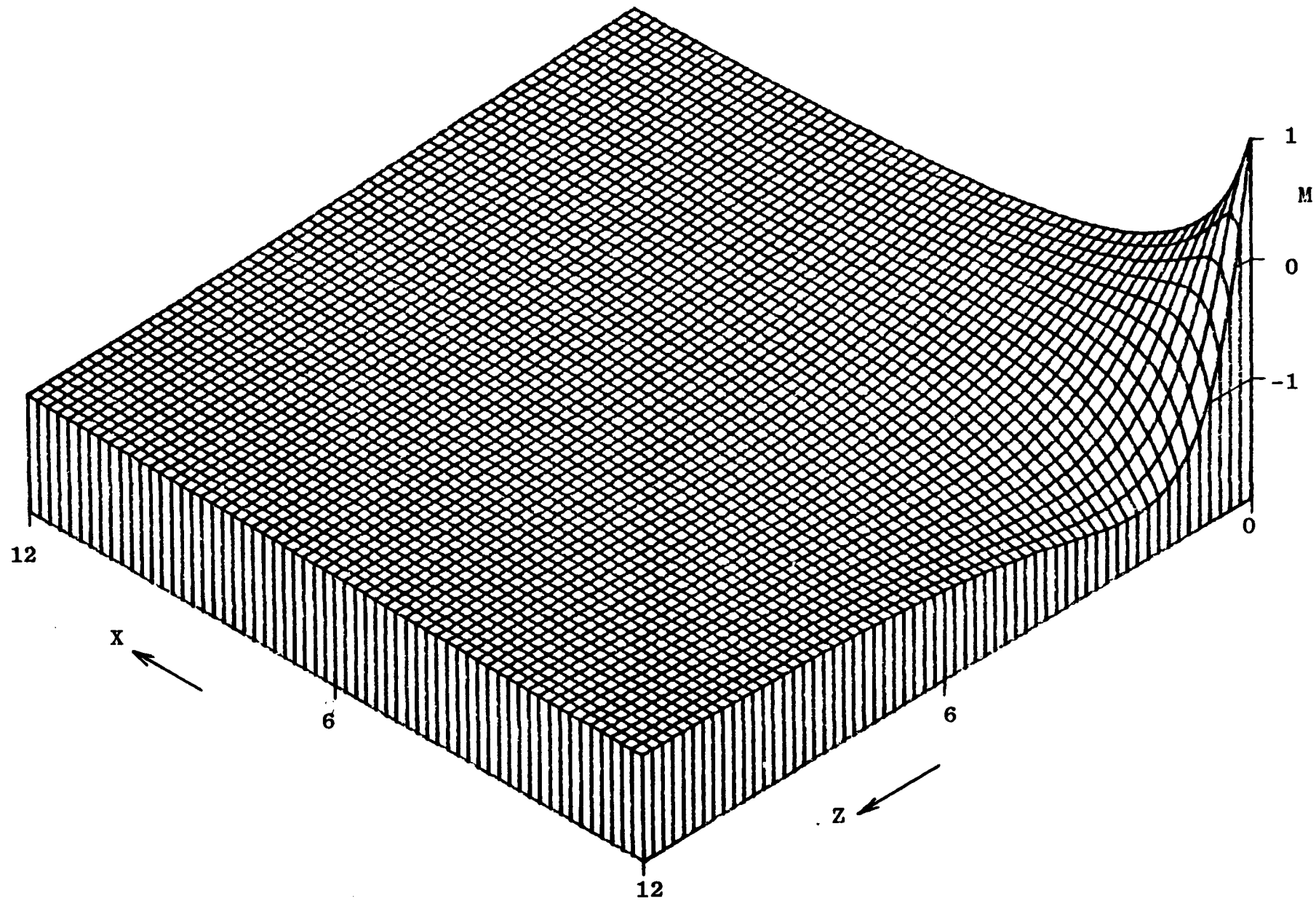


Figure 5.2 Sketches of the normalised nearfield disturbance $M(\tilde{X}) = N(\tilde{X})/R$.

(a) $Y = 0$

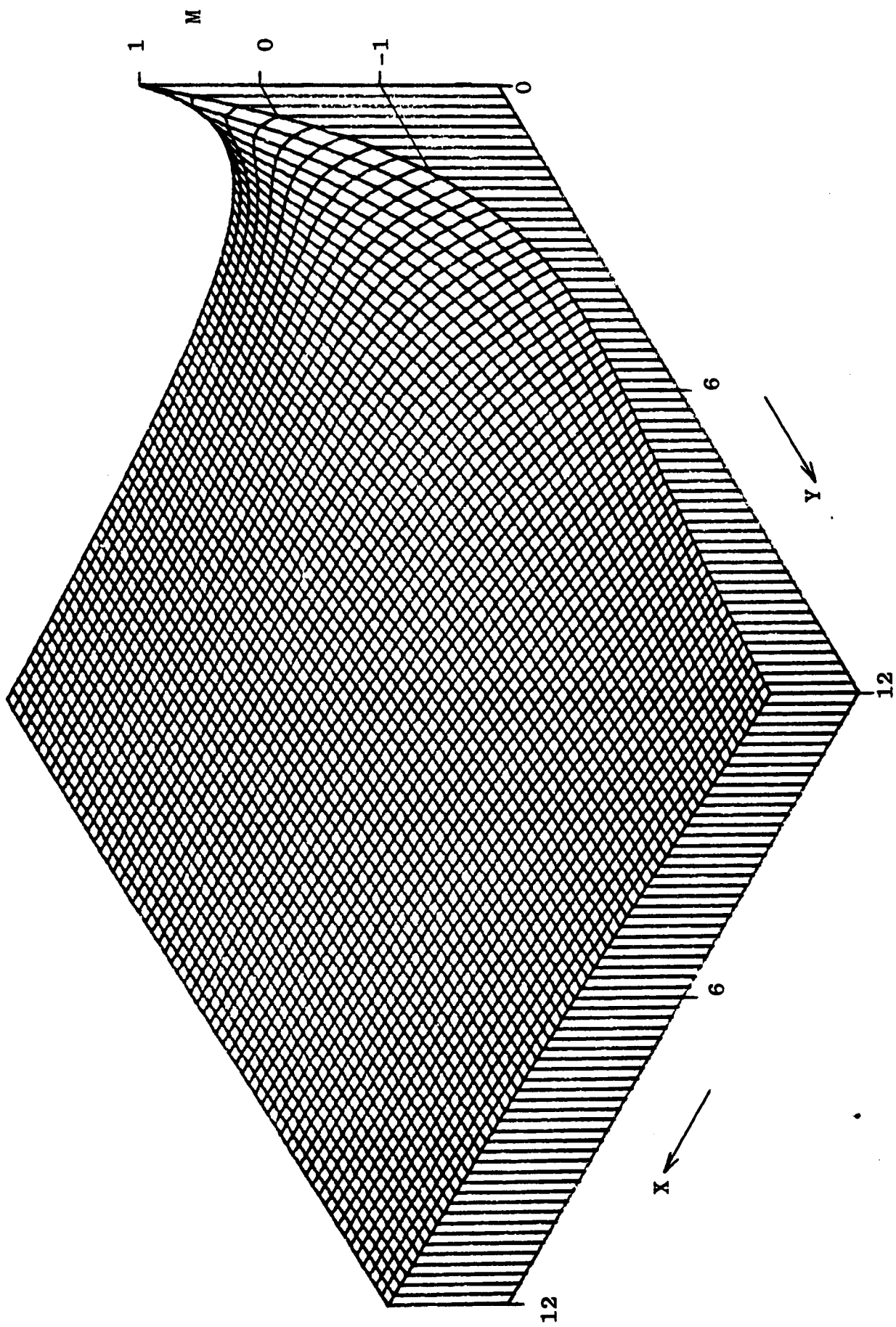


Figure 5.2 Continued. (b) $Z = 0$

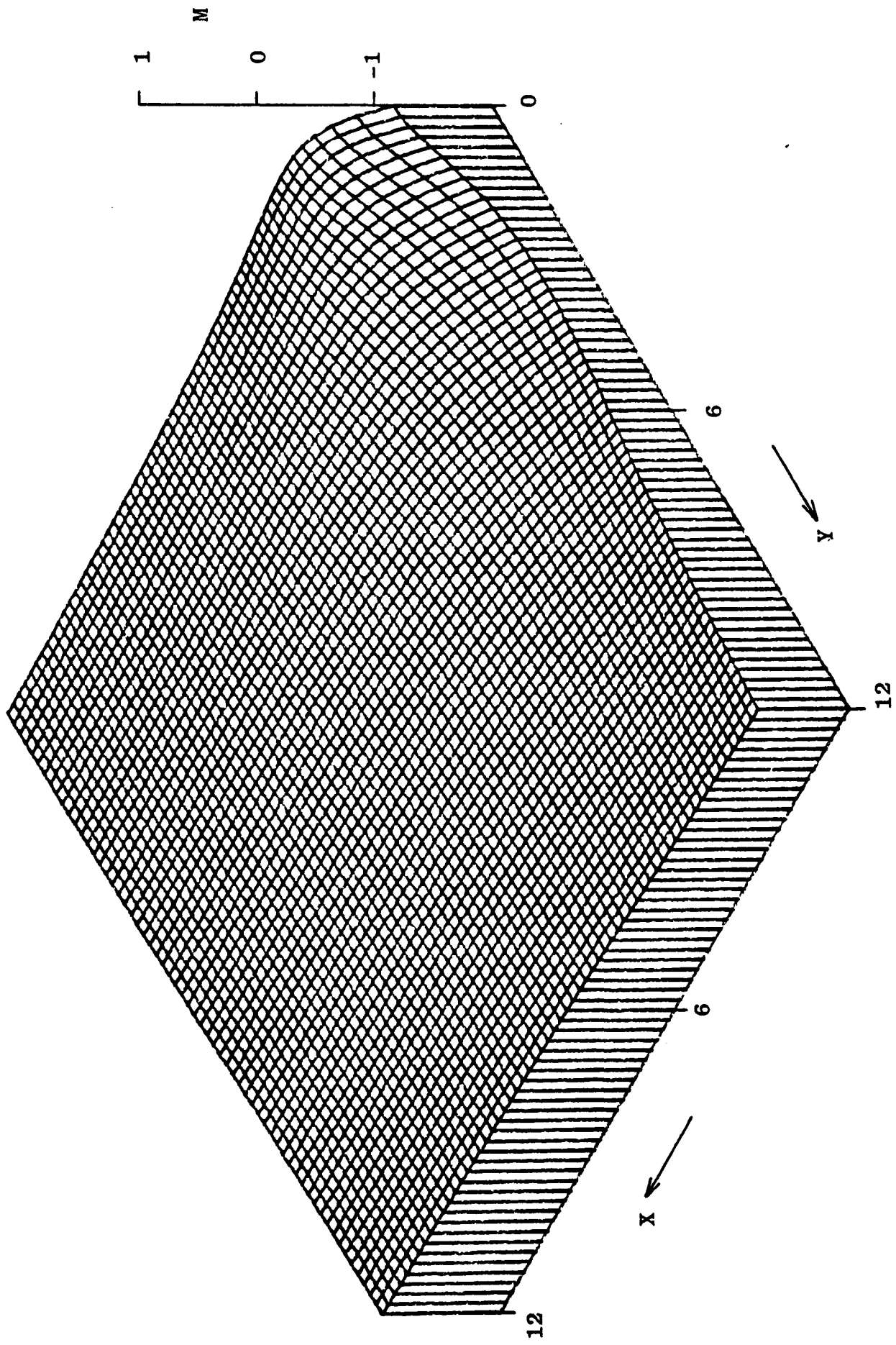


Figure 5.2 Continued. (c) $Z = 1$

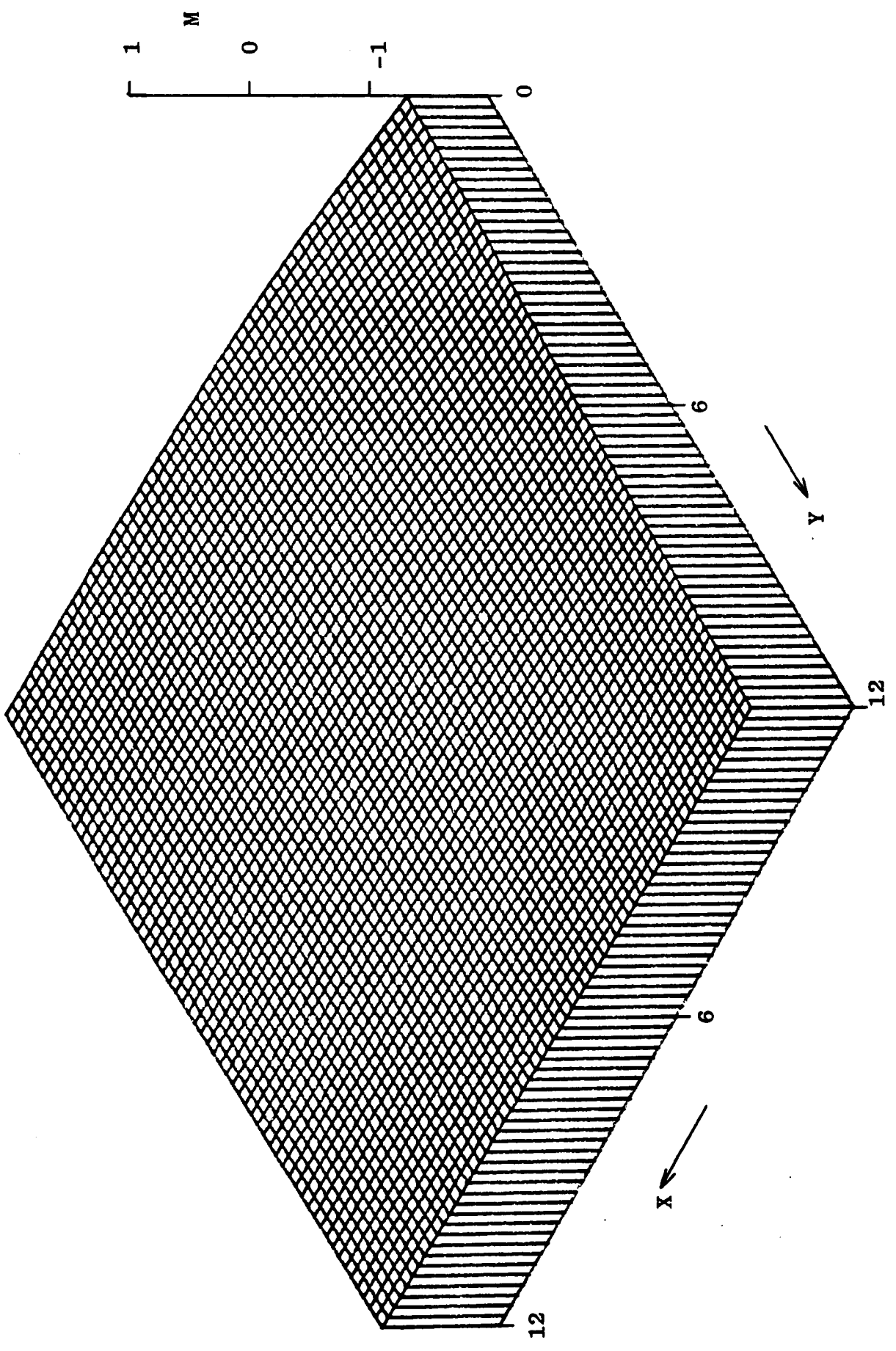


Figure 5.2 Continued. (d) $Z = 5$

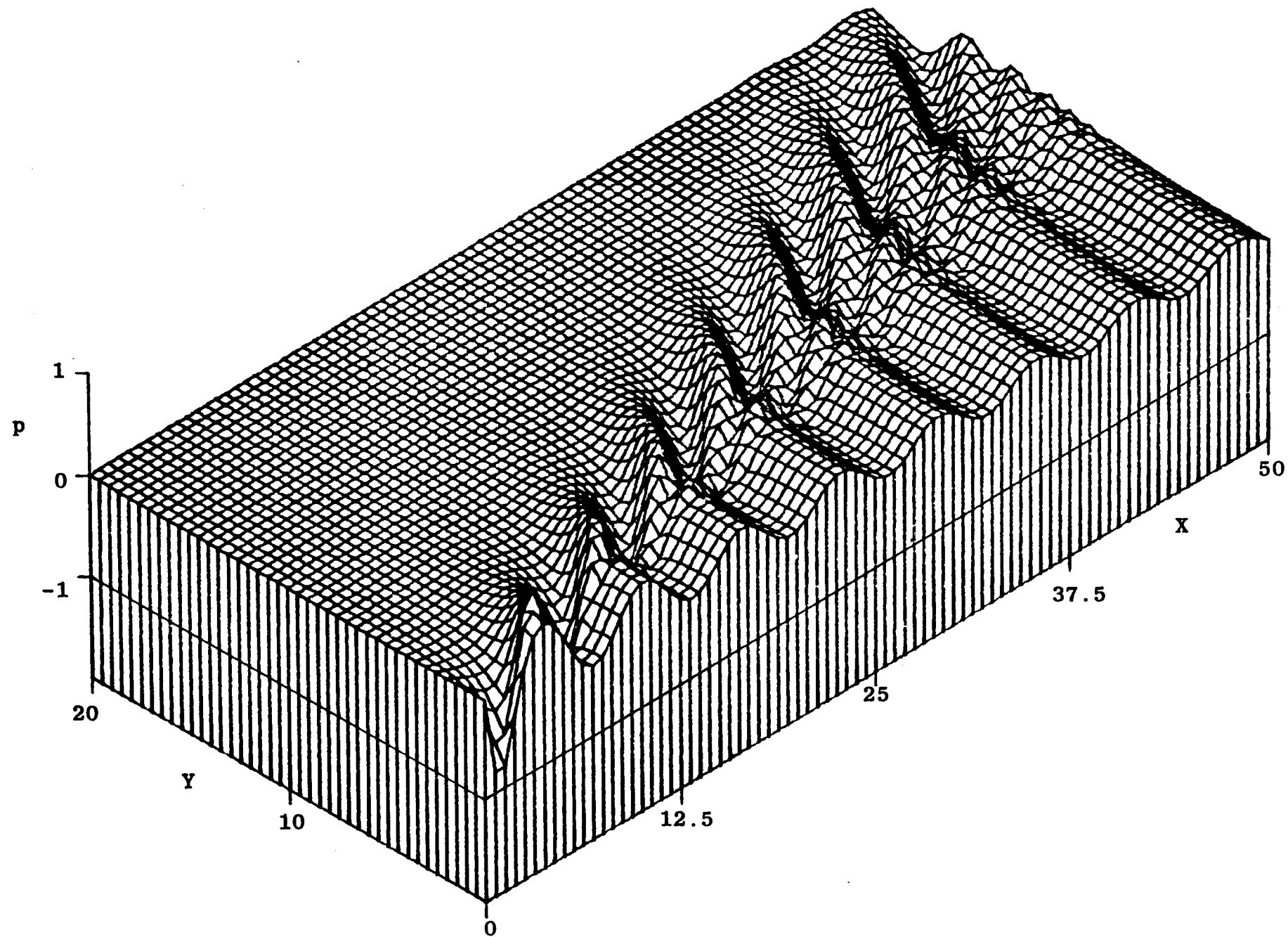


Figure 5.3 Sketches of the normalised wavelike disturbance $p(\underline{X}) = P(\underline{X}) / \{ \frac{1}{2} \exp(-Z) \sqrt{\pi/Z} \}$.

(a) $Z = 0.3$

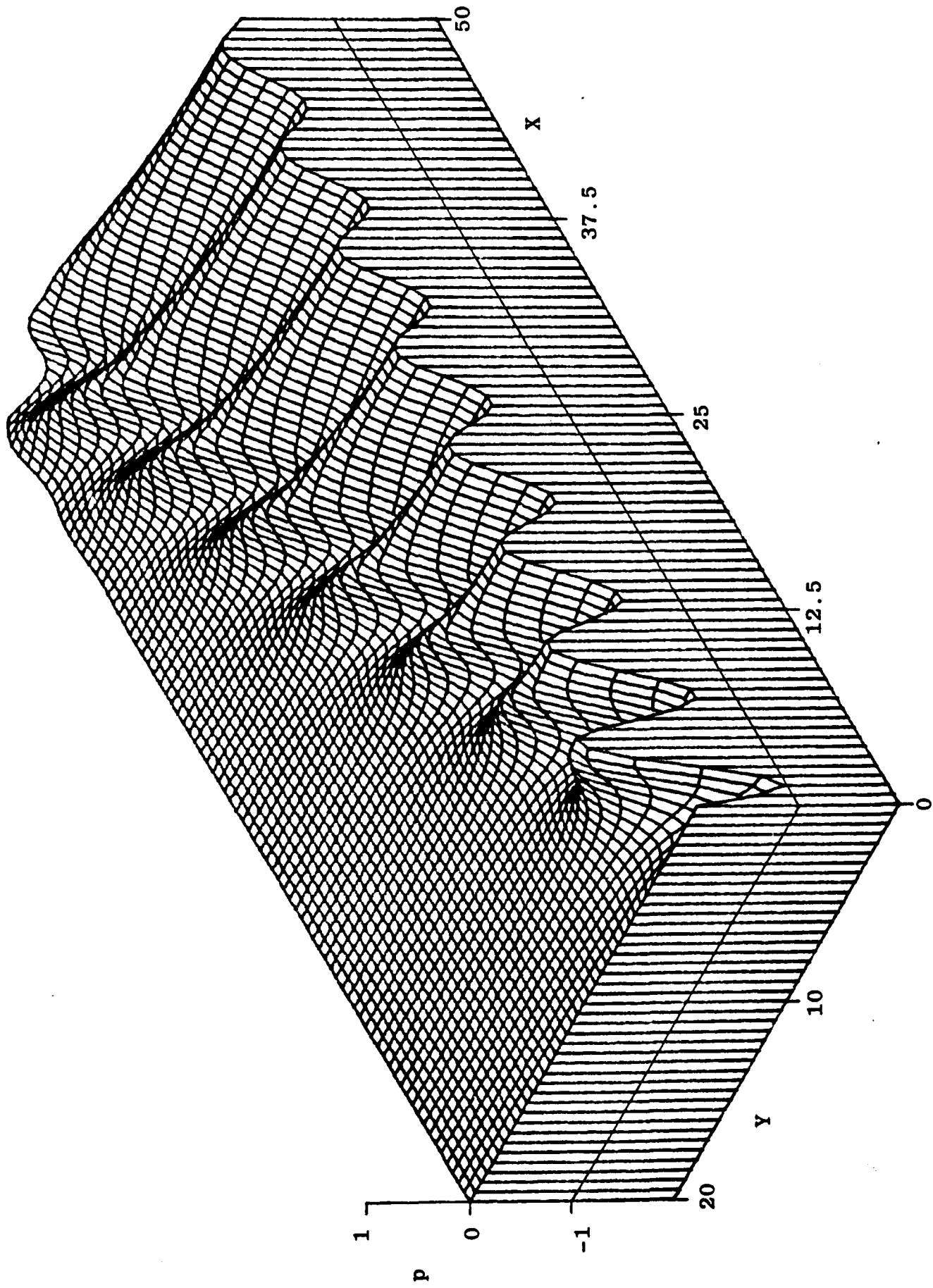


Figure 5.3 Continued. (b) $Z = 1.5$

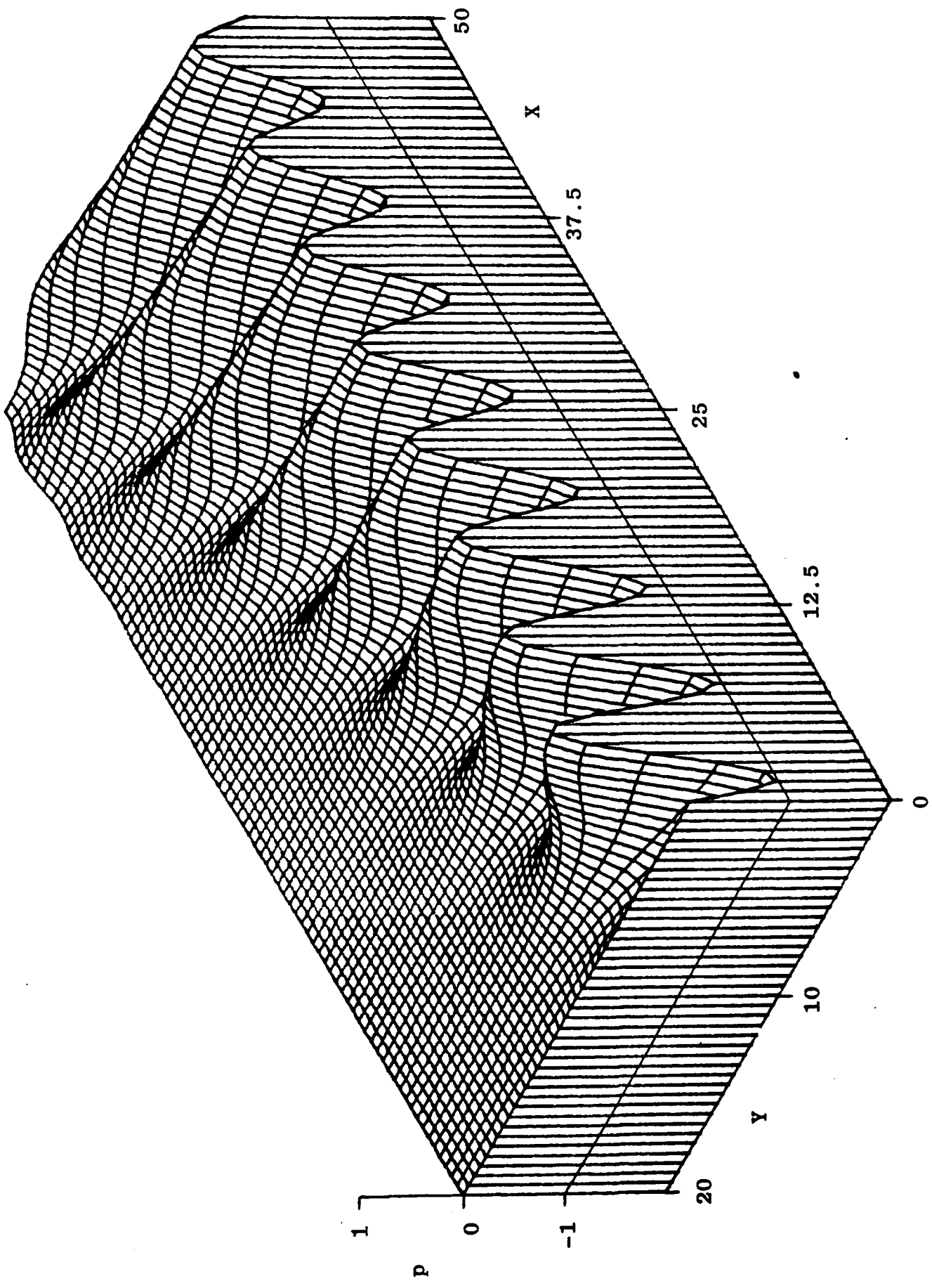


Figure 5.3 Continued. (c) $Z = 6$

6. APPLICATIONS OF THE THEORY

6.1 HULL DATA

The theory developed in the foregoing chapters is presently used to analyse the steady flow parameters for five different hull forms. Results are presented over prescribed ranges of the Froude number and compared with experimental data, as well as other theoretical predictions. Both the exact Neumann-Kelvin solution (see section 4.2) and the explicit slender ship approximation (see section 4.3) are considered. In order to gain insight in the performance and limitations of the linearised potential flow model a wide variety of flow parameters is investigated. These include the wave resistance, lift force, trimming moment, sinkage, trim, wave profile, pressure signatures and vertical force distributions.

The five hull forms include one mathematically defined fully submerged ship, one mathematically defined surface ship, and three realistic surface ships (see Andrew et al (1986)). The main particulars of the considered hull forms are summarised in Table 6.1 and the schematic body planes of the surface ships are shown in Figure 6.1. Table 6.1 gives for each hull form the beam/length and draft/length ratio, the block coefficient, the numbers of panels used to discretise the port side of the hull surface, and the range of Froude numbers.

The submerged prolate spheroid is considered in section 6.2.1. For this hull form an exact analytical solution of the Neumann-Kelvin wave resistance is available (see Farell (1973)). Wigley's parabolic hull form has been the subject of extensive experimental and theoretical studies. Experimental data and theoretical predictions of the wave resistance, wave profile and hull pressure signatures are presented and discussed in section 6.2.2. The HSVA tanker represents an extreme case of a very full hull form and was selected in order to assess the possible limitations of the linearised potential flow model. Predictions of the wave resistance and wave profile are presented in section 6.3.1. The 'Friesland' class destroyer represents an other extreme case of a very fast ship with transom stern. Andrew (1985) has measured the vertical force distributions in calm water. These data, as well as total lift force, trimming moment, sinkage and trim, are compared with the theoretical predictions in section 6.3.2. Finally, a 1930's Cruiser was selected to illustrate the versatility of the developed theory to deal with the prediction of other flow parameters. For one value of the Froude number predictions of the pressure field within the fluid surrounding the hull are presented in section 6.3.3.

All presented flow data are nondimensional in terms of the fluid density, the ship speed and the ship length (see Table 2.1).

6.2 MATHEMATICALLY DEFINED HULL FORMS

6.2.1 SUBMERGED PROLATE SPHEROID.

Evidently the water line integral terms (see chapter 4) are no longer present in the case of a fully submerged body and this implies a major theoretical simplification. Havelock (1931a) was among the first to investigate the wave resistance of a submerged prolate spheroid and derived a simple wave resistance approximation formula by using the axial source distribution corresponding to the motion of the spheroid in an infinite fluid and applying Lagally's theorem to evaluate the wave resistance. Of course, the axial source distribution does not produce a spheroid in the presence of a free surface, but the accuracy of Havelock's approximation increases with increasing immersion depth. Later Farell (1973) obtained the complete analytical solution of the Neumann-Kelvin problem by expanding the potential and the source strength in equations (4.12-13) into series of spheroidal harmonics. Havelock's approximation is obtained by retaining only the first term in Farell's exact expansion. By comparing Farell's solution with the present theoretical predictions the accuracy of the computational methods discussed in the previous chapter can be assessed.

Figure 6.2 depicts the relationship between the wave resistance coefficient C_w ($\equiv R_w / \rho V^2 L^2$) and the Froude number F_n ($\equiv V / \sqrt{gL}$). Havelock's approximation is seen to be in poor agreement with Farell's exact solution. This discrepancy is due to the small immersion depth of the spheroid's centroid (the present immersion depth/length ratio equals 0.1242, see Table 6.1). The Neumann-Kelvin theoretical predictions (i.e. the numerically exact solutions of equations (4.12-13)) are in excellent agreement with Farell's exact solution. This result confirms the accuracy of the developed computer program. The explicit slender ship approximation given by equation (4.16) is in good agreement with Farell's solution. The small differences may possibly be ascribed to the rather large value of the spheroid's beam/length ratio (this ratio equals 0.1667, see Table 6.1).

6.2.2 WIGLEY'S PARABOLIC HULL

Wigley's (1942) parabolic hull form has been the subject of extensive experimental and theoretical studies, see Chen and Noblesse (1983b) and McCarthy (1985) for a review. The nondimensional offsets of the Wigley hull are given by the equation $y = \pm \frac{1}{2} b (1 - 4x^2) (1 - z^2/d^2)$ for $-\frac{1}{2} \leq x \leq \frac{1}{2}$, $-d \leq z \leq 0$, where b and d are constants representing the beam/length and draft/length ratio respectively ($b=0.1$, $d=0.0625$). Chen and Noblesse (1983b) investigated eleven sets of experimental wave resistance data and

concluded that considerable variations occur (for example, the experiments scatter is 65% at $F_n = 0.2$). Recently new experiments have been carried out by Ju (1983) and Kajitani et al (1983) (see also McCarthy (1985)) and these data are used in the present section.

The results of Ju's (1983) wave resistance measurements with a 10 ft restrained model are summarised in Figure 6.3. For Froude numbers between 0.16 and 0.34 this figure shows the measured total resistance C_t , the calculated frictional resistance C_f (represented by the Schoenherr flat plate friction formula), the estimated viscous resistance $C_v = 1.1 C_f$, the measured viscous wake resistance C_{vw} (derived from wake survey measurements), the residual resistance $C_r = C_t - C_f$, the wavemaking resistance $C_w = C_t - C_v$ and the wave pattern resistance $C_{wp} = C_t - C_{vw}$. At low Froude numbers (F_n less than about 0.25) the viscous resistance is more than 80% of the total resistance and the wave pattern resistance derived from wake-survey measurements is expected to be more reliable than the wave pattern resistance derived from wave pattern analysis (see McCarthy (1985)).

Figures 6.4(a)-(c) show comparisons between the measured wavemaking and wave pattern resistance and theoretical predictions. The theoretical data shown in figures 6.4(a)-(b) were obtained by Chen and Noblesse (1983a). Figure 6.4(a) compares the experimental data with the thin and slow ship theoretical predictions calculated using equations (4.24) and (4.25a) respectively. Both theoretical curves are in poor agreement

with the experimental data. The theoretical humps and hollows are exaggerated and, more seriously, they occur at rather lower values of the Froude number than in the experimental data. Figure 6.4(b) shows the zeroth and first order wave resistance approximations corresponding to the sequence of slender ship approximations defined by equation (4.18). Chen and Noblesse (1983b) made several assumptions in order to simplify the calculations. Most notably the nearfield disturbance component $N(\underline{X})$ of the Kelvin wave source potential was approximated by the zero Froude number Green's function (i.e. $N(\underline{X}) = -1/|\underline{X}|$, see the discussion surrounding equation (3.15)), and the water line integral term was neglected. The zeroth order wave resistance approximation is essentially a generalisation of the classic thin ship approximation and the zeroth order curve in figure 6.4(b) suffers from the same defects as the theoretical curves in figure 6.4(a). The first order wave resistance approximation shown in figure 6.4(b) implies a major qualitative improvement of the theoretical predictions. Although the humps are still exaggerated, their positions are in good agreement with the experimental data.

The present results are shown in figure 6.4(c). Calculations were made at 19 different Froude numbers and both the 'exact' Neumann-Kelvin theoretical predictions and the explicit slender ship approximations are in good agreement with the experimental data. At values of the Froude number less than about 0.25 the theoretical predictions overestimate the

experimental data. Comparison between the first order curve in figure 6.4(b) and the slender ship approximation curve in figure 6.4(c) shows that the inclusion of the nearfield disturbance component has an important (decreasing) effect on the magnitude of the humps of the wave resistance curve. Because of the large variation in the high Froude number theoretical predictions obtained by other authors (see Table 1.1) no direct comparison with these data has been included in figure 6.4(c). The presently obtained results confirm the usefulness of the Neumann-Kelvin approximation for a practical range of Froude numbers.

Figures 6.5(a)-(d) show a typical comparison between the measured and calculated wave profile and hull pressures at a fixed value of the Froude number ($F_n = 0.316$). The wave profiles ζ_w / F_n^2 ($\equiv gZ_w / V^2$) were measured by Kajitani et al (1983) using restrained models. Figure 6.5(a) indicates that there is good agreement between the measured and calculated wave profiles except in the bow regime. The theoretical bow wave crest amplitudes are lower than the experimental values. Figure 6.5(b)-(d) show the comparisons of the measured and calculated hull pressure p ($\equiv P / \rho V^2$) at three different depths ($z/d = -0.20, -0.52$ and -0.84). The measurements were obtained using a short 2.5 m restrained model (see Kajitani et al (1983)) and it is difficult to draw a conclusion from the results shown in these figures. Both the exact Neumann-Kelvin solution and the slender ship approximation have the same characteristics as the measured pressure signatures.

6.3 REALISTIC HULL FORMS

6.3.1 HSVA TANKER

The HSVA tanker is a limiting case with its high value of block coefficient and low range of Froude numbers (see Table 6.1 and figure 6.1). Figure 6.6 shows the measured wave resistance data which were obtained from the total resistance measurements carried out by Collatz (1972). Free-running models of three different sizes were used (the effects of sinkage and trim are assumed to be negligible for this hull form). The estimated wave resistance is given by $C_w = C_t - (C_{vt} + C_{vp})$, where C_t is the total resistance, C_{vt} is the viscous tangential resistance (here assumed to be given by the ITTC 1957 line) and C_{vp} is the viscous pressure (or form) drag. For this hull form C_{vp} is very large and assumed to be constant ($C_{vp} = 0.895 \times 10^{-4}$). The resistance curve for the smallest model has a hump at $F_n \approx 0.17$ which does not show up in the curves for the two larger models.

Holtrop and Mennen (1978) have derived estimation formulas for the wave resistance by applying statistical regression to a large number of existing model and full scale ship measurements. The results obtained by applying these formulas to the HSVA tanker are shown in figure 6.6 and are in good agreement with the measured data. Also shown in figure 6.6 are the slow ship approximation

predictions of Baba (1979). These data are in excess of the measurements by a factor three to four (Baba applied his theory to a variety of ships but felt that the beam/draft ratio of the HSVA tanker is too large for his method to apply).

The present calculations shown in figure 6.6 are in remarkably good qualitative agreement with the experimental data. Apparently the absence of interference between the bow and stern wave systems due to the long parallel middle body is correctly modelled by the linearised potential flow theory. However, the Neumann-Kelvin theoretical predictions and the explicit slender ship approximation are in excess of the measurements by factors of about 1.5 and 2 respectively. The author has not been able to explain these differences. Both theoretical curves predict a small hump at $F_n \approx 0.17$ in agreement with the measurements for the smallest model and Holtrop and Mennen's predictions.

In order to make a full assessment of the performance of the linearised potential flow model in this case, further comparisons must be made with other experimental data, such as wave profiles, observations of wave breaking, and sinkage and trim measurements (see McCarthy (1985)). Unfortunately these data were not available to the author, but figure 6.7 shows a typical comparison of calculated wave profiles at $F_n = 0.15$. Included in this figure are the theoretical predictions of Gadd (1979) who used a modified Rankine source method (see Gadd (1976)), and Chan and Chan (1979) who solved an initial value problem by means of the

finite difference method. Chan and Chan's prediction of the bow wave amplitude is close to the maximum theoretical stagnation point value ($\zeta_w/F_n^2 = \frac{1}{2}$, see equation (2.5)). In both Gadd's and Chan and Chan's predictions the bow wave trough is positioned slightly more forward than in the present calculations. However, effective conclusions cannot be made without reference to further measurements.

6.3.2 'FRIESLAND' CLASS DESTROYER

The Dutch 'Friesland' class destroyer is a fast naval ship with transom stern (see figure 6.1). Andrew (1985) has measured the steady lift force distribution in calm water. The experimental set-up is sketched in figure 6.8. A 3.4 m model was built-up from 19 separate segments connected by sensitive strain-gauge dynamometers to a stiff longitudinal beam firmly attached to the carriage structure. During the experiments the model was kept restrained (i.e. prevented from sinkage and trim). Figures 6.9(a)-(e) show the measured steady lift force distributions $d\ell_w/dx$ ($= (dL_w/dx)/\rho V^2 L$) at five Froude numbers $F_n = 0.15$ (0.1) 0.55 (corresponding to full scale ship speeds $V = 9.68$ (6.45) 35.5 knots). It can be seen that for F_n up to 0.35 the lift force is relatively uniformly distributed along the ship length. For F_n above 0.35 the (downward) sectional force peaks markedly over the aft body and increases steeply with increasing speed.

The present theoretical curves obtained by sectionwise integration of the calculated pressures, are also shown in figures 6.9(a)-(e). In this case, where only the steady lift force distribution of the restrained model is considered, no difficulties were encountered in the modelling of the transom stern effects (when the wave resistance of the free running model is calculated precautions must be taken to model the effect of the transom stern on the sinkage and trim, see Salvesen (1979)). At low Froude numbers the present calculations are seen to be in good agreement with the measurements, but at high values of the Froude number both theoretical curves peak less markedly than the experimental curves. The slender ship approximation fares less well than the Neumann-Kelvin theoretical predictions.

Figures 6.10(a)-(b) show the total lift force $l_w (=L_w/\rho V^2 L^2)$ and trimming moment $m_w (=M_w/\rho V^2 L^3)$ as functions of the Froude number. The experimental and theoretical curves were derived from the lengthwise integration of the distributions shown in figures 6.9(a)-(e). The lift force increases relatively smoothly with increasing speed and reaches a peak value at $F_n=0.45$, whilst the trimming moment is small up to nearly $F_n=0.35$ after which there is a rapid rise with increasing speed. This corresponds to the peak distributed vertical force moving aft as seen in figures 6.9 (d)-(e), whilst the total moment increases with speed above $F_n=0.35$ but does not peak. The qualitative agreement between the experimental data and theoretical predictions is generally good. At low speed ($F_n \leq 0.35$) the quantitative agreement is also very

encouraging, but less satisfactory at higher speeds. As might be expected after the earlier remarks the slender ship approximation compares less favourably as the speed increases.

Figures 6.10(c)-(d) show the calculated sinkage $s_w (=S_w/L)$ and trim by the stern $\theta_w (\approx(D_a - D_f)/L)$ derived from the solution of equations (2.22b-c). Also included in this figure are the results of direct sinkage and trim measurements of the free-running model (see Andrew (1985)). These data quantify the differences in attitude between the restrained and free-running model. Sinkage is seen to increase steadily up to $F_n = 0.45$ and appears to level off thereafter; the trim is small up to $F_n = 0.35$ and then increases markedly. As might be expected from the previous comparison the sinkage and trim are poorly predicted except for $F_n < 0.35$ when the quantities are small anyway. Using the measured lift force and trimming moment in equations (2.22b-c) does not significantly improve the predictions. This serves to illustrate the invalidity of equations (2.22b-c) at high Froude numbers when it would appear that the sinkage and trim should be determined iteratively (see section 2.4).

6.3.3 CRUISER HULL FORM

This 1930's cruiser hull was selected as a final test case to illustrate the versatility of the developed theory.

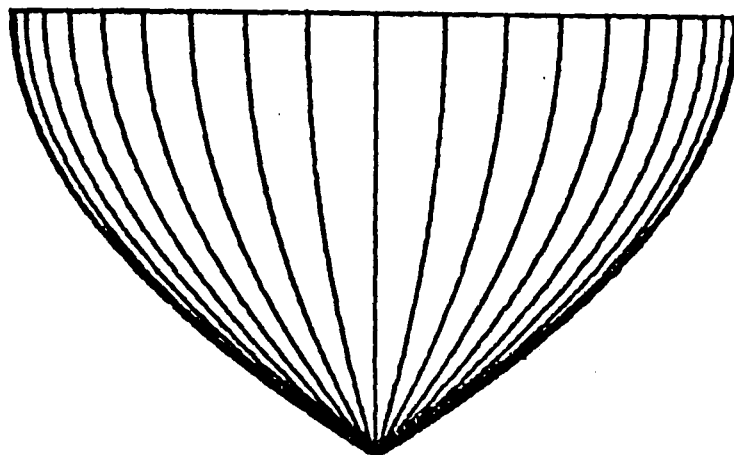
For the hull form the calm water pressure field below the hull has been recorded at $F_n = 0.126$ (see Andrew (1986)). The arrays of measurement positions below the hull are sketched in figure 6.11. At two different depths both the keel and transverse pressure signature have been measured. The measured and calculated data are compared in figures 6.12(a)-(d). It is seen that the experimental data and theoretical predictions are in good agreement, both along and transverse to the track of the ship. For this slender ship form (see Tables 6.1 and figure 6.1) travelling at fairly low speed the slender ship approximation agrees very well with the Neumann-Kelvin theoretical predictions.

| ship | beam/ length | draft/ length | block coefficient | number of panels on port hull surface | water line | Froude number |
|-----------------------------------|---------------------|---------------------|----------------------|--|------------|------------------|
| submerged prolate spheroid | 0.1667 | 0.1242 ¹ | 0.5236 | 220 | - | 0.40-0.80 |
| Wigley's parabolic hull | 0.1000 | 0.0625 | 0.4444 | 252 | 36 | 0.16-0.34 |
| HSVA tanker | 0.1515 ² | 0.0561 ² | 0.8503 ² | 226 | 32 | 0.13-0.18 |
| 'Friesland' class destroyer | 0.1044 ² | 0.0347 ² | 0.5540 ² | 227 | 35 | 0.15-0.55 |
| Cruiser | 0.1161 | 0.0362 | 0.5327 | 231 | 30 | 0.1257 |

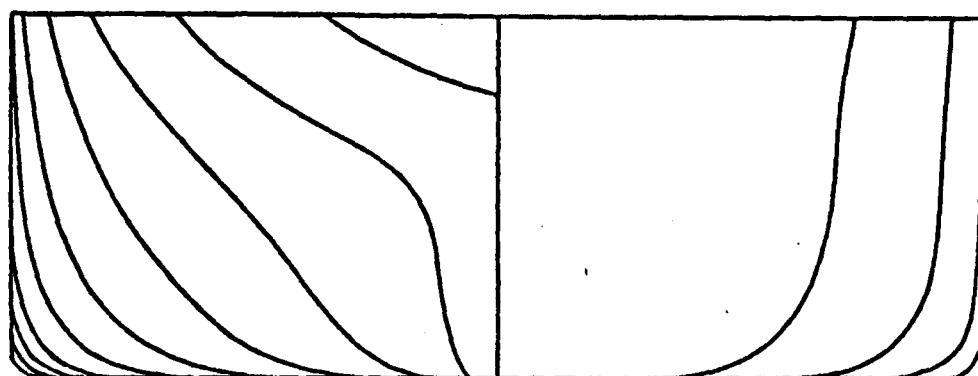
¹ draft \equiv immersion depth of centroid

² length \equiv length between perpendiculars

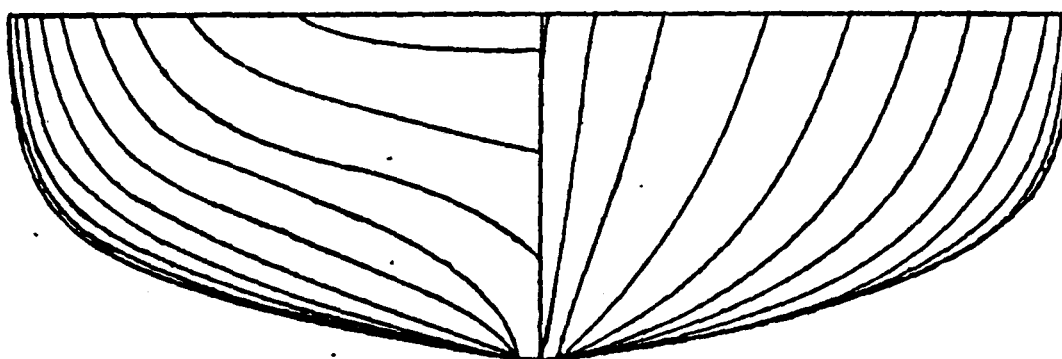
Table 6.1 Hull data.



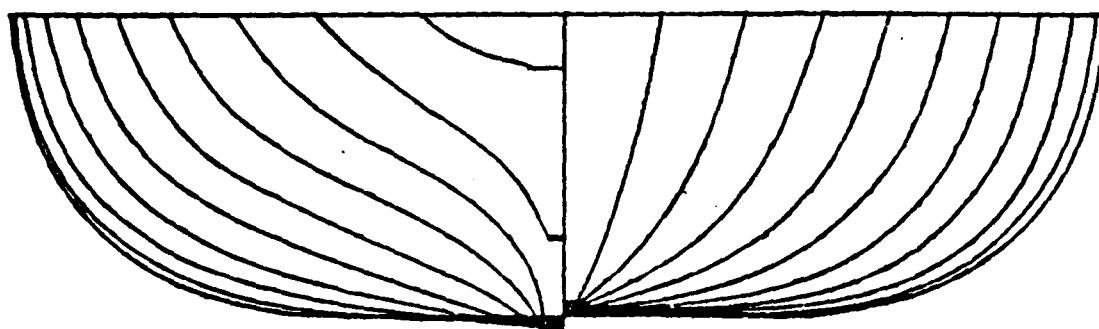
Wigley's
parabolic
hull



HSVA
tanker



'Friesland'
class
destroyer



Cruiser

Figure 6.1 Schematic body plans of four surface ships.

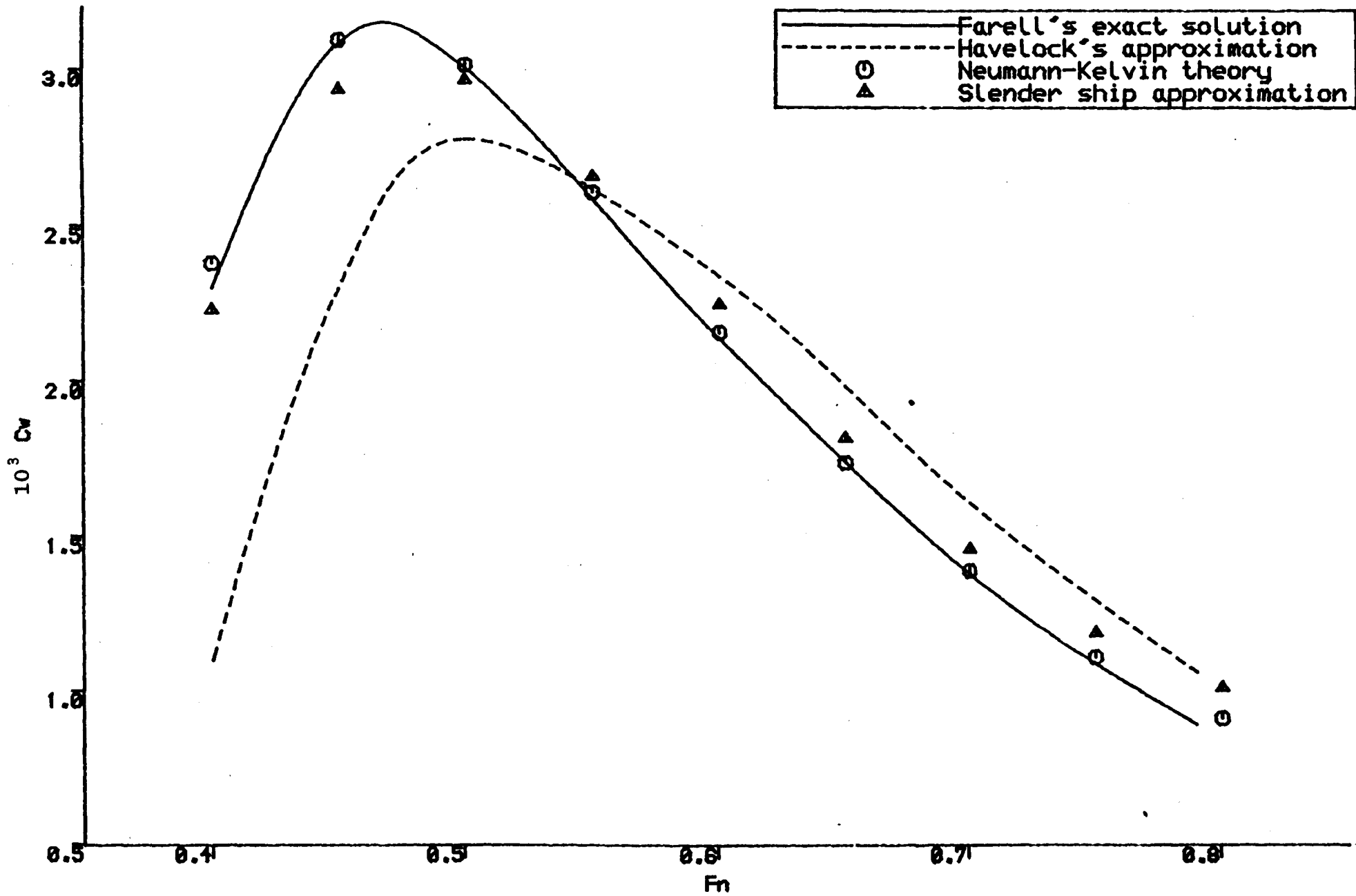


Figure 6.2 Wave resistance of submerged prolate spheroid.

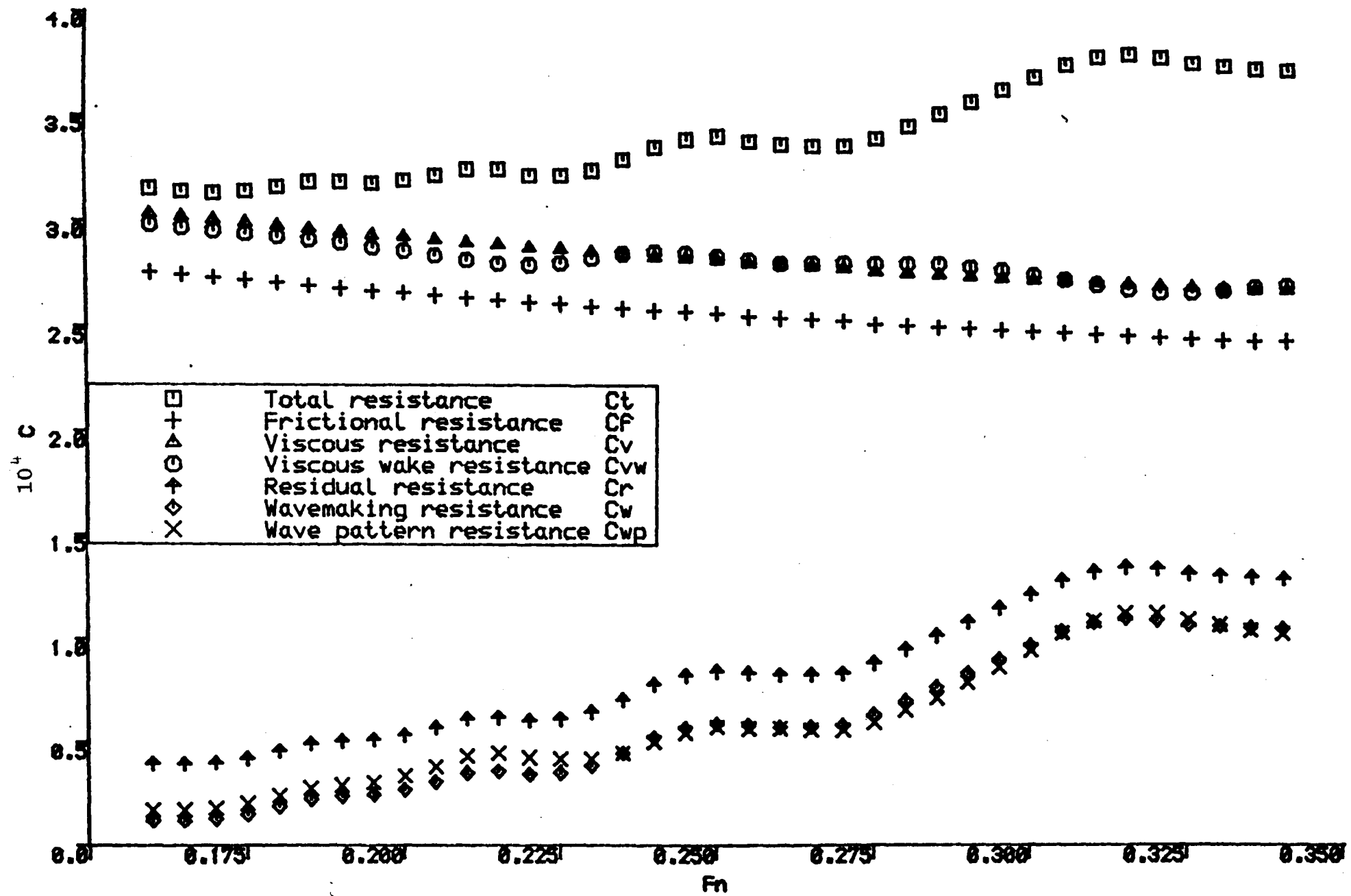


Figure 6.3 Resistance components of Wigley hull as measured by Ju (1983).

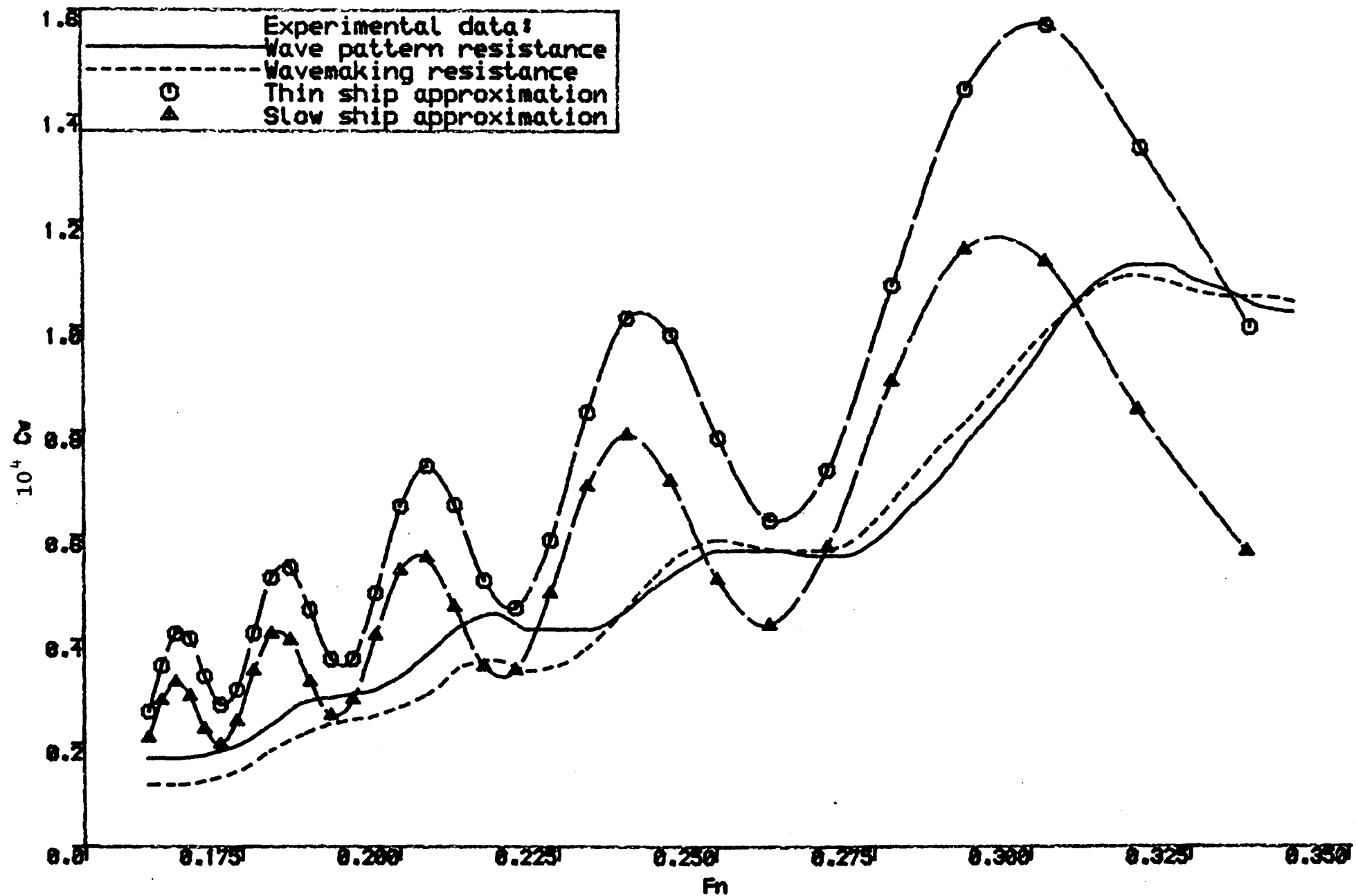


Figure 6.4 Comparison of measured and calculated wave resistance for the Wigley hull.

(a) Thin and slow ship approximations.

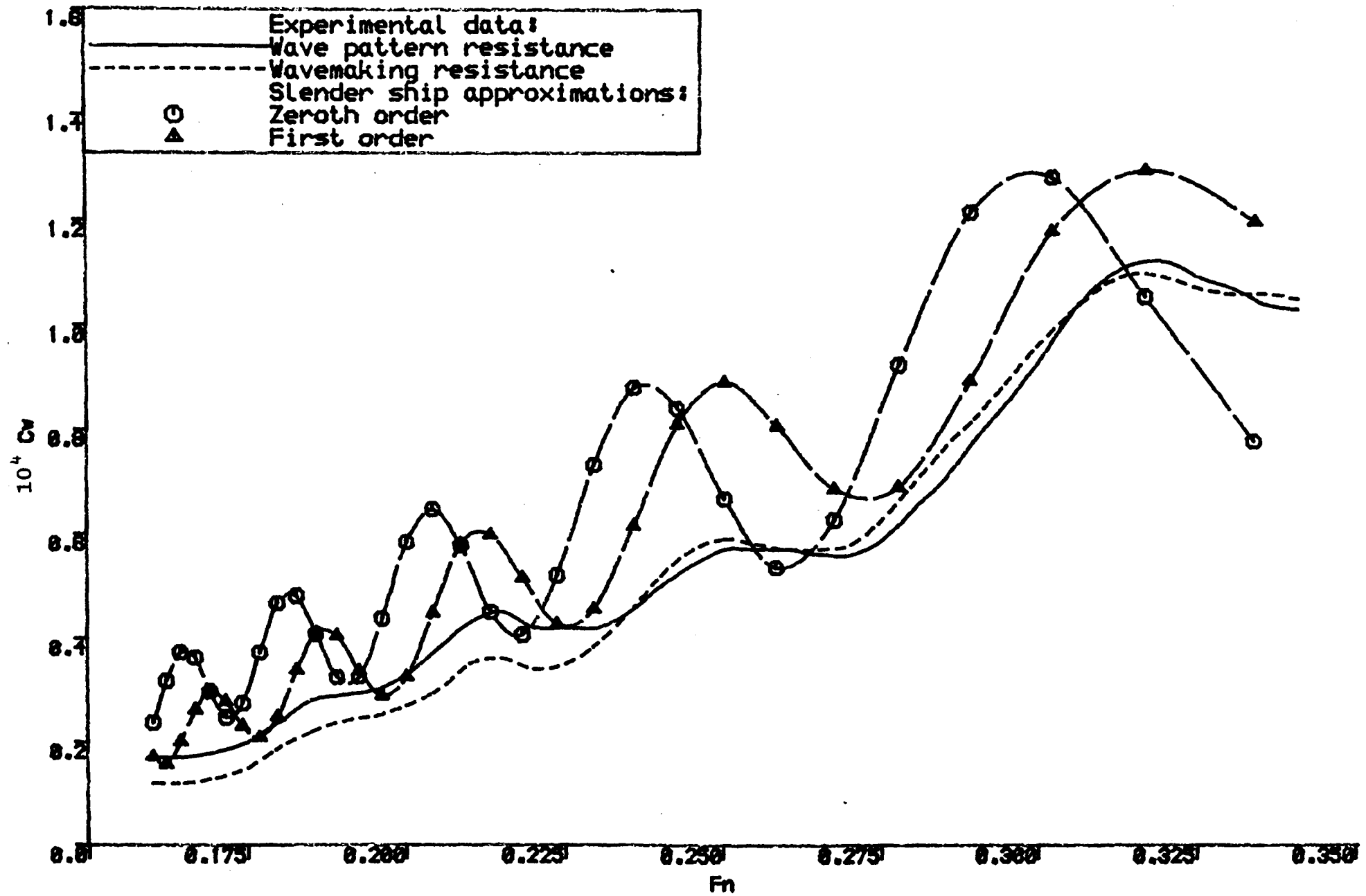


Figure 6.4 Continued. (b) Zeroth and first order slender ship approximations.

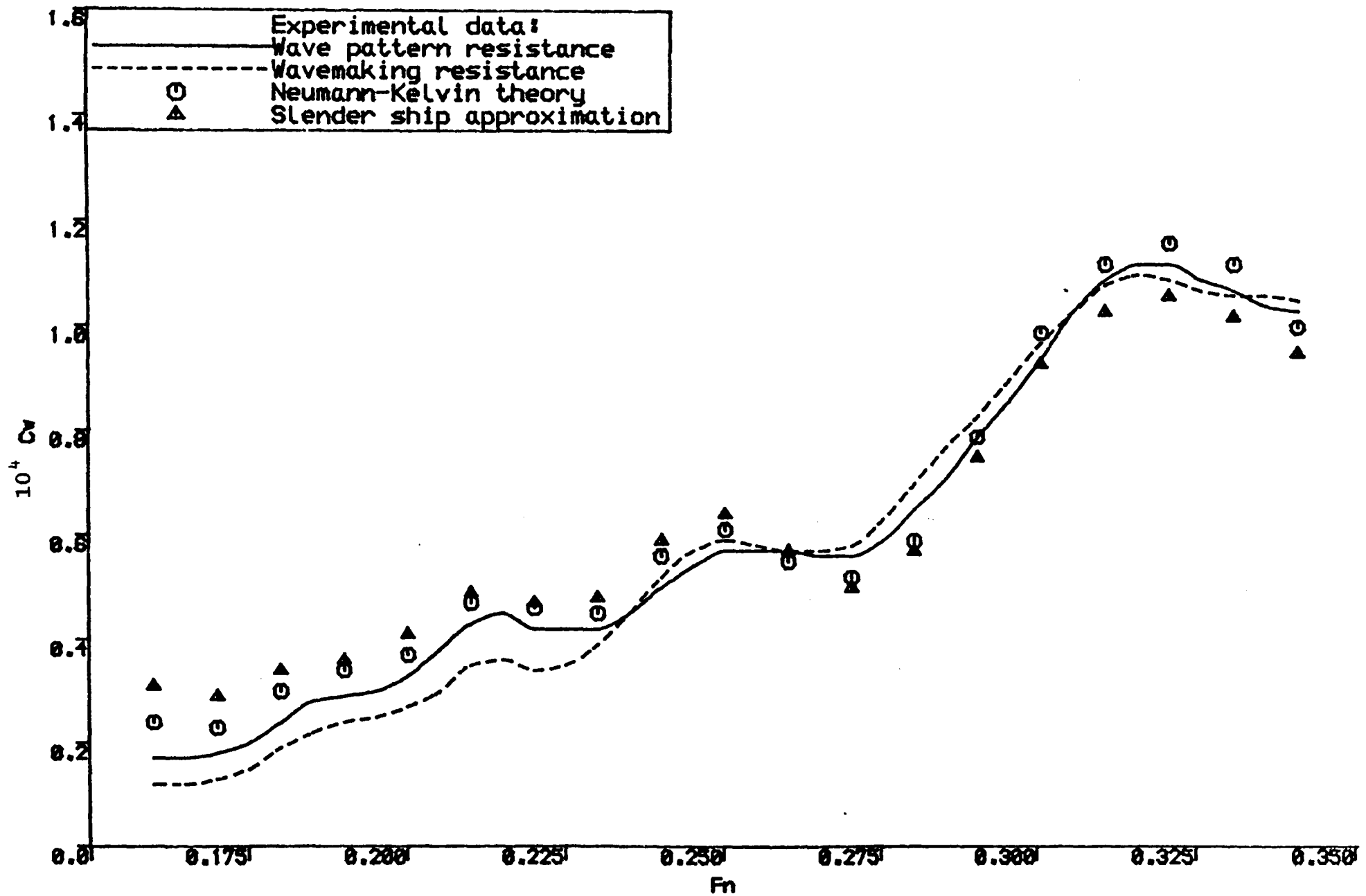


Figure 6.4 Continued. (c) Present calculations.

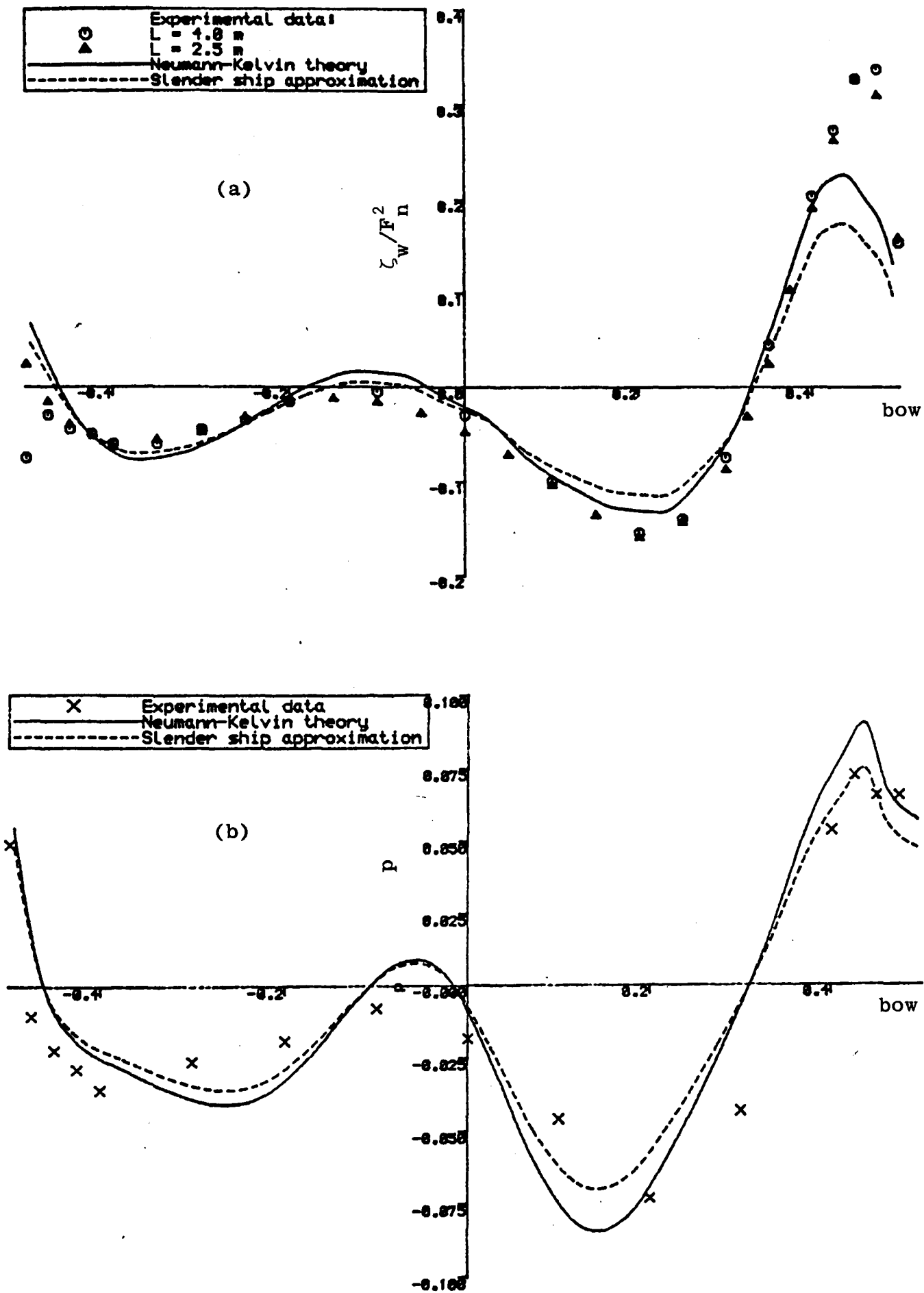


Figure 6.5 Comparison of measured and calculated wave profiles and hull pressures for the Wigley hull at $F_n = 0.316$.
 (a) wave profile
 (b) hull pressure for $z/d = -0.20$

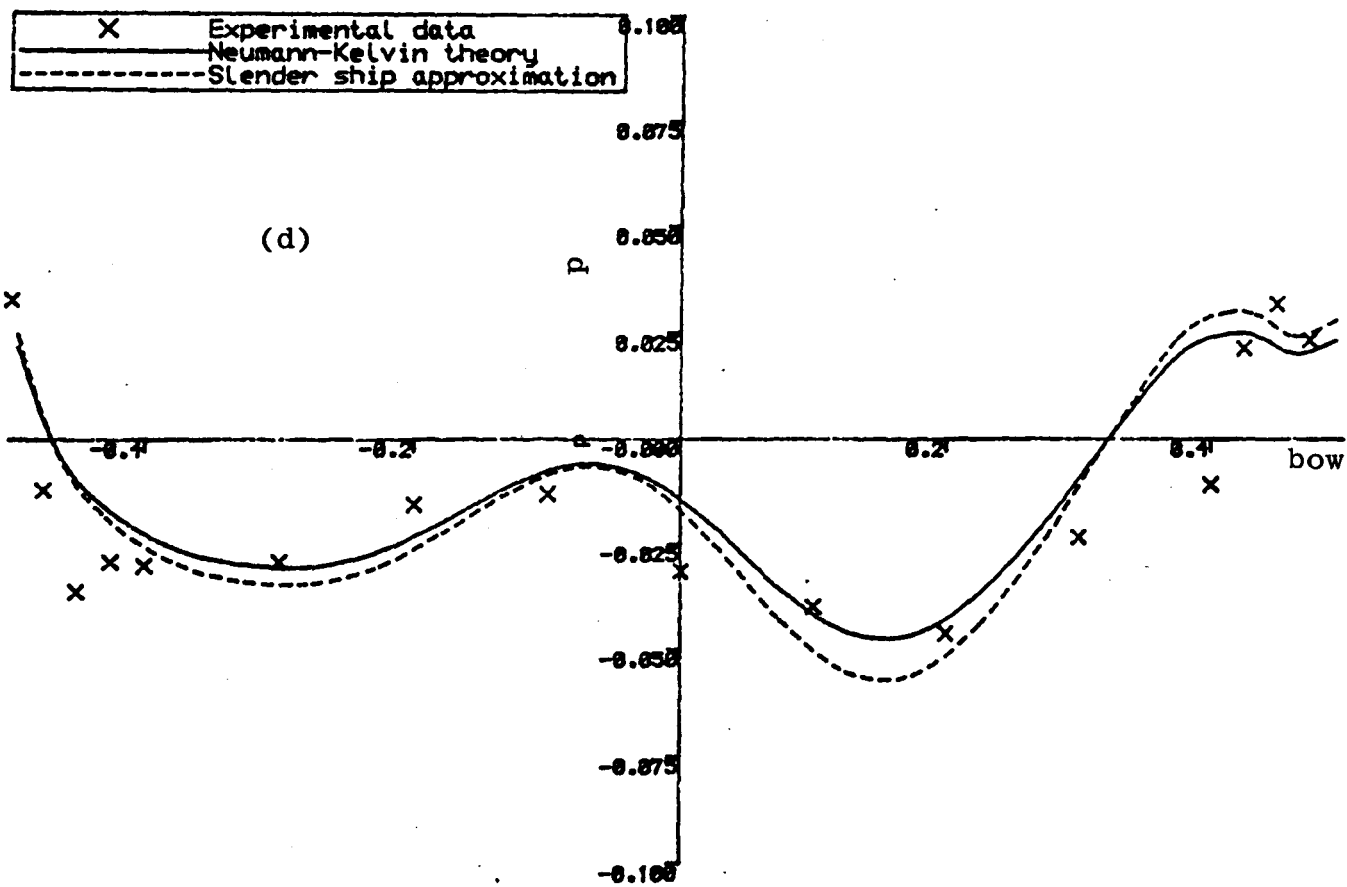
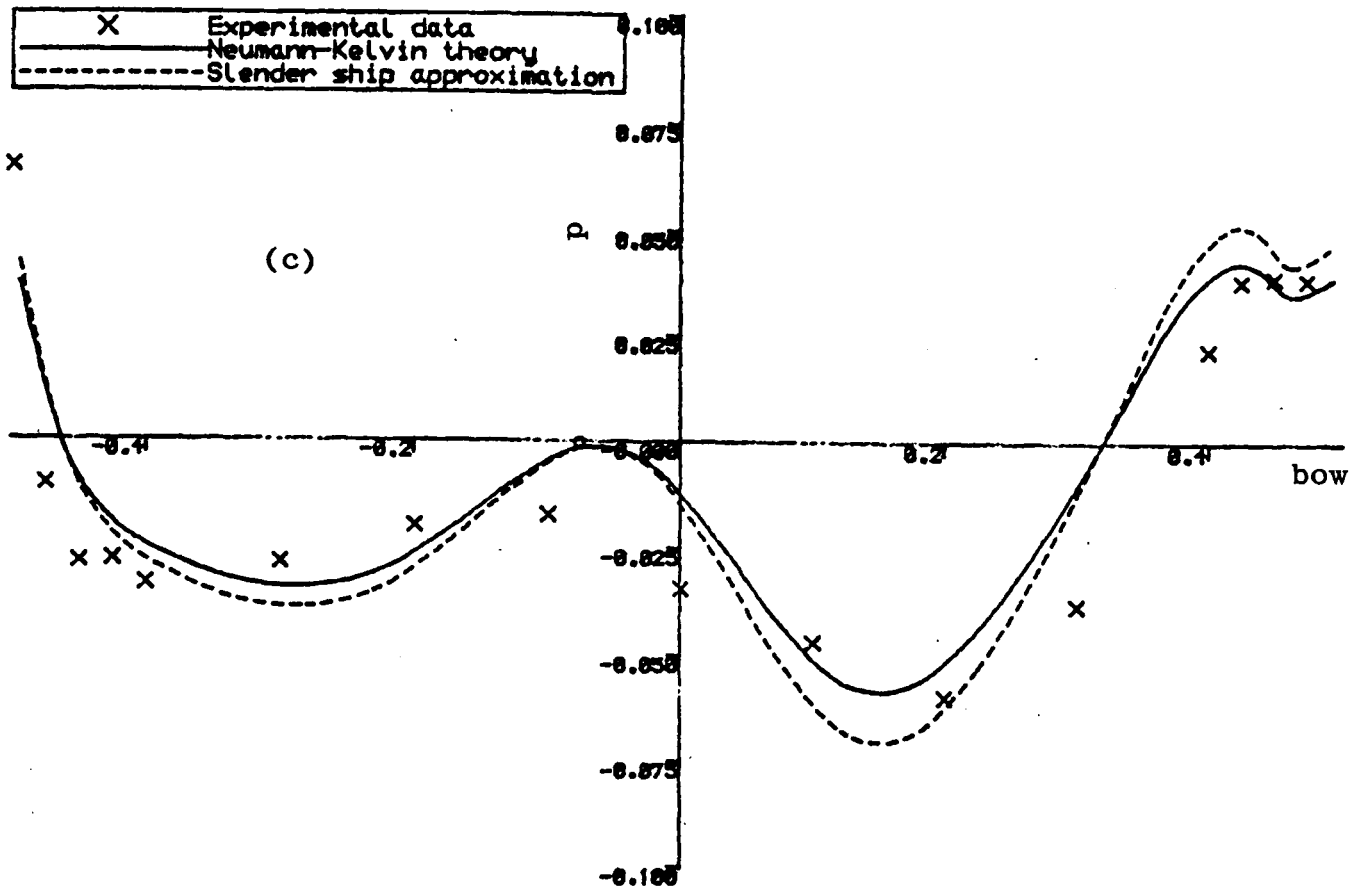


Figure 6.5 Continued.

(c) hull pressure for $z/d = -0.52$

(d) hull pressure for $z/d = -0.84$

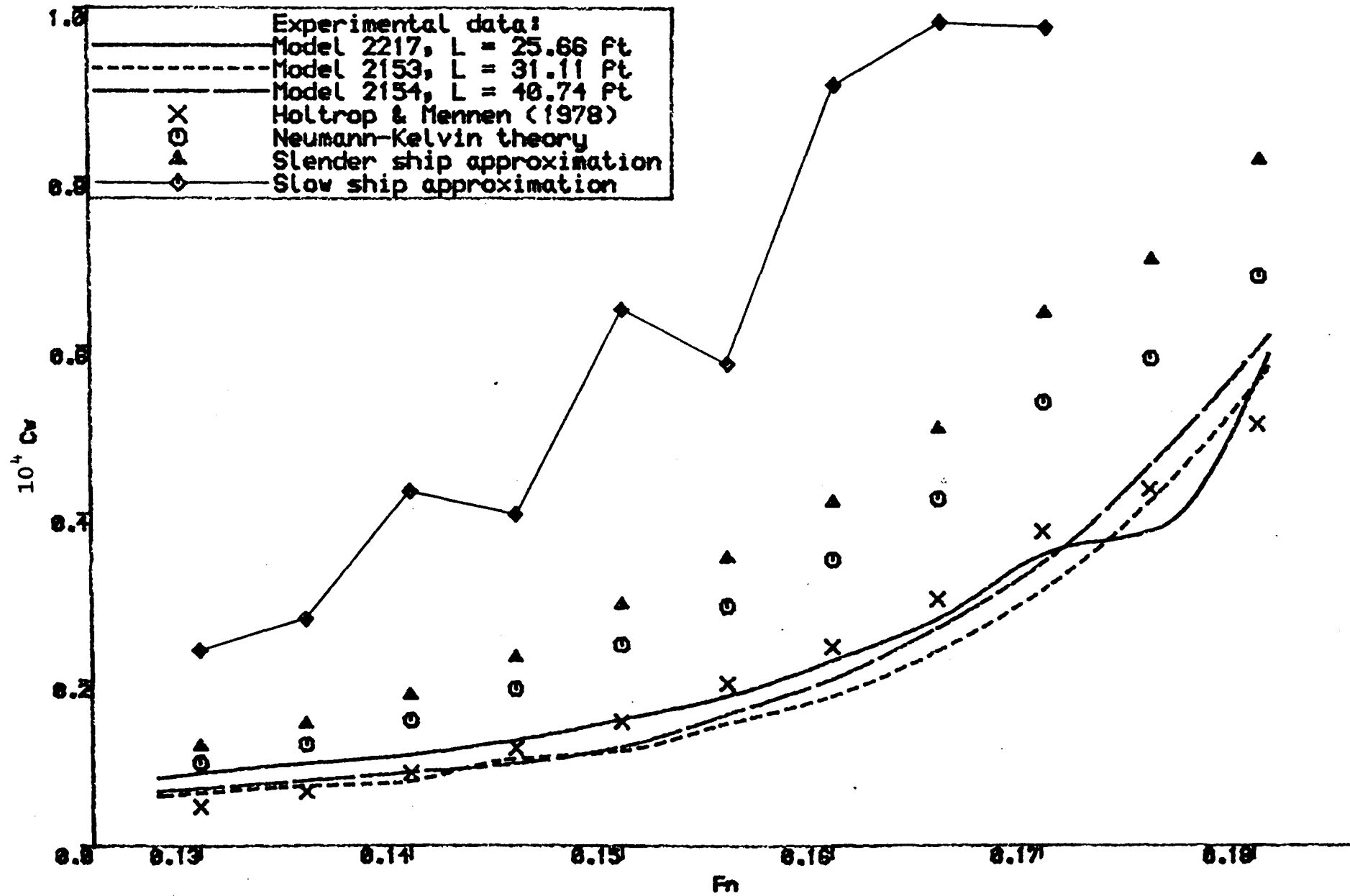


Figure 6.6 Comparison of measured and calculated wave resistance for the HSVA tanker.

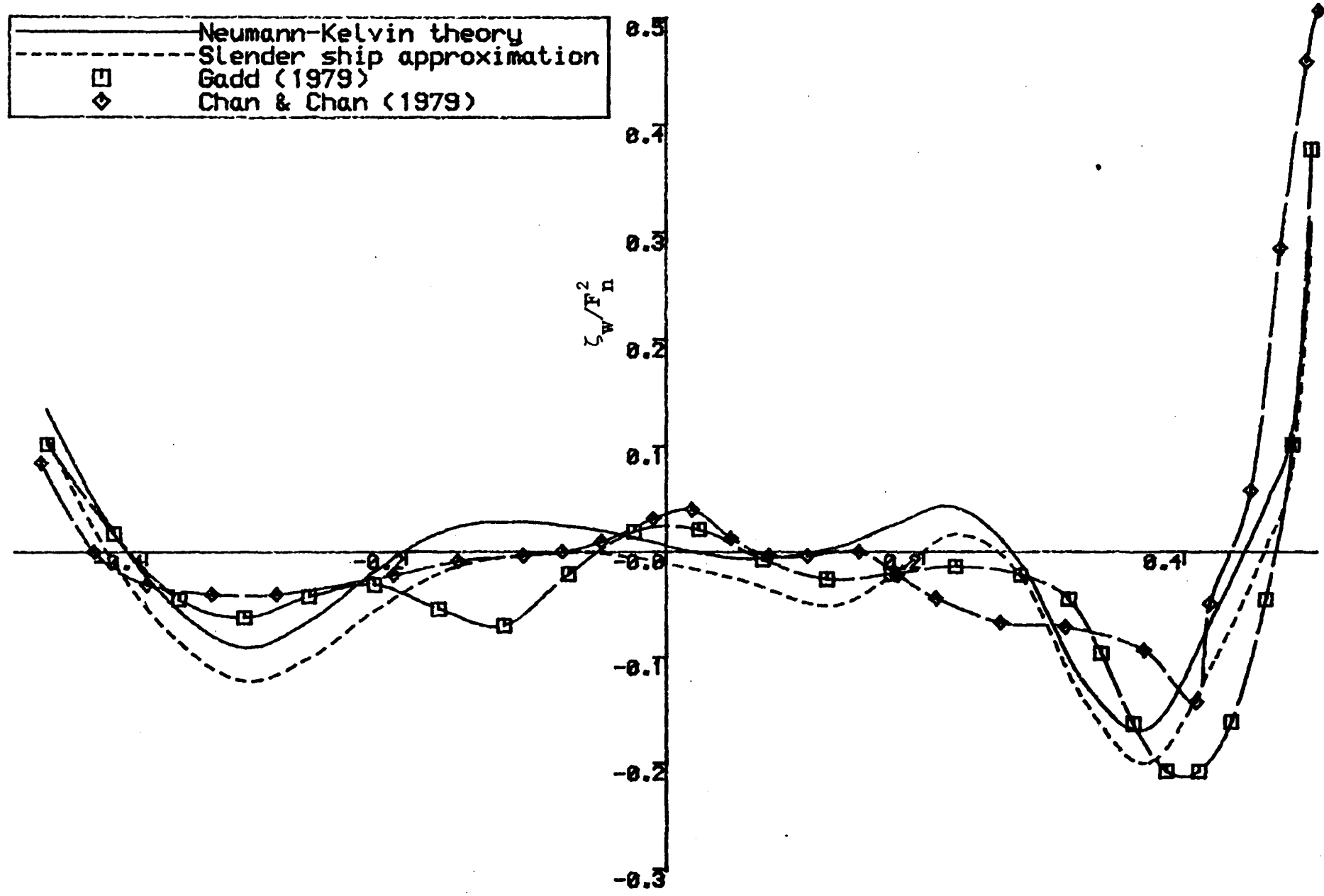


Figure 6.7 Comparison of calculated wave profiles for the HSVA tanker at $F_n = 0.15$.

CROSS-BEAMS CONNECTED TO CARRIAGE STRUCTURE (152 mm x 152 mm x 6.4 mm 'I' SECTION)

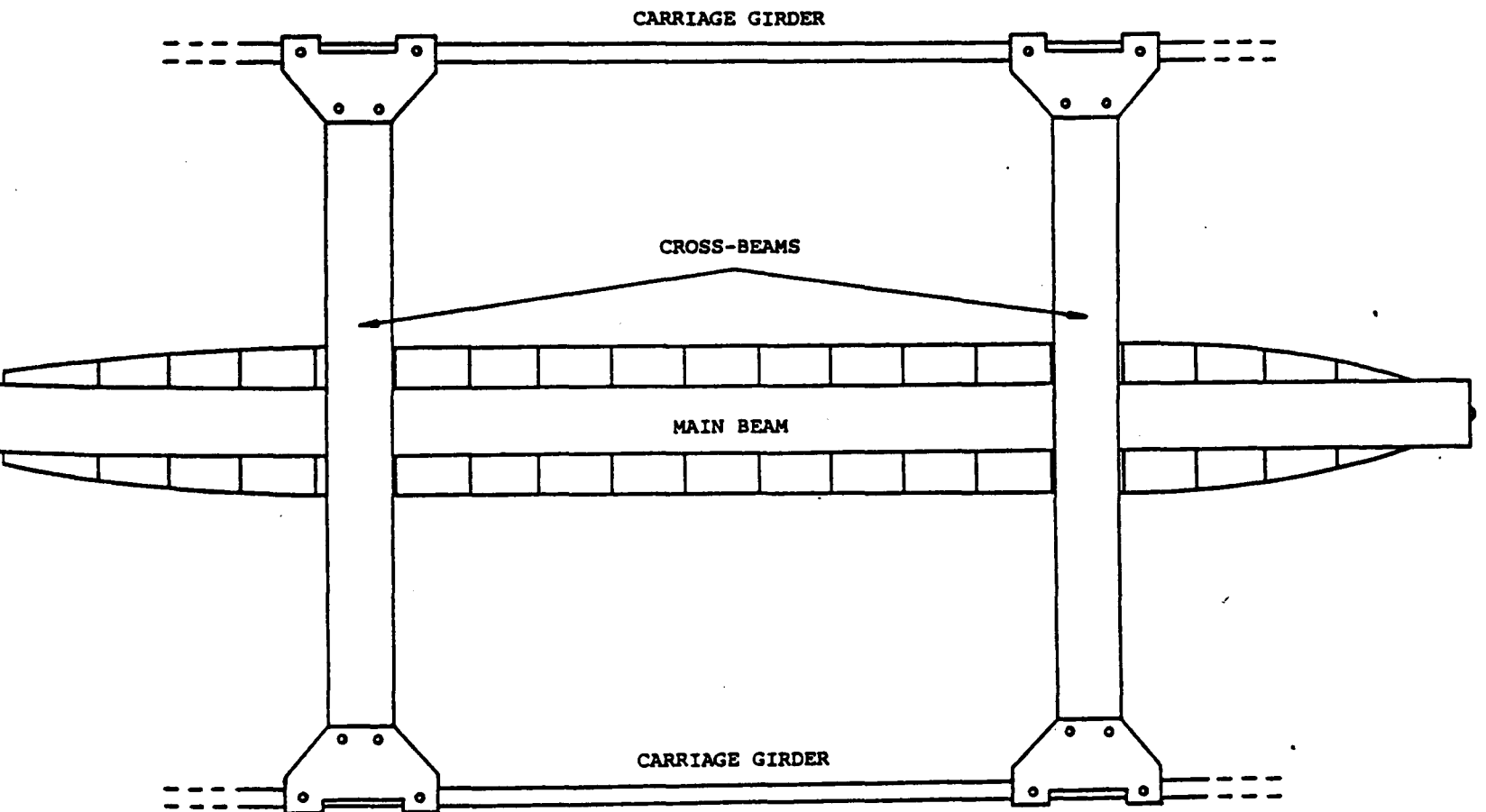
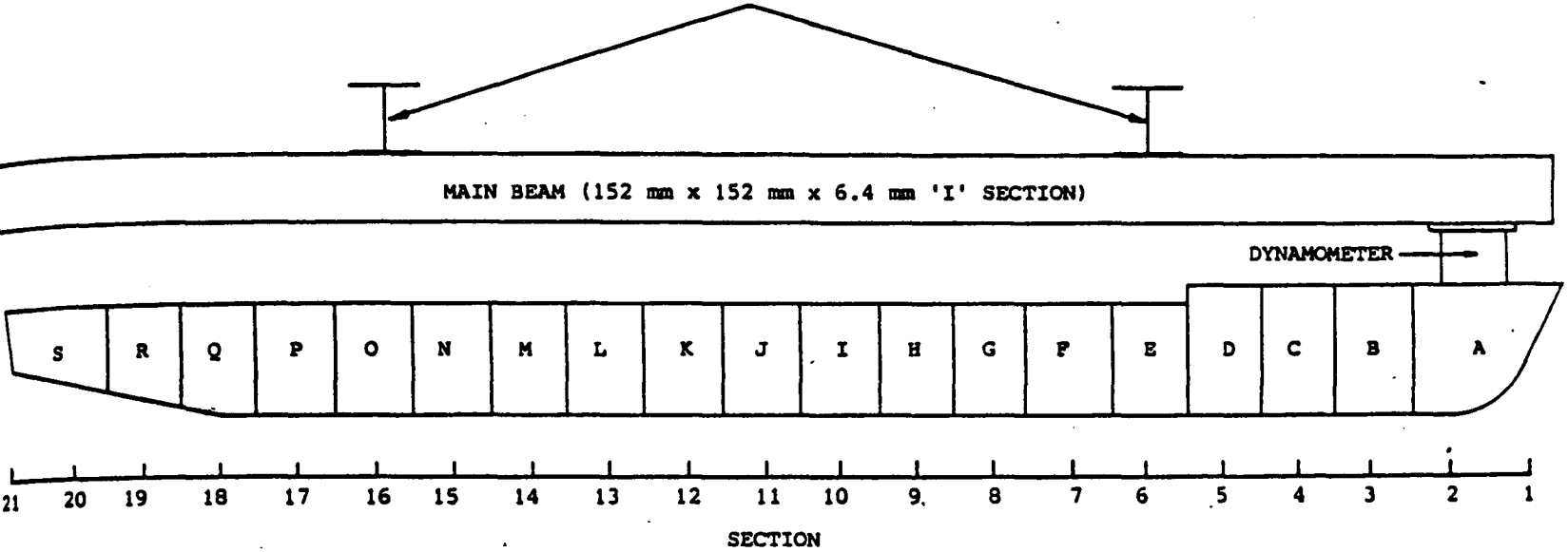


Figure 6.8 Schematic of segments and supporting and model mounting arrangements during 'Friesland' experiments (from Andrew (1985)).

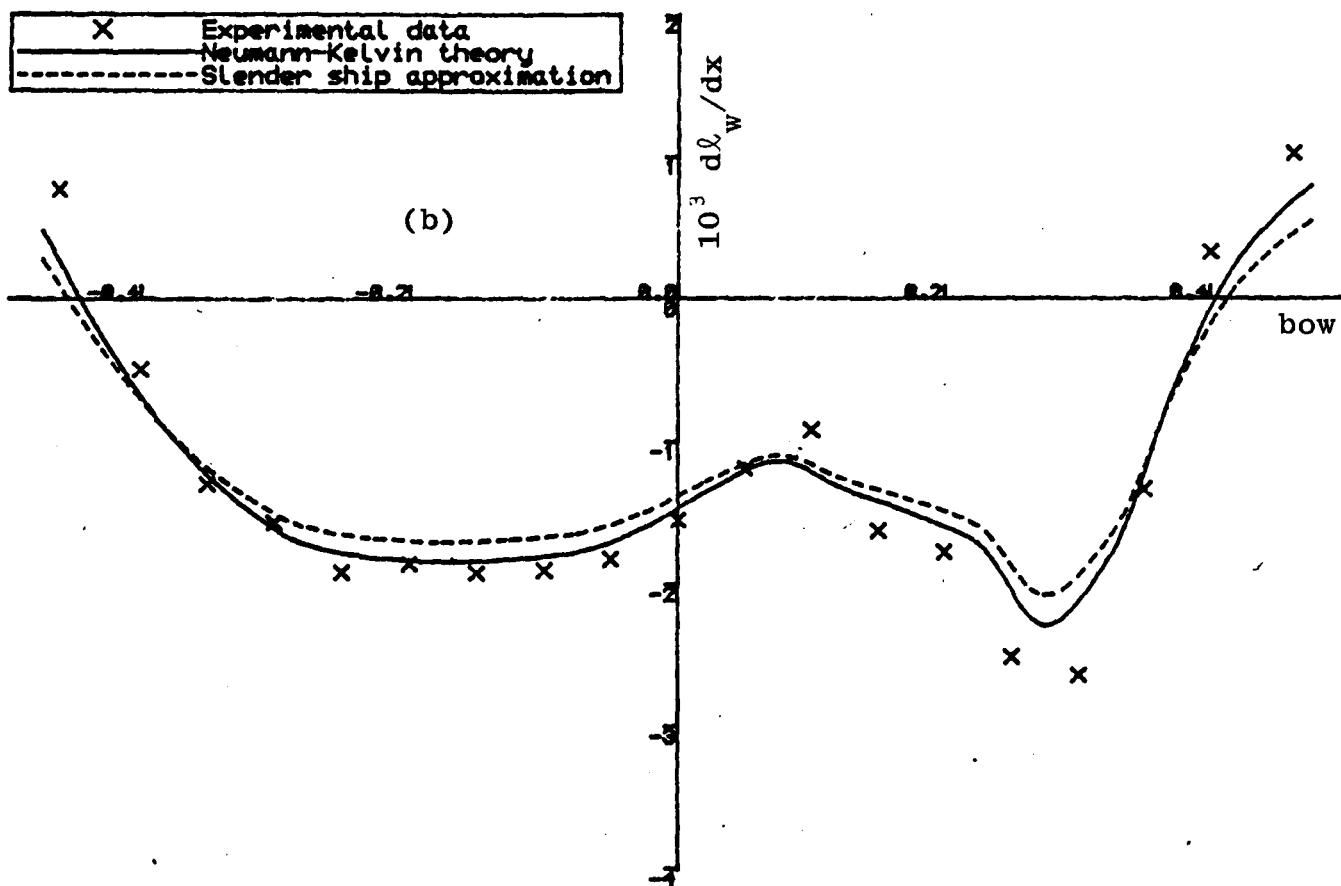
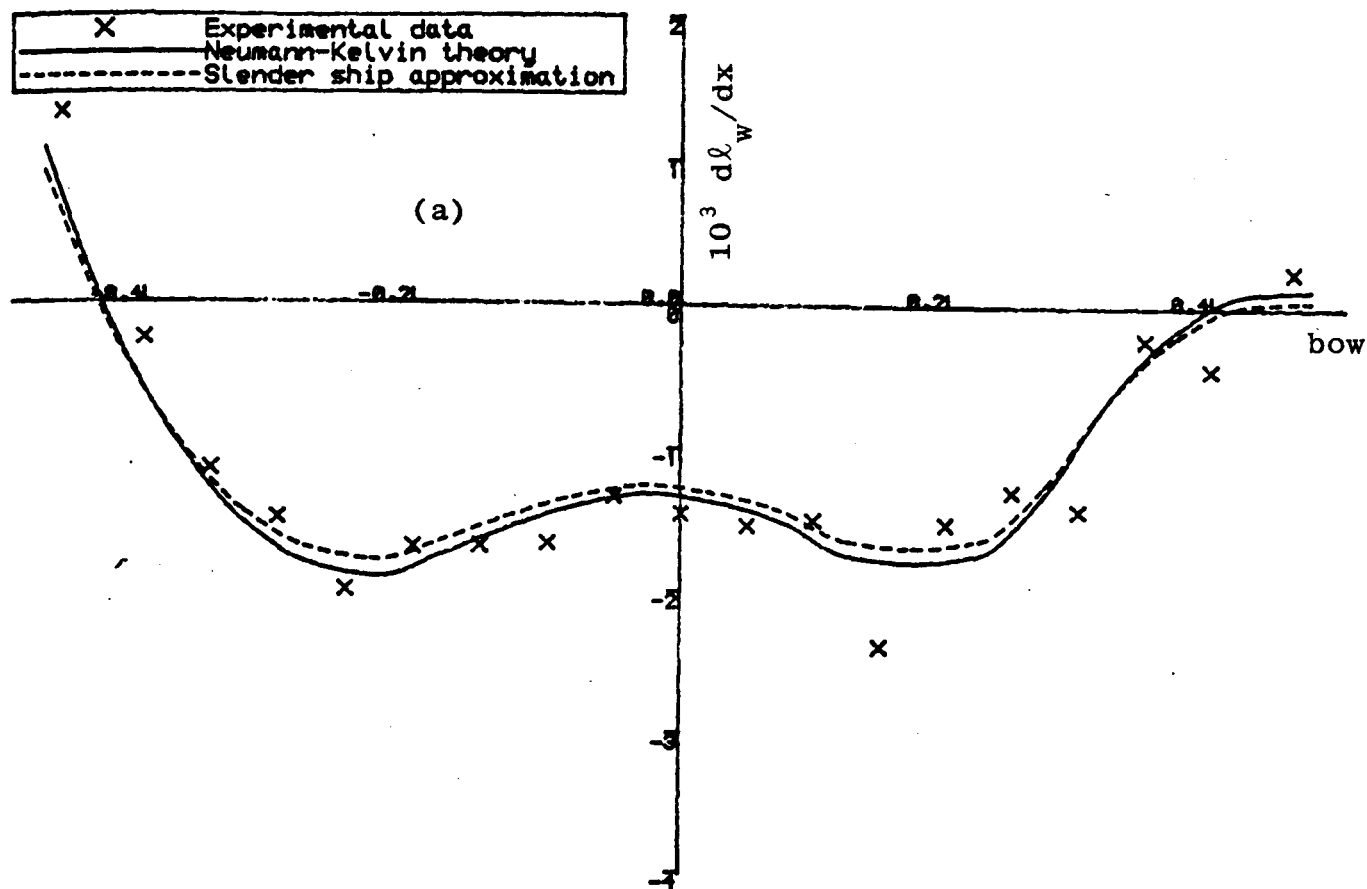


Figure 6.9 Comparison of measured and calculated lift force distributions.

(a) $F_n = 0.15$

(b) $F_n = 0.25$

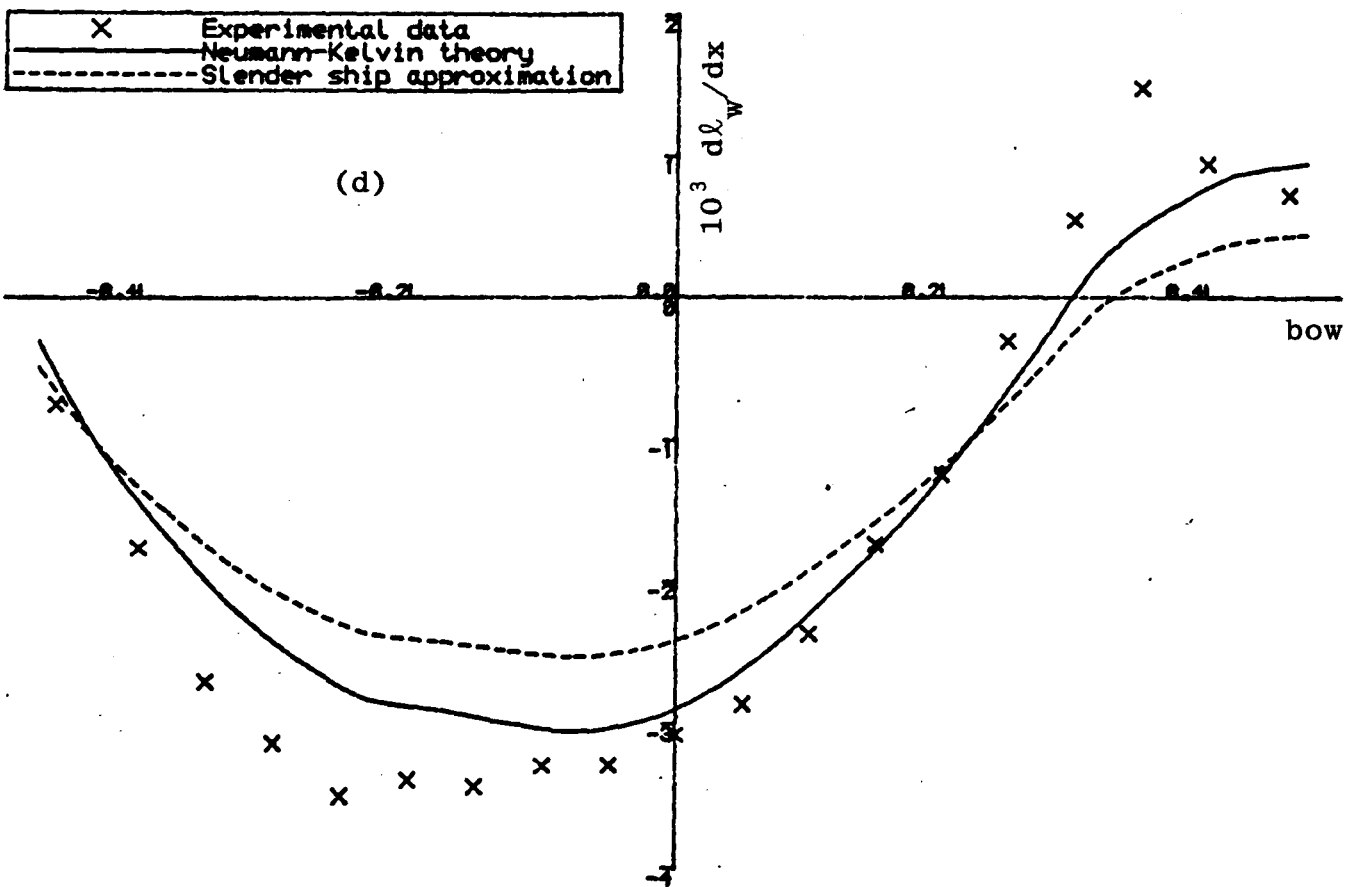
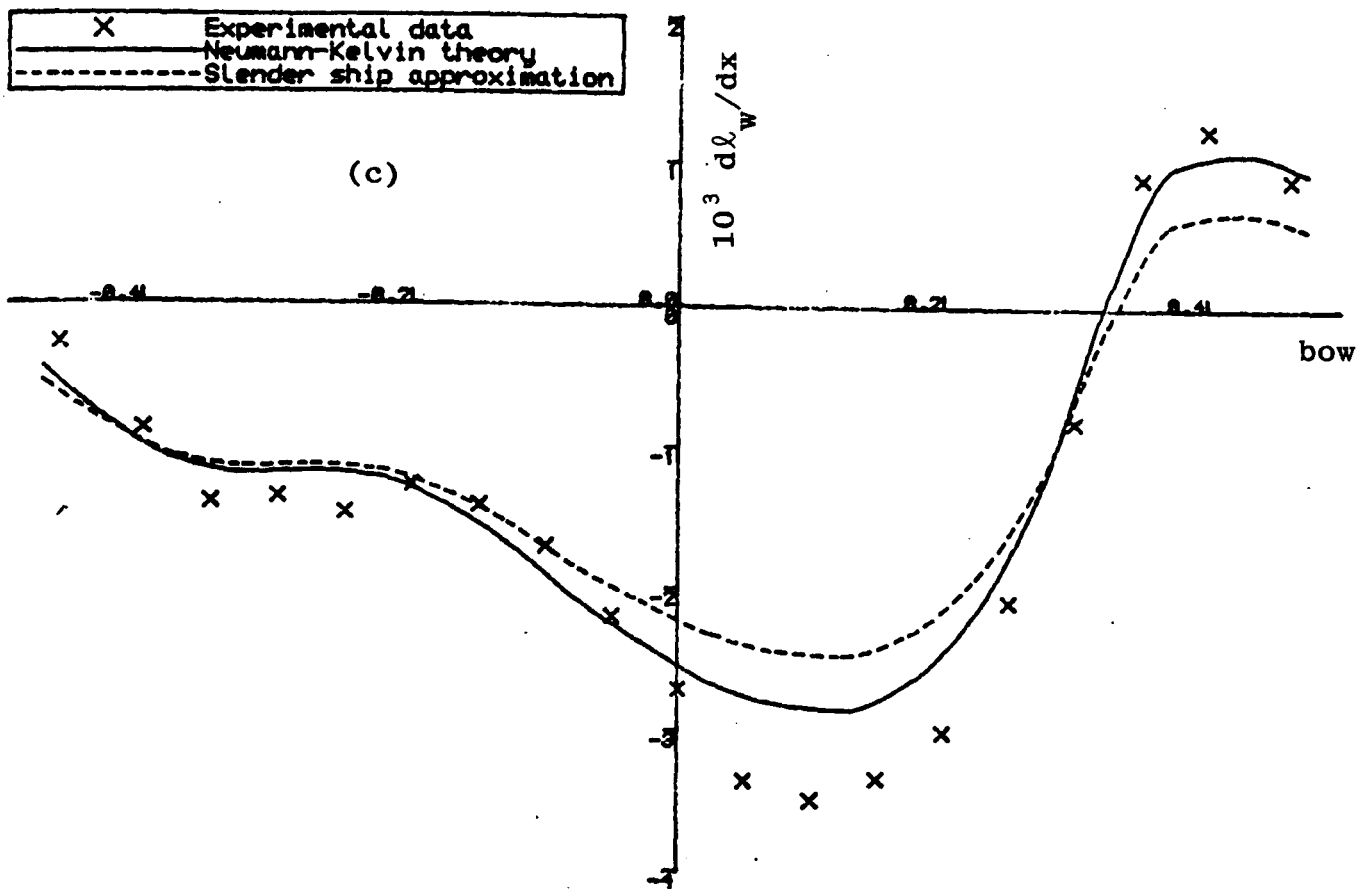


Figure 6.9 Continued.

(c) $F_n = 0.35$

(d) $F_n = 0.45$

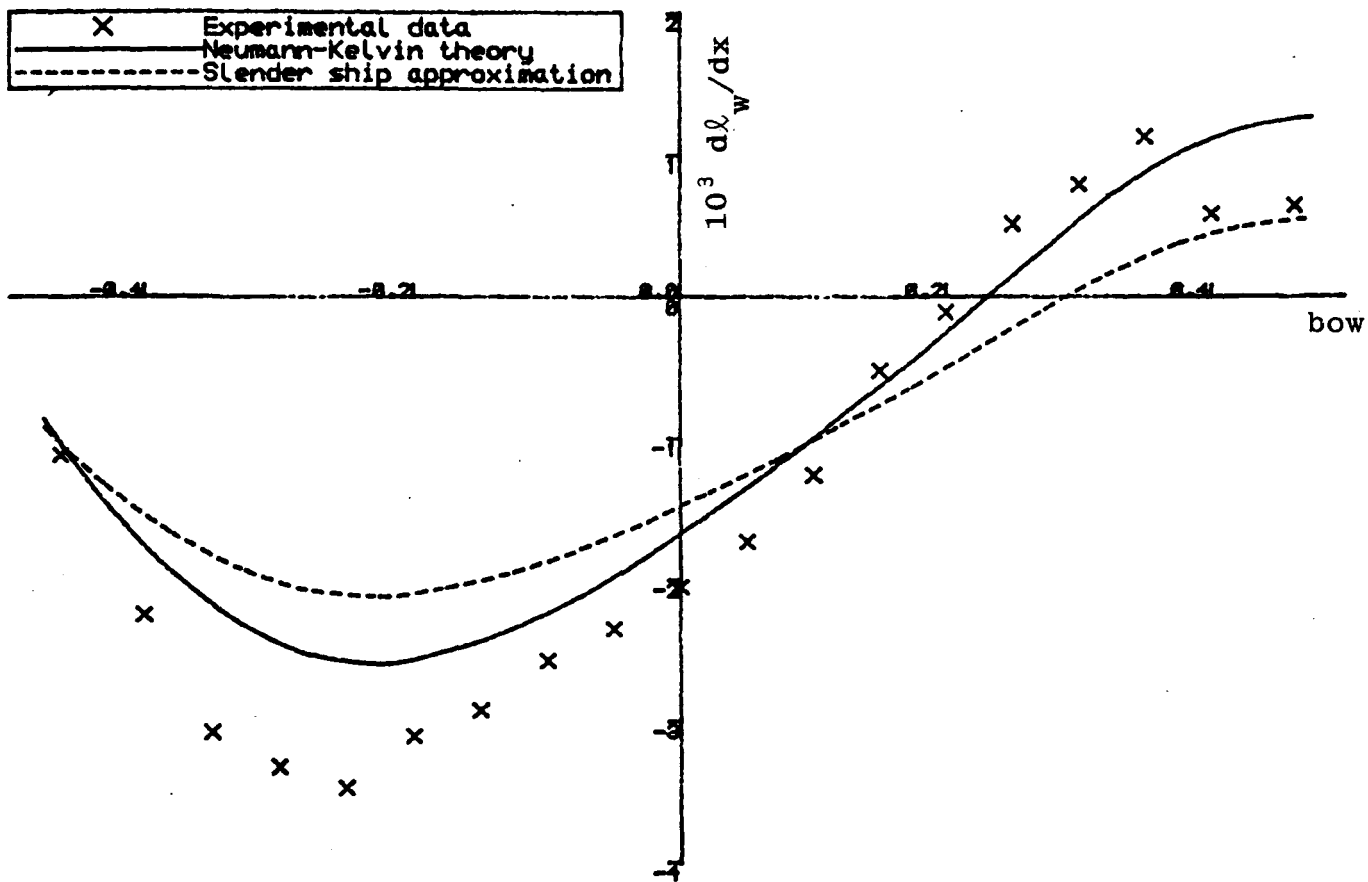


Figure 6.9 Continued. (e) $F_n = 0.55$

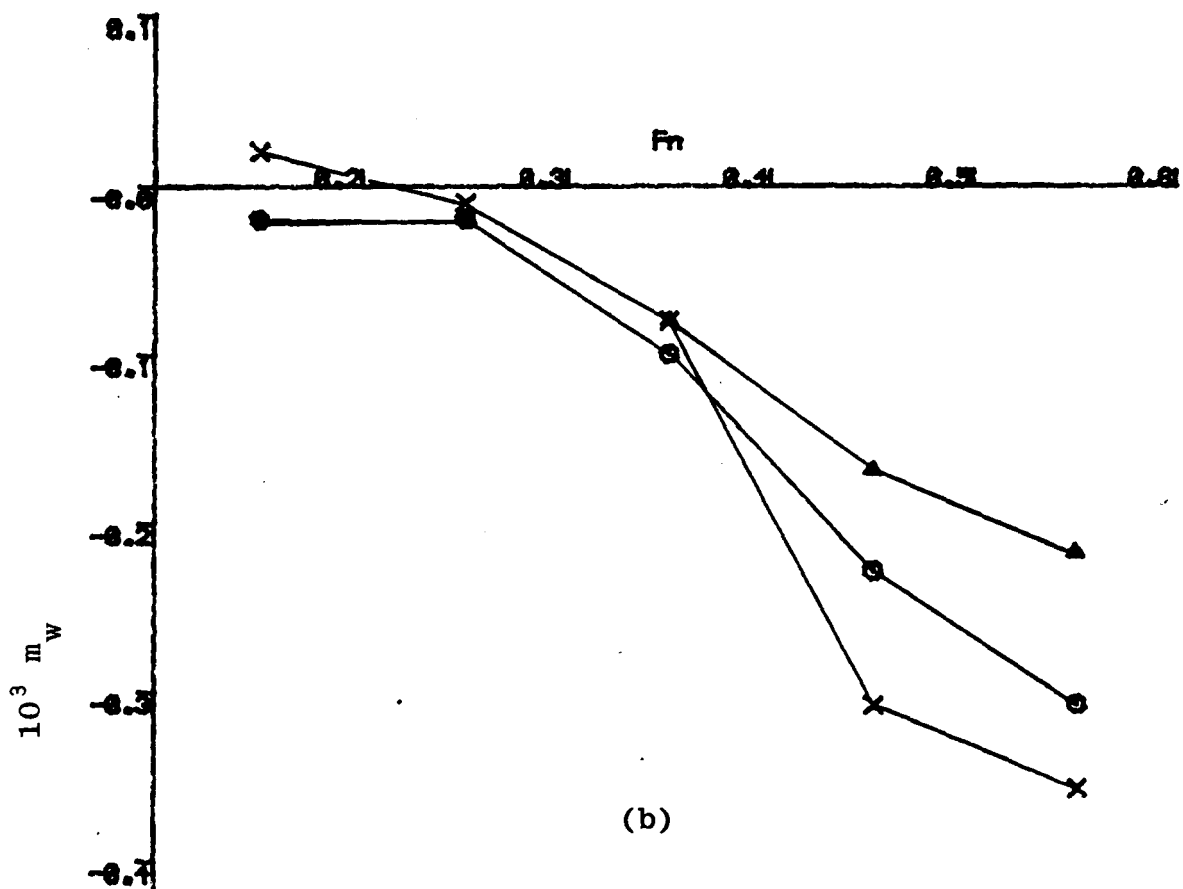
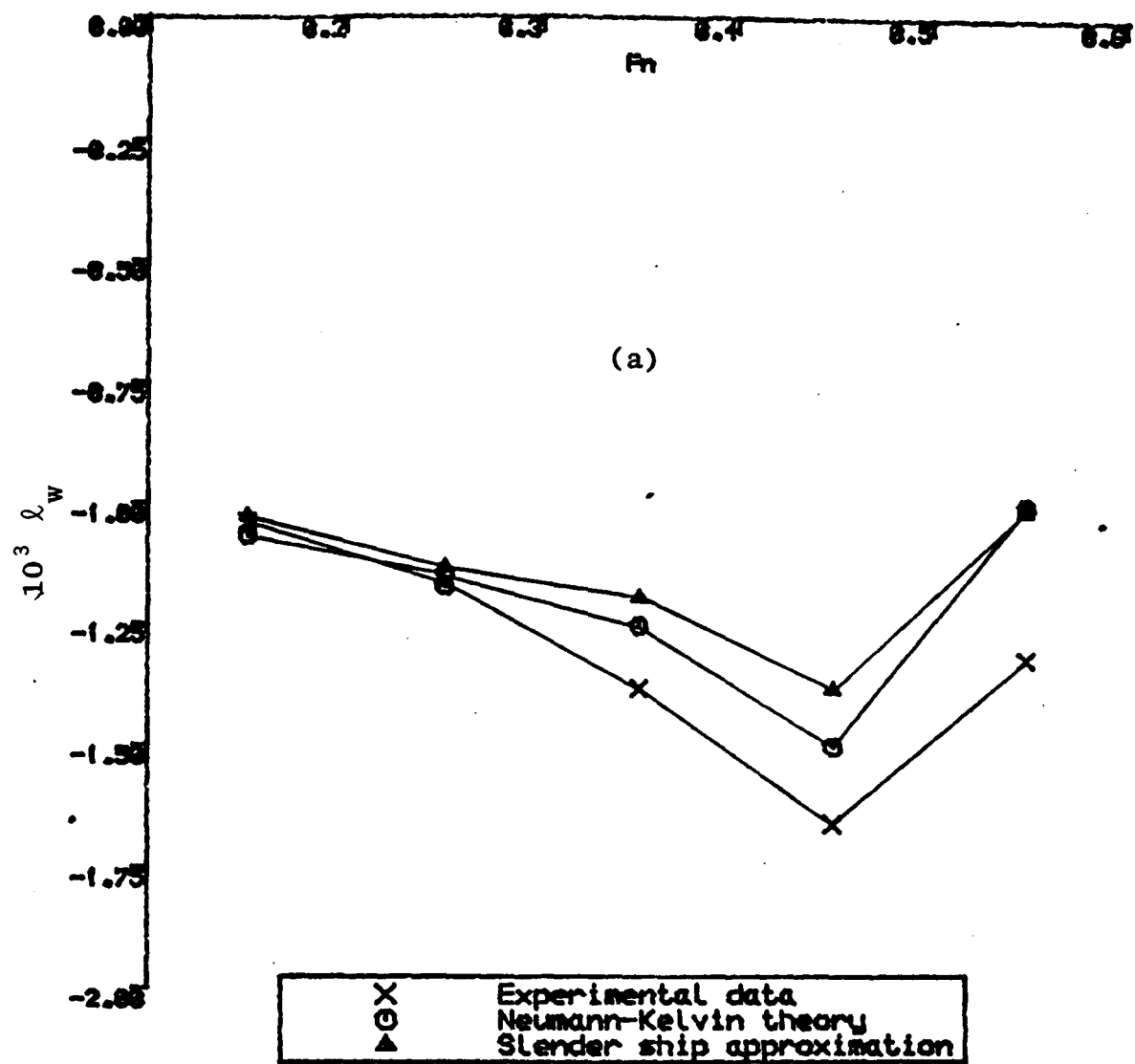


Figure 6.10 Comparison of measured and calculated total lift force (a) and trimming moment (b).

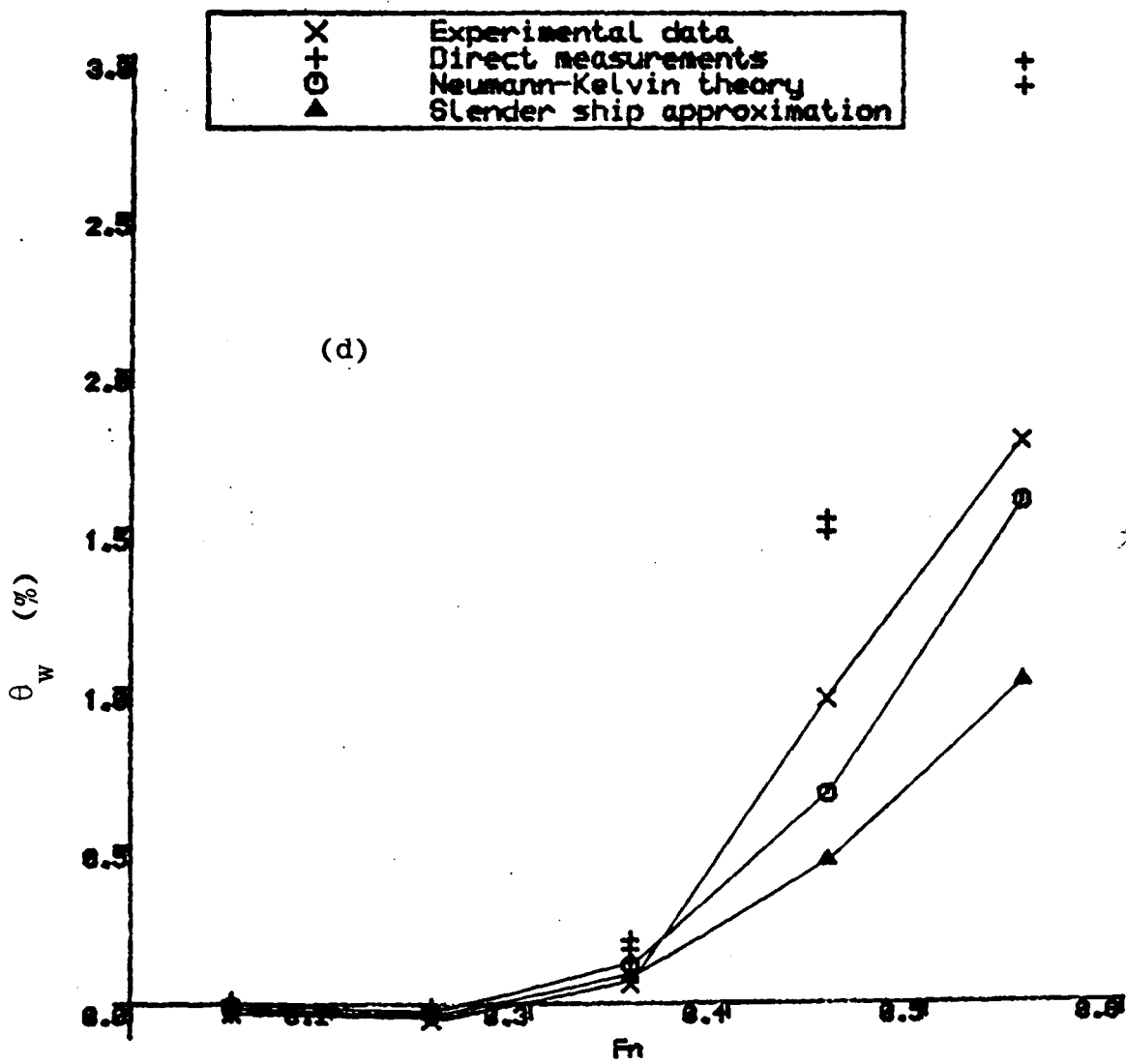
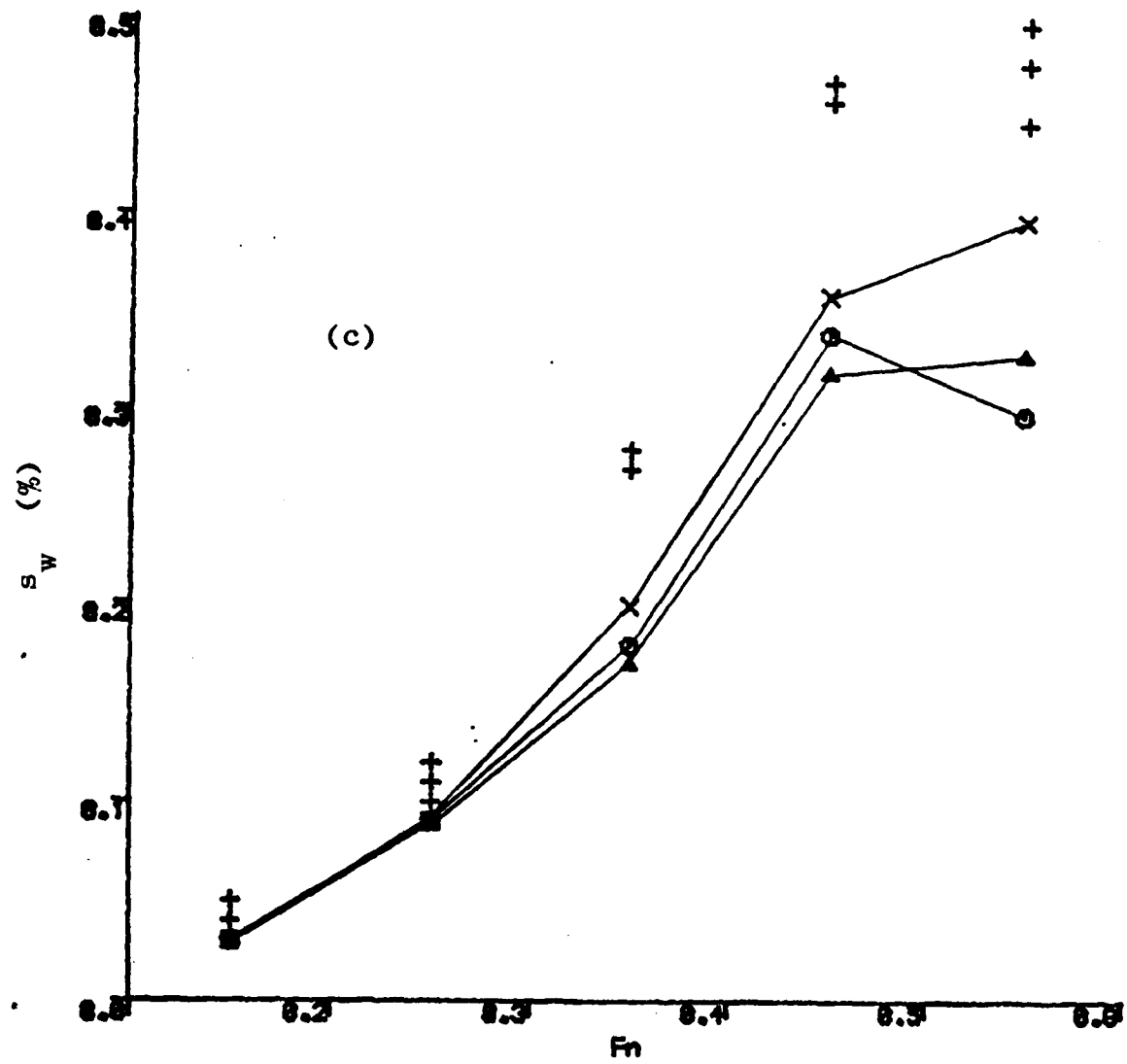


Figure 6.10 Comparison of measured and calculated sinkage (c) and trim by the stern (d).

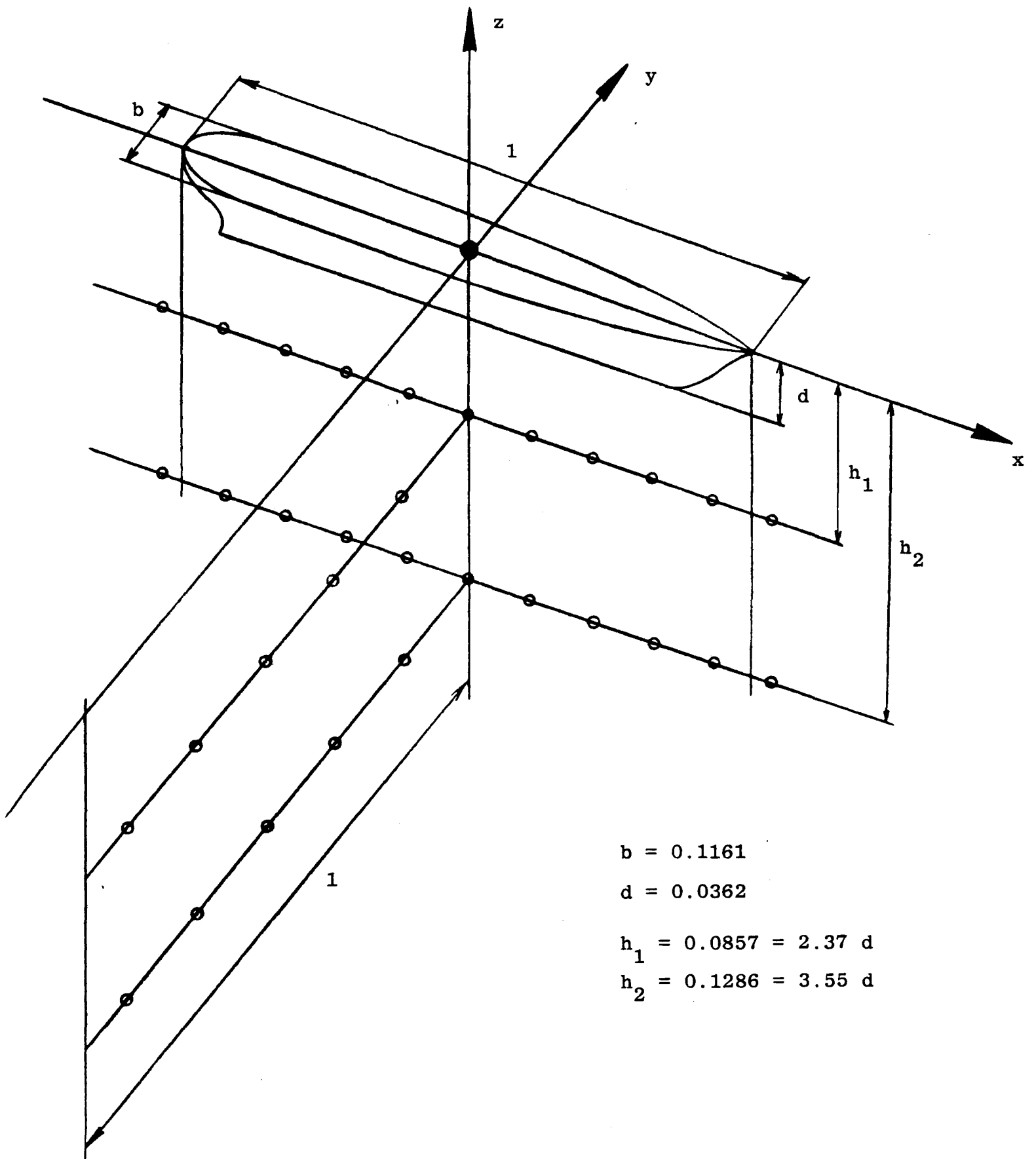


Figure 6.11 Sketch of the pressure measurement positions beneath the cruiser travelling at $F_n = 0.1257$.

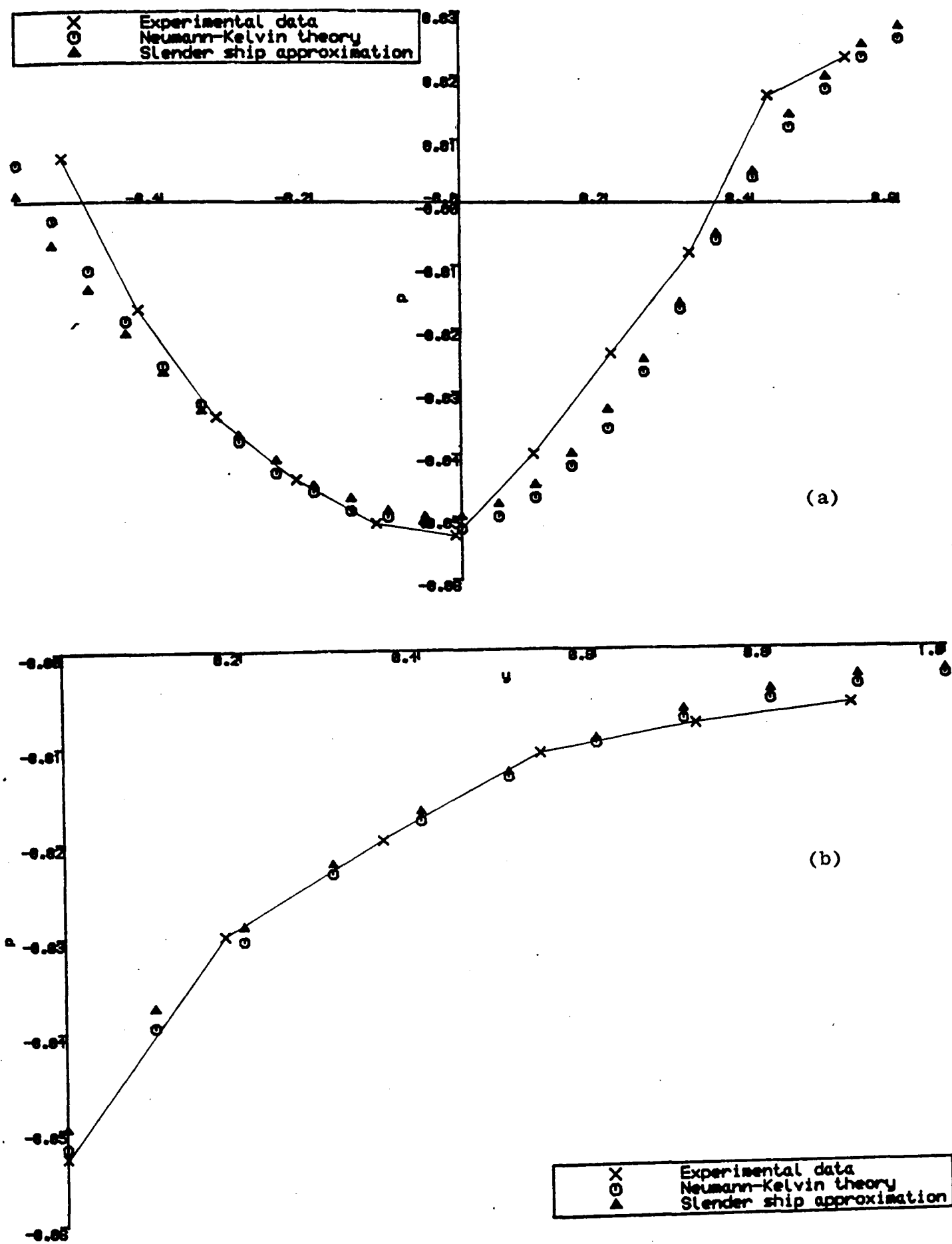
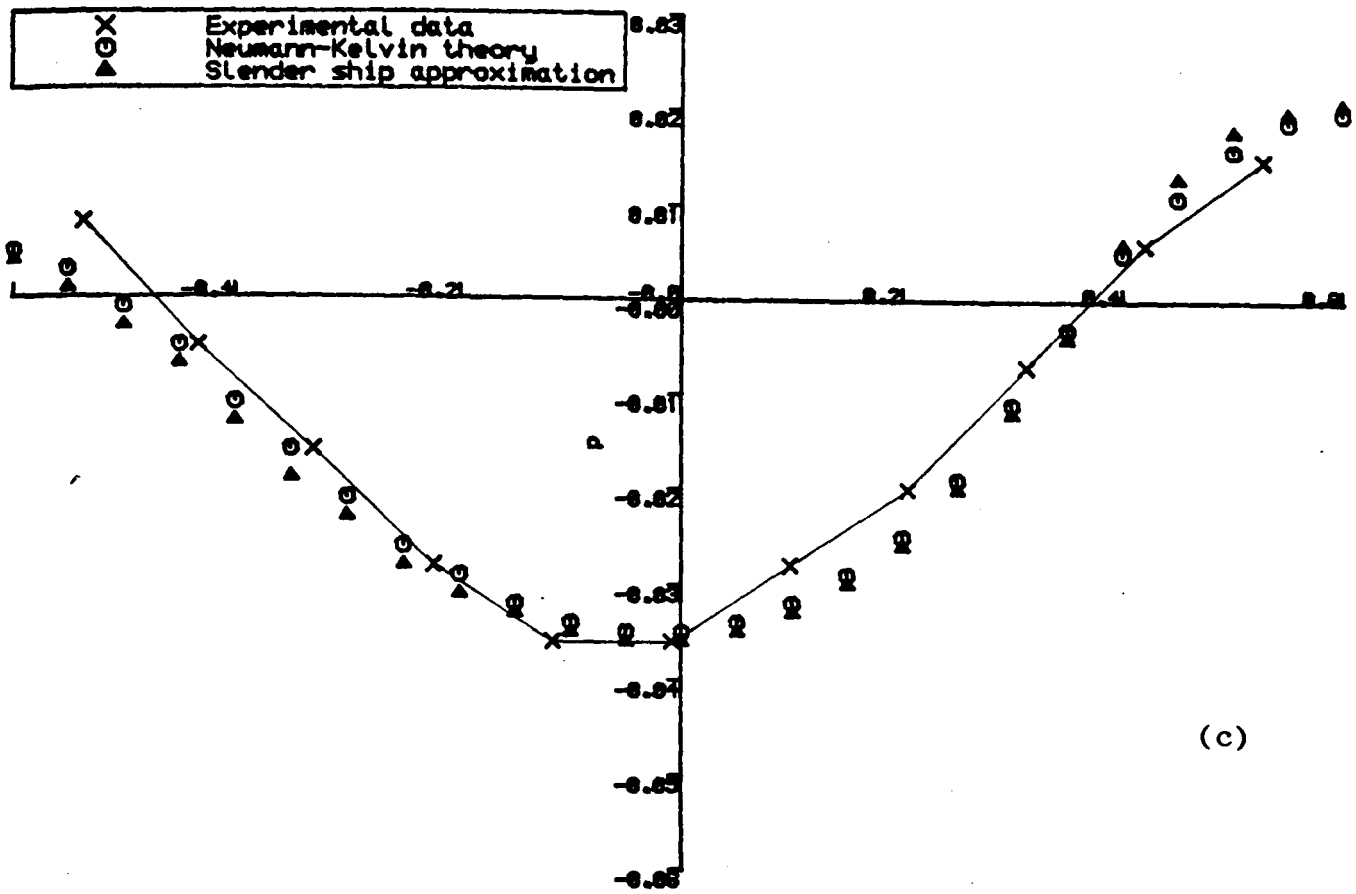
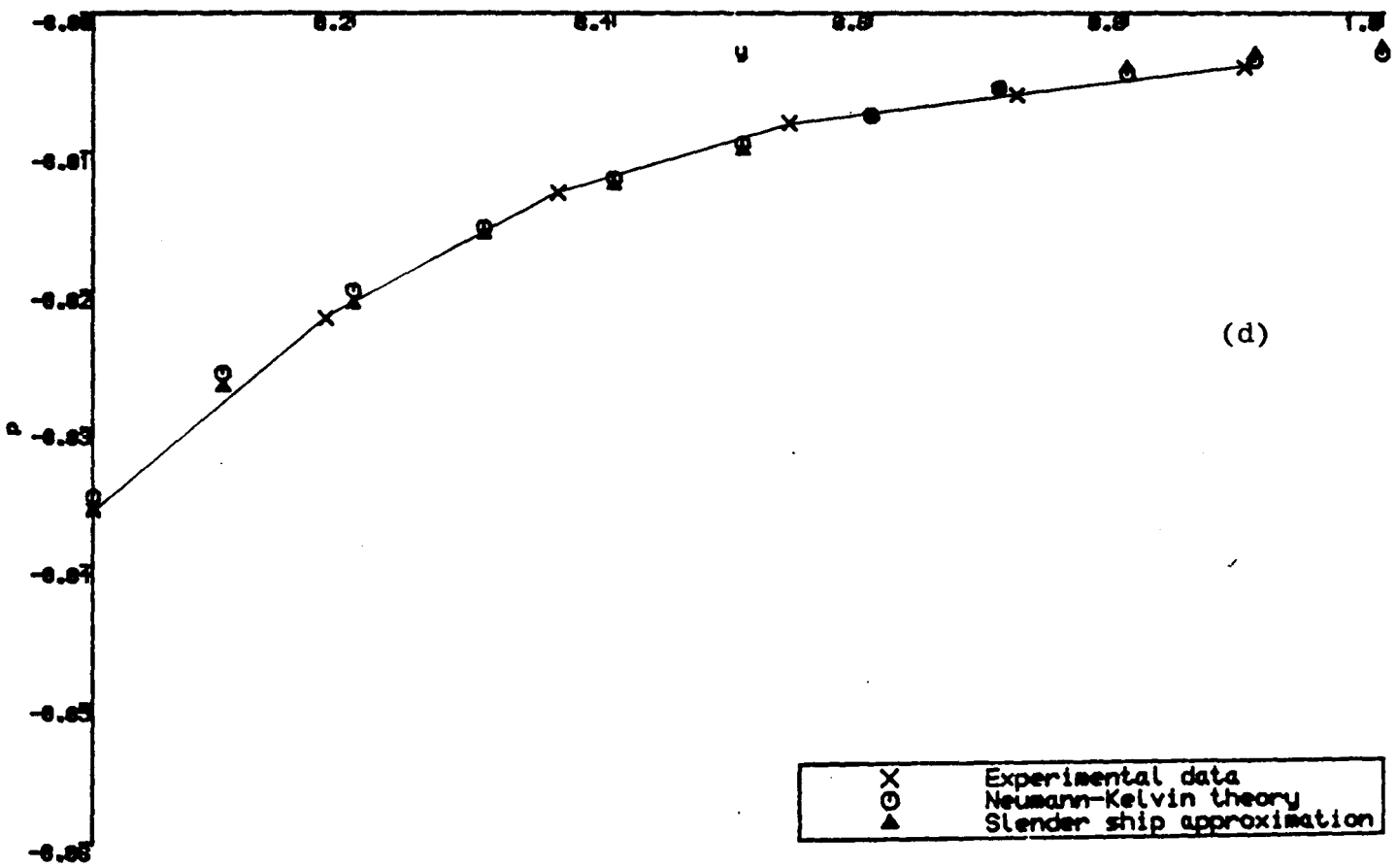


Figure 6.12 Longitudinal keel (a) and transverse amidships (b) pressure signatures for $z/d = -2.37$.



(c)



(d)

Figure 6.12 Longitudinal keel (c) and transverse amidships (d) pressure signatures for $z/d = -3.55$.

7. CONCLUSIONS

As a result of the investigations the following conclusions can be drawn:

- (i) The adopted formulation of the Kelvin wave source potential is very convenient from both physical, mathematical and numerical points of view. Due care is required when evaluating this function in order to avoid unacceptable numerical errors. The nearfield and wavelike disturbance components can be calculated in an accurate and efficient manner by means of Chebyshev and Neumann series expansions respectively. Certain questions regarding the behaviour of the wavelike disturbance in the vicinity of the free surface require further investigation.
- (ii) For an adequate description of the steady ship motion problem the three-dimensional features of the fluid flow and hull geometry cannot be neglected. The transfer of the hull surface condition to the ship's centreplane in the consistent Michell thin ship theory seems particularly inappropriate from this point of view and may be more restrictive than the linearisation of the free surface condition.
- (iii) The use of the inconsistent Neumann-Kelvin approximation can be justified from a practical point of view when the ship-

generated free surface disturbance is sufficiently small. This assumption is usually violated in the vicinity of the ship's bow where the quality of the theoretical predictions of the wave profile and hull pressures deteriorates, but this does not affect significantly the theoretical predictions of the wave resistance and other global flow parameters for ships which are sufficiently slender and operate at low to moderate values of the Froude number.

- (iv) The solution of the Fredholm integral equation for the source strength is rendered superfluous by adopting the explicit slender ship approximation, where the source strength is approximated by the perturbed normal hull velocity. This approximation should only be used however for ships with low block coefficients operating at low Froude number.
- (v) The quantitative agreement between the experimental data and theoretical predictions becomes less satisfactory when the ship is full-bodied. This is probably due to a combination of nonlinear free surface effects and viscous interaction effects. Further detailed comparisons with experimental data are required in order to assess the capability of the Neumann-Kelvin theory in this respect.
- (vi) At high Froude numbers the quality of the theoretical predictions is less satisfactory and a nonlinear flow description incorporating the dynamic effects of sinkage and trim might

be required. In particular, when calculating the sinkage and trim at high ship speeds, the application of the hull surface boundary condition at the mean position of the hull is no longer acceptable and an iterative procedure is required to determine the sinkage and trim.

APPENDIX

EVALUATION OF SPECIAL FUNCTIONS

THE EXPONENTIAL INTEGRAL

Let $E_1(z)$, $|z| > 0$, denote the complex-valued exponential integral function of z , as defined in Abramowitz and Stegun (1972). Because of the symmetry relationship $E_1(\bar{z}) = \overline{E_1(z)}$ only values of $z=x+iy$ for which $y \geq 0$ are considered.

For moderate and large values of $|z|$ the exponential integral may be evaluated from its continued fraction representation given by (see Abramowitz and Stegun (1972)):

$$\exp(z)E_1(z) = \frac{1}{z + 1 + \frac{1}{z + 1 + \frac{2}{z + 1 + \frac{2}{z + \dots}}} = \lim_{n \rightarrow \infty} w_n(z) \quad . \quad (A.1)$$

This continued fraction converges in a larger domain than the asymptotic series given by equation (3.13). The successive convergents w_n may be generated recursively as follows (see Gautschi (1967)):

$$u_{n+1} = z / (z + a_{n+1} u_n) \quad ,$$

$$v_{n+1} = v_n (u_{n+1} - 1) \quad ,$$

$$w_{n+1} = w_n + v_{n+1} \quad ,$$

for $n=1,2,\dots$, where $a_{n+1} = \langle (n+1)/2 \rangle$ ($\langle x \rangle$ denotes the integer part of x) and the initial values are given by $u_1=1$, $v_1=w_1=1/z$. Using this algorithm an absolute accuracy of at least six significant digits can be achieved throughout the domain where $e(x,y) = x^2 + 14x + 5.0625y^2 \geq 32$, see Baar (1985).

For small values of $|z|$ the exponential integral may be evaluated from its ascending series representation given by equation (3.12), which may be written in the form:

$$E_1(z) + \ln(z) + \gamma = \lim_{n \rightarrow \infty} p_n(z) \quad (\text{A.2})$$

Successive convergents p_n are generated by means of:

$$q_{n+1} = -nzq_n / (n+1)^2, \quad ,$$

$$p_{n+1} = p_n + q_{n+1} \quad ,$$

for $n=1,2,\dots$, the initial values being $p_1=q_1=z$. This method is used if $e(x,y) < 32$ and $-8 < x < 2$.

In the remaining domain near the negative real axis, where $e(x,y) < 32$ and $-16 < x < 8$, the ascending series is slowly converging and it is more efficient to use the Taylor series about $y=0$ given by (see Newman (1985)):

$$\exp(z)E_1(z) = \sum_{n=0}^{\infty} P_n(|x|)(iy)^n \quad , \quad (\text{A.3})$$

where $nP_n(x) = P_{n-1}(x) + 1/x^n$ for $n \geq 0$, $x > 0$, the initial value being $P_0(x) = -\exp(-x)\{Ei(x) + i\pi\}$. In the range $8 < x < 16$ the exponential integral $Ei(x)$ may be computed using the special polynomial approximation:

$$\begin{aligned} x \exp(-x) Ei(x) = & 1.1029749 - 0.0442424t + 0.0198195t^2 \\ & - 0.0089561t^3 + 0.0039184t^4 - 0.0015478t^5 \\ & + 0.0003842t^6 - 0.0000052t^7 + \epsilon(x) \end{aligned}$$

where $t = \frac{1}{4}x - 3$ and $|\epsilon| < 4.7E-7$, see Baar (1985).

THE BESSEL FUNCTIONS

Let $J_n(x)$, $Y_n(x)$, $I_n(x)$ and $K_n(x)$, $n \geq 0$, $x > 0$ denote the usual Bessel functions of x and integer order n , as defined in Abramowitz and Stegun (1972). For $n=0,1$ the Bessel functions $J_n(x)$ and $Y_n(x)$ can be computed by means of the polynomial approximations developed by Newman (1984). Similar approximations for the modified Bessel functions $I_n(x)$ and $K_n(x)$ were derived by Allen (1956) and these are quoted in Abramowitz and Stegun (1972). From a numerical point of view it is slightly better to compute $\exp(-x)I_n(x)$ and $\exp(x)K_n(x)$ since this removes most of the variation in $I_n(x)$ and $K_n(x)$ respectively.

When $n \geq 2$ the following procedures proposed by Baar and Price (1986b) are very convenient. Following Gautschi (1967) consider the general three-term recurrence relationship:

$$f_{n+1} + a_n f_n + b_n f_{n-1} = 0 \quad , \quad (A.4)$$

where $f_n = f_n(x)$ and $n \geq 1$. For the Bessel functions the coefficients $a_n(x)$ and $b_n(x)$ are given by Abramowitz and Stegun (1972) as:

$$(a_n, b_n) = \begin{cases} (-2n/x, 1) \\ (2n/x, -1) \\ (-2n/x, -1) \end{cases} \quad \text{if } f_n = \begin{cases} J_n, Y_n \\ I_n \\ K_n \end{cases} \quad (A.5)$$

From equation (A.4) it follows that the ratio $r_n(x) = f_{n+1}/f_n$ satisfies the relationship:

$$r_n + a_n + b_n/r_{n-1} = 0 \quad (A.6)$$

for $n \geq 1$, provided that $f_n \neq 0$ (this restriction is not serious from the practical point of view, as explained by Gautschi (1967)).

The functions $Y_n(x)$ and $K_n(x)$ are numerically increasing functions of n and the ratios r_n can simply be computed by means of the forward recurrence:

$$r_n = -(a_n + b_n/r_{n-1})$$

for $n \geq 1$, the initial value being $r_0 = f_1/f_0$.

The functions $J_n(x)$ and $I_n(x)$ are numerically decreasing functions of n (i.e. 'minimal' solutions of equation (A.4)) and therefore the recurrence relationship given by equation (A.6) is only stable when applied in the backward direction. That is:

$$r_{n-1} = -b_n / (a_n + r_n)$$

for $n=N, N-1, \dots, 1$, where it is assumed that the ratio r_n is known for some value $n=N$. Gautschi (1967) shows that r_N is given by the continued fraction:

$$r_N = \frac{-b_{N+1}}{a_{N+1}} - \frac{b_{N+2}}{a_{N+2}} - \frac{b_{N+3}}{a_{N+3}} - \dots = \lim_{n \rightarrow \infty} w_n,$$

where a_n and b_n are given by equation (A.5). The successive convergent values of w_n may be generated recursively as follows:

$$u_{n+1} = 1 / \{ 1 - (b_{N+n+1} / a_{N+n} a_{N+n+1}) u_n \},$$

$$v_{n+1} = v_n (u_{n+1} - 1),$$

$$w_{n+1} = w_n + v_{n+1}$$

for $n=1, 2, \dots$, the initial values being $u_1=1$, $v_1=w_1=-b_{N+1}/a_{N+1}$.

The presented algorithms are very well suited to the computation of the sequences of Bessel function ratios defined in equations (5.7a-d). In order to verify the relationships given by equations (5.8a-b), as well as to derive similar relationships

for the evaluation of the gradient of the wavelike disturbance, the following derivative relations are useful:

$$cf'_n = f_{n-1} + df_{n+1}, \quad (A.7)$$

where $f'_n = df_n(x)/dx$ and

$$(c,d) = \begin{cases} (2,-1) \\ (2,1) \\ (-2,1) \end{cases} \text{ if } f_n = \begin{cases} J_n, Y_n \\ I_n \\ K_n \end{cases}, \quad (A.8)$$

see Abramowitz and Stegun (1972). In particular:

$$(J'_0, Y'_0, I'_0, K'_0) = (-J_1, -Y_1, I_1, -K_1).$$

REFERENCES

- Abramowitz, M. and Stegun, I.A. (eds), 1972, Handbook of mathematical functions. Dover Publ., New York.
- Adachi, H. and Takeshi, H., 1983, 'Neumann-Kelvin problem solved by the iterative procedure using Hess and Smith solver program'. Proc. 2nd DTNSRDC Workshop Ship Wave-Resistance Comp., Bethesda, pp. 281-320.
- Allen, E.E., 1956, 'Polynomial approximations to some modified Bessel functions'. Math. Tables Aids Comp., vol. 10, pp. 162-164.
- Andersson, B.J., 1975, 'Notes on the theory of ship waves'. Dept. Hydromech., Roy. Inst. Tech., Stockholm.
- Andrew, R.N., 1985, 'Distributed vertical wave force on a ship with forward speed'. Univ. London, Ph.D. thesis.
- Andrew, R.N., 1986, private communication.
- Andrew, R.N., Baar, J.J.M. and Price, W.G., 1986, 'Prediction of ship wavemaking resistance and other steady flow parameters using Neumann-Kelvin theory'. Trans. Roy. Inst. Naval Arch., to appear.
- Baar, J.J.M., 1984a, 'On the use of Green's functions in marine hydromechanics. Part 1: Singularity distributions'. Mech. Eng. Dept., Brunel Univ., Uxbridge.
- Baar, J.J.M., 1984b, 'On the use of Green's functions in marine hydromechanics. Part 2: Translating, pulsating source in shallow water'. Mech. Eng. Dept., Brunel Univ., Uxbridge.

- Baar, J.J.M., 1985, 'Evaluation of the complex-valued exponential integral function'. Mech. Eng. Dept., Brunel Univ., Uxbridge.
- Baar, J.J.M. and Price, W.G., 1986a, 'Developments in the calculation of the wavemaking resistance of ships'. Proc. Roy. Soc., to appear.
- Baar, J.J.M. and Price, W.G., 1986b, 'Evaluation of the wavelike disturbance in the Kelvin wave source potential'. J. Ship Res., to appear.
- Baba, E., 1976, 'Wave resistance of ships in low speed'. Mitsubishi Heavy Ind., Nagasaki, Tech. Bull. No. 199.
- Baba, E., 1977, 'Numerical evaluation of a wave-resistance theory for slow ships'. Proc. 2nd Int. Conf. Num. Ship Hydrodyn., Berkeley, pp. 17-29.
- Baba, E., 1979, 'Wave-resistance computations by low speed theory'. Proc. Workshop Ship Wave-Resistance Comp., Bethesda, pp. 306-317.
- Bai, K.J., 1977, 'A localized finite-element method for steady three-dimensional ship-wave problems'. Proc. 2nd Int. Conf. Num. Ship Hydrodyn., Berkeley, pp. 78-87.
- Bai, K.J., 1979, 'Wave resistance in a restricted water by the localized finite element method'. Proc. Workshop Ship Wave-Resistance Comp., Berkeley, pp. 407-419.
- Bernoulli, D., 1757, 'Principes hydrostatiques et mecaniques, ou memoire sur la maniere de diminuer le roulis et le tangage d'un navire sans qu'il perde sensiblement aucune des bonnes qualites que sa construction doit lui donner'. Prix de l'Academie des Sciences, Paris.
- Bessho, M., 1961, 'On the wave-making resistance of submerged prolate spheroids'. J. Zosen Kiokai, vol. 109, pp. 59-72.

- Bessho, M., 1964, 'The fundamental function in the theory of the wave-making resistance of ships'. Mem. Def. Acad. Japan, vol. 4, pp. 99-119.
- Bessho, M., 1976, 'Line integral, uniqueness and diffraction of wave in the linearized theory'. Proc. Int. Sem. Wave Resistance, Tokyo and Osaka, pp. 45-55.
- Bishop, R.E.D. and Price, W.G., 1979, Hydroelasticity of ships. Cambridge Univ. Press, Cambridge.
- Brard, R., 1971, 'The Neumann-Kelvin problem for surface ships'. Bassin d'Essais des Carenes, Paris, Rep. No. 11 CST.
- Brard, R., 1972, 'The representation of a given ship form by singularity distributions when the boundary condition on the free surface is linearized'. J. Ship Res., vol. 16, pp. 79-92.
- Brard, R., 1974a, 'Le probleme de Neumann-Kelvin'. C.-R. Acad. Sci., Paris, Serie A, vol. 278, pp. 163-167.
- Brard, R., 1974b, 'Complements sur le probleme de Neumann-Kelvin'. C.-R. Acad. Sci., Paris, Serie A, vol. 278, pp. 379-384.
- Chamberlain, R.R. and Yen, S.M., 1985, 'Numerical solution of the nonlinear ship wave problem'. Proc. 4th Int. Conf. Num. Ship Hydrodyn., Washington, pp. 246-258.
- Chan, R.K.-C. and Chan, F.W.-K., 1979, 'Nonlinear calculations of three-dimensional flow about a ship'. Proc. Workshop Ship Wave-Resistance Comp., Bethesda, pp. 420-433.
- Chang, M.S., 1979, 'Wave resistance predictions using a singularity method'. Proc. Workshop Ship Wave-Resistance Comp., Bethesda, pp. 202-213.

Chang, M.S. and Pien, P.C., 1975, 'Hydrodynamic forces on a body moving beneath a free surface'. Proc. 1st Int. Conf. Num. Ship Hydrodyn., Gaitherburg, pp. 539-559.

Chen, C.Y. and Noblesse, F., 1983a, 'Preliminary numerical study of a new slender-ship theory of wave resistance'. J. Ship. Res., vol. 27, pp. 172-186.

Chen, C.Y. and Noblesse, F., 1983b, 'Comparison between theoretical predictions of wave resistance and experimental data for the Wigley hull'. J. Ship Res., vol. 27, pp. 215-226.

Chow, S.K., Hou, A.Y. and Landweber, L., 1976, 'Hydrodynamic forces and moments acting on a body emerging from an infinite plane'. Phys. Fluids, vol. 19, pp. 1439-1449.

Chung, Y.K., 1984, 'Ray theory and Kelvin wave'. J. Ship Res., vol. 28, pp. 213-217.

Collatz, G., 1972, 'Mass-Stabsuntersuchungen fur ein Modell grosser Volligkeit'. Forschungszentrum Deutschen Schiffbau, Hamburg, Bericht Nr. 28.

Daube, O., 1980, 'Contribution au calcul non lineaire de la resistance de vagues du'n navire'. Univ. Nantes, Ph. D. thesis.

Daube, O. and Dulieu, A., 1981, 'A numerical approach to the nonlinear wave resistance problem'. Proc. 3rd Int. Conf. Num. Ship Hydrodyn., Paris.

Davis, P.J. and Rabinowitz, P., 1975, Methods of numerical integration. Acad. Press, New York, 2nd edn.

Dawson, C.W., 1977, 'A practical computer method for solving ship-wave problems'. Proc. 2nd Int. Conf. Num. Ship Hydrodyn., Berkeley, pp. 30-38.

- Demanche, J.F., 1981, 'Potential of a moving pulsating source'. Proc. 3rd Int. Conf. Num. Ship Hydrodyn., Paris, pp.27-36.
- Dern, J.C., 1977, 'Existence, uniqueness and regularity of the solution of the Neumann-Kelvin problem for two- or three-dimensional submerged bodies'. Proc. 2nd Int. Conf. Num. Ship Hydrodyn., Berkeley, pp. 57-77.
- Eggers, K.W.H., 1966, 'Second-order contributions to ship waves and wave resistance'. Proc. 6th Symp. Naval Hydrodyn., Washington, pp. 649-672.
- Eggers, K.W.H., 1980, 'On the irregularities of the wave-flow due to source panels and how to compensate them by adding Kelvin-source line elements'. Proc. Cont. Workshop Ship Wave-Resistance Comp., Izu Shuzenji, pp. 101-106.
- Eggers, K.W.H. and Choi, H.S., 1975, 'On the calculation of stationary ship flow components'. Proc. 1st Int. Conf. Num. Ship Hydrodyn., Gaithersburg, pp. 455-479.
- Eggers, K.W.H., Sharma, S.D. and Ward, L.W., 1967, 'An assessment of some experimental methods for determining the wavemaking characteristics of a ship form'. Trans. Soc. Naval Arch. Mar. Eng., vol. 75, pp. 112-144.
- Emerson, A., 1967, 'The calculation of ship resistance: an application of Guilloton's method'. Trans. Inst. Naval Arch., vol. 109, pp. 241-248.
- Emerson, A., 1971, 'Hull form and ship resistance'. N.-E. Coast Inst. Eng. Shipb. Trans., vol. 87, pp. 139-150.
- Erdelyi, A., 1956, Asymptotic expansions. Dover Publ., New York.

Euler, L., 1749, *Scientia navalis, seu tractatus de construendis ac dirigendis navibus*. St Peterburg.

Euvrard, D., 1983, 'Les mille et une facettes de la fonction de Green du probleme de la Resistance de Vagues'. Ecole Nationale Superieure de Techniques Avancees, Paris, Rep. No. 144.

Farell, C., 1973, 'On the wave resistance of a submerged spheroid'. *J. Ship Res.*, vol. 17, pp. 1-11.

Fox, L. and Parker, I.B., 1968, *Chebyshev polynomials in numerical analysis*. Oxford Univ. Press, London.

Froude, R.E., 1889, 'On the leading phenomena of the wave-making resistance of ships'. *Trans. Inst. Naval Arch.*, vol. 22, pp. 220-224.

Froude, W., 1868, 'Observations and suggestions on the subject of determining by experiment the resistance of ships'. Memo. to E.J. Reed, Chief Constructor of the Navy.

Froude, W., 1876, 'The fundamental principles of the resistance of ships'. *Proc. Roy. Inst. Gt. Brit.*, vol. 8, pp. 188-213.

Froude, W., 1877, 'On experiments upon the effect produced on the wave-making resistance of ships by length of parallel middle body'. *Trans. Inst. Naval Arch.*, vol. 18, pp. 77-87.

Gadd, G.E., 1968, 'On understanding ship resistance mathematically'. *J. Inst. Math. Appl.*, vol. 4, pp. 43-57.

Gadd, G.E., 1970, 'A method for calculating the flow over ship hulls'. *Trans. Roy. Inst. Naval Arch.*, Vol.112, pp.335-345.

- Gadd, G.E., 1973, 'Wave resistance calculations by Guilloton's method'.
Trans. Roy. Inst. Naval Arch., vol. 115, pp. 377-384.
- Gadd, G.E., 1976, 'A method of computing the flow and surface wave
pattern around full forms'. Trans. Roy. Inst. Naval Arch., vol.
118, pp. 207-219.
- Gadd, G.E., 1979, 'Contribution to Workshop on Ship Wave-Resistance
Computations'. Proc. Workshop Ship Wave-Resistance Comp., Bethesda,
pp. 117-161.
- Gamst, A., 1979, 'Existenz, Eindeutigkeit und Regularitat stationarer
Wellen Stromungen, die von Druck Verteilungen an der Wasserober-
flache verursacht werden. Lineare Theorie'. Univ. Hamburg. Ph. D.
Thesis.
- Gautschi, W., 1967, 'Computational aspects of three-term recurrence
relations'. SIAM Rev., vol. 9, pp. 24-82.
- Gautschi, W., 1970, 'Efficient computation of the complex Error function'.
SIAM J. Num. Anal., vol. 7, pp. 187-198.
- Gawn, R.W.L., 1955, 'The Admiralty Experimental Works, Haslar'. Trans.
Inst. Naval Arch., vol. 97, pp. 1-35.
- Goodwin, E.T., 1956, 'Note on the computation of certain highly
oscillatory integrals'. Math. Tables Aids Comp., vol. 10, pp. 96-97.
- Gradshteyn, I.S. and Ryzhik, I.M. (eds.), 1980, Table of integrals, series
and products. Acad. Press, New York, 4th edn.
- Griffel, D.H., 1981, Applied functional analysis. Ellis Horwood Publ.,
Chichester.

- Guevel, P., Delhommeau, G. and Cordonnier, J.P., 1977, 'Numerical solution of the Neumann-Kelvin problem by the method of singularities'. Proc. 2nd Int. Conf. Num. Ship Hydrodyn., Berkeley, pp. 107-213.
- Guevel, P., Delhommeau, G. and Cordonnier, J.P., 1979, 'The Guilloton's method'. Proc. Workshop Ship Wave-Resistance Comp., Bethesda, pp. 434-448.
- Guevel, P., Vaussy, P. and Kobus, J.M., 1974, 'The distribution of singularities kinematically equivalent to a moving hull in the presence of a free surface'. Int. Shipb. Prog., vol. 21, pp. 311-324.
- Guilloton, R., 1960, 'The waves generated by a moving body'. Trans. Roy. Inst. Naval Arch., vol. 102, pp. 157-173.
- Guilloton, R., 1964, 'L'etude theorique et numerique du bateau en fluide parfait'. Bull. Ass. Tech. Mar. Aeron., vol. 64, pp. 538-561.
- Guilloton, R., 1965, 'La pratique du calcul des isobares sur une carene linearisee'. Bull. Ass. Tech. Mar. Aeron., vol. 65, pp. 379-394.
- Guttman, C., 1983, 'Etude theorique et numerique du probleme de Neumann-Kelvin tridimensionnel pour un corps totalement immerge'. Ecole Nationale Superieure de Techniques Avancees, Paris, Rep. No. 177.
- Havelock, T.H., 1908, 'The propagation of groups of waves in dispersive media, with application to waves on water produced by a travelling disturbance'. Proc. Roy. Soc., Ser. A, vol. 81, pp. 398-430.
- Havelock, T.H., 1923, 'Studies in wave resistance: influence of the form of the water-plane section of the ship'. Proc. Roy. Soc., Ser. A, vol. 103, pp. 571-585.

- Havelock, T.H., 1925, 'Studies in wave resistance: the effect of a parallel middle body'. Proc. Roy. Soc., Ser. A, vol. 108, pp. 77-92.
- Havelock, T.H., 1931a, 'The wave resistance of a spheroid', Proc. Roy. Soc., Ser. A, vol. 131, pp. 275-285.
- Havelock, T.H., 1931b, 'The wave resistance of an ellipsoid'. Proc. Roy. Soc., Ser. A, vol. 132, pp. 480-486.
- Havelock, T.H., 1932, 'The theory of wave resistance'. Proc. Roy. Soc., Ser. A, vol. 138, pp. 339-348.
- Havelock, T.H., 1934, 'Wave patterns and wave resistance'. Trans. Inst. Naval Arch., vol. 76, pp. 430-442.
- Hess, J.L. and Smith, A.M.O., 1966, 'Calculation of potential flow about arbitrary bodies'. Prog. Aeron. Sci., vol. 8, pp. 1-138.
- Hirata, M.H. and Levi da Conceicao, C.A., 1976, 'The line integral term in the wave resistance'. Proc. Int. Sem. Wave Resistance, Tokyo and Osaka, pp. 245-248.
- Hogner, E., 1922, 'A contribution to the theory of ship waves'. Ark. Mat., Astron. Fys., vol. 17, pp. 1-50.
- Hogner, E., 1932, 'Eine Interpolationsformel für den Wellenwiderstand von Schiffen'. Jahrb. Schiffbautech. Gesellschaft, vol. 33, pp. 452-456.
- Holtrop, J. and Mennen, G.G.J., 1978, 'A statistical power prediction method'. Int. Shipb. Prog., vol. 25, pp. 1-4.
- Inglis, R.B., 1980, 'A three-dimensional analysis of the motion of a rigid ship in waves'. Univ. London, Ph.D. thesis.

- Inui, T., 1962, 'Wave-making resistance of ships'. Trans. Soc. Naval Arch. Mar. Eng., vol. 70, pp. 282-326.
- Inui, T., 1976, 'Introductory lecture'. Proc. Int. Sem. Wave Resistance, Tokyo and Osaka, pp. 7-18.
- Inui, T. and Kajitani, H., 1977, 'Study on local non-linear free surface effects in ship waves and wave resistance', Schiffstechnik, vol. 24, pp. 178-213.
- Ju, S., 1983, 'Study of total and viscous resistance for the Wigley parabolic ship form'. Proc. 2nd DTNSRDC Workshop Ship Wave-Resistance Comp., Bethesda, pp. 36-49.
- Kajitani, H., Miyata, H., Ikehata, M., Tanaka, H., Adachi, H., Namimatsu, M. and Ogiwara, S., 1983, 'Summary of the cooperative experiment on Wigley parabolic model in Japan'. Proc. 2nd DTNSRDC Workshop Ship Wave-Resistance Comp., Bethesda, pp. 5-35.
- Kantorovich, L.V. and Akilov, G.P., 1982, Functional analysis. Pergamon Press, Oxford, 2nd edn.
- Kayo, Y., 1978, 'A note on the uniqueness of wave-making resistance when the double-body potential is used as the zero-order approximation'. Trans. West-Japan Soc. Naval Arch., vol. 55, pp. 1-11.
- Keller, J.B., 1974, 'Wave patterns of non-thin or full-bodied ships'. Proc. 10th Symp. Naval Hydrodyn., Cambridge (Ma), pp. 543-547.
- Keller, J.B., 1979, 'The ray theory of ship waves and the class of streamlined ships'. J. Fluid Mech., vol. 91, pp. 465-488.
- Kellogg, O.D., 1954, Foundations of potential theory. Dover Publ., New York.

- Kobayashi, M. and Ikehata, M., 1970, 'On the source distribution representing ship hull form'. J. Soc. Naval Arch. Japan, vol. 128, pp. 1-9.
- Kochin, N.E., 1951, 'On the wave resistance and lift of bodies submerged in a fluid'. Soc. Naval Arch. Mar. Eng., Tech. Bull. 1-8, transl.
- Korving, C. and Hermans, A.J., 1977, 'The wave resistance for flow problems with a free surface'. Proc. 2nd Int. Conf. Num. Ship Hydrodyn., Berkeley, pp. 285-291.
- Kostyukov, A.A., 1968, Theory of ship waves and wave resistance. Eff. Comm. Inc., Iowa, transl.
- Kotik, J. and Morgan, R., 1969, 'The uniqueness problem for wave resistance calculated from singularity distributions which are exact at zero Froude number'. J. Ship Res., vol. 13, pp. 61-68.
- Kreyszig, E., 1983, Advanced engineering mathematics. Wiley, New York, 5th edn.
- Kusaka, Y., 1976, 'On the contribution of line integral to the wave resistance of surface ships'. Proc. Int. Sem. Wave Resistance, Tokyo and Osaka, pp. 249-254.
- Lamb, H., 1932, Hydrodynamics. Cambridge Univ. Press, Cambridge, 6th edn.
- Lenoir, M., 1982, 'Methodes de couplage en hydrodynamique navale et application a la resistance de vagues bidimensionnelle'. Ecole Nationale Superieure de Techniques Avancees, Paris, Rep. No. 164.
- Lighthill, J.H., 1978, Waves in fluids. Cambridge Univ. Press, Cambridge.
- Luke, Y.L., 1969, The special functions and their approximations. Volume II. Acad. Press, New York.

- Lunde, J.K., 1951, 'On the linearized theory of wave resistance for displacement ships in steady and accelerated motion'. Trans. Soc. Naval Arch. Mar. Eng., vol. 59, pp. 25-76.
- Maruo, H., 1962, 'Calculation of the wave resistance of ships, the draught of which is as small as the beam'. J. Zosen Kiokai, vol. 112, pp. 21-37.
- Maruo, H., 1966, 'A note on the higher-order theory of thin ships'. Bull. Fac. Eng., Yokohama Nat. Univ., vol. 15, pp. 1-21.
- Maruo, H., 1977, 'Wave resistance of a ship with finite beam at low Froude numbers'. Bull. Fac. Eng., Yokohama Nat. Univ., vol. 26, pp. 59-75.
- Maruo, H., 1982, 'New approach to the theory of slender ships with forward velocity'. Bull. Fac. Eng., Yokohama Nat. Univ., vol. 31, pp. 85-100.
- Maruo, H. and Ikehata, M., 1983, 'An application of new slender ship theory to Series 60, $C_b=0.60$ '. Proc. 2nd DTNSRDC Workshop Ship Wave-Resistance Comp., Bethesda, pp. 141-160.
- Maruo, H. and Ogiwara, S., 1985, 'A method of computation for steady ship waves with nonlinear free surface conditions'. Proc. 4th Int. Conf. Num. Ship Hydrodyn., Washington, pp. 218-233.
- Massie, W.W. (ed.), 1978, 'Coastal engineering. Volume III: Harbour and beach problems'. Coastal Eng. Group, Tech. Univ. Delft.
- McCarthy, J.H. (ed.), 1985, 'Collected experimental resistance component and flow data for three surface ship model hulls'. David W. Taylor Naval Ship Res. Dev. C., Bethesda, Rep. No. DTNSRDC-85/011.
- Mei, C.C., 1978, 'Numerical methods in water-wave diffraction and radiation'. Ann. Rev. Fluid Mech., vol. 10, pp. 393-416.

- Michell, J.H., 1898, 'The wave resistance of a ship'. Phil. Mag., Ser. 5, vol. 45, pp. 106-123.
- Milne-Thomson, L.M., 1968, Theoretical Hydrodynamics. MacMillan Press, London, 5th edn.
- Miyata, H., Nishimura, S. and Kajitani, H., 1983, 'Numerical simulation of ship waves by direct integration of Navier-Stokes equations'. Proc. 2nd DTNSRDC Workshop Ship Wave-Resistance Comp., Bethesda, pp. 441-457.
- Nakatake, K., 1969, 'On the wave pattern created by singular points'. Coll. Eng., Univ. Michigan, Ann Arbor, transl.
- Newman, J.N., 1976, 'Linearized wave resistance theory'. Proc. Int. Sem. Wave Resistance, Tokyo and Osaka, pp. 31-43.
- Newman, J.N., 1977, Marine hydrodynamics. MIT Press, Cambridge (Ma).
- Newman, J.N., 1978, 'The theory of ship motions'. Adv. Appl. Mech., vol. 18, pp. 221-283.
- Newman, J.N., 1984, 'Approximations for the Bessel and Struve functions'. Math. Comp., vol. 43, pp. 551-556.
- Newman, J.N., 1985, 'The evaluation of free-surface Green functions'. Proc. 4th Int. Conf. Num. Ship Hydrodyn., Washington, pp. 4-19.
- Newman, J.N., 1986a, 'Evaluation of the wave-resistance Green function. Part 1: The double integral'. Submitted to J. Ship Res.
- Newman, J.N., 1986b, 'Evaluation of the wave-resistance Green function. Part 2: The single integral on the centerplane'. Private comm.
- Newman, J.N., 1986c, private communication.

- Noblesse, F., 1975, 'The near-field disturbance in the centerplane Havelock source potential'. Proc. 1st Int. Conf. Num. Ship Hydrodyn., Gaithersburg, pp. 481-501.
- Noblesse, F., 1976, 'What is the proper linear model and perturbation scheme for the flow around a ship?'. Proc. Int. Sem. Wave Resistance, Tokyo and Osaka, pp. 393-398.
- Noblesse, F., 1977, 'The fundamental solution of the theory of steady motion of a ship'. J. Ship Res., vol. 21, pp. 82-88.
- Noblesse, F., 1978a, 'The steady wave potential of a unit source, at the centerplane'. J. Ship Res., vol. 22, pp. 80-88.
- Noblesse, F., 1978b, 'On the fundamental function in the theory of steady motion of ships'. J. Ship Res., vol. 22, pp. 212-215.
- Noblesse, F., 1981, 'Alternative integral representations for the Green function of the theory of ship wave resistance'. J. Eng. Math., vol. 15, pp. 241-265.
- Noblesse, F., 1983, 'A slender-ship theory of wave resistance'. J. Ship Res., vol. 27, pp. 13-33.
- Noblesse, F., 1984, 'Convergence of a sequence of slender-ship low-Froude-number wave-resistance approximations'. J. Ship Res., vol. 28, pp. 155-162.
- Noblesse, F. and Dagan, G., 1976, 'Nonlinear ship-wave theories by continuous mapping'. J. Fluid Mech., vol. 75, pp. 347-371.
- Noblesse, F. and Triantafyllou, G., 1983, 'Explicit approximations for calculating potential flow about a body'. J. Ship Res., vol. 27, pp. 1-12.

- Nonweiler, T.N.R., 1984, Computational mathematics. Ellis Horwood Publ., Chichester.
- Ogilvie, T.F., 1970, 'Singular-perturbation problems in ship hydrodynamics'. Adv. Appl. Mech., vol. 17, pp. 91-188.
- Oomen, A.C.W.J., 1979, 'Ship wave-resistance computations by finite element method'. Proc. Workshop Ship Wave-Resistance Comp., Bethesda, pp. 407-419.
- Oomen, A.C.W.J., 1981, 'Free surface potential flow computation using a finite element method'. Proc. 3rd Int. Conf. Num. Ship Hydrodyn., Paris, pp.27-36.
- Patterson, T.N.R., 1973, 'Algorithm 468: Algorithm for automatic numerical integration over a finite interval'. Comm. Ass. Comp. Mach., vol. 16, pp. 694-699.
- Peters, A.S., 1949, 'A new treatment of the ship wave problem'. Comm. Pure Appl. Math., vol. 2, pp. 123-148.
- Peters, A.S. and Stoker, J.J., 1957, 'The motion of a ship, as a rigid floating body, in a seaway'. Comm. Pure Appl. Math., vol. 10, pp. 399-490.
- Price, W.G. and Bishop, R.E.D., 1974, Probabilistic theory of ship dynamics. Chapman and Hall, London.
- Roach, G.F., 1982, Green's functions. Cambridge Univ. Press, Cambridge, 2nd edn.
- Salvesen, N., 1979, 'Athena Model group discussion'. Proc. Workshop Ship Wave-Resistance Comp., Bethesda, pp. 75-85.

- Saunders, H.E., 1957, Hydrodynamics in ship design. Volume 2. Soc. Naval Arch. Mar. Eng., New York.
- Schendel, U., 1984, Introduction to numerical methods for parallel computers. Ellis Horwood Publ., Chichester.
- Sclavounos, P. and Lee, C.H., 1985, 'Topics on boundary-element solutions of wave radiation-diffraction problems'. Proc. 4th Int. Conf. Num. Ship Hydrodyn., Washington, pp. 175-184.
- Sharma, S.D., 1965, 'Zur Problematik der Aufteilung des Schiffswiderstandes in zahigkeits- und wellenbedingte Anteile'. Jahrb. Schiffbautech. Gesellschaft, vol. 59, pp. 458-504.
- Shen, H.-T. and Farell, C., 1977, 'Numerical calculation of the wave integrals in the linearized theory of water waves'. J. Ship Res., vol. 21, pp. 1-10.
- Simmgen, M., 1968, 'Ein Beitrag zur linearisierten Theorie des periodisch instationar angestromten Unterwassertragflugels'. Z. Ang. Math. Mech., vol. 48, pp. 255-264.
- Sneddon, I.H., 1972, The use of integral transforms. McGraw-Hill, New York.
- Sorensen, R.M., 1973, 1973, 'Ship-generated waves'. Adv. Hydrosci., vol. 9, pp. 49-83.
- Standing, R.G., 1975, 'Experience in computing the wavemaking of source/sink models'. Nat. Phys. Lab., Teddington, NPL Rep. Ship 190.
- Suzuki, K., 1979, 'Calculation of ship wave resistance with special reference to sinkage'. Proc. Workshop Ship Wave-Resistance Comp., Bethesda, pp. 256-281.

- Swanson, C.V., 1984, 'Radar observability of ship wakes'. Appl. Phys. Tech., Rep. No. 1, 109 pp.
- Thomson, W. (Lord Kelvin), 1887, 'On ship waves'. Proc. Inst. Mech. Eng., vol. 3, pp. 409-434.
- Thomson, W. (Lord Kelvin), 1904, 'Deep water ship waves'. Proc. Roy. Soc. (Edinb.), vol. 25, pp. 562-587.
- Todd, F.H., 1966, 'Viscous resistance of ships'. Adv. Hydrosci., vol. 3, pp. 1-62.
- Tsai, W., Lin, Y. and Liao, C., 1983, 'Numerical solution of the Neumann-Kelvin problem and its application to ship wave-resistance computations'. Proc. 2nd DTNSRDC Workshop Ship Wave-Resistance Comp., Bethesda, pp. 233-280.
- Tsutsumi, T., 1979, 'Calculation of the wave resistance of ships by the numerical solution of the Neumann-Kelvin problem'. Proc. Workshop Ship Wave-Resistance Comp., Bethesda, pp. 162-201.
- Tuck, E.O., 1964, 'A systematic asymptotic expansion procedure for slender ships'. J. Ship Res., vol. 8, pp. 15-23.
- Tulin, P., 1984, 'Surface waves from the ray point of view'. Proc. 4th Int. Conf. Num. Ship Hydrodyn., Washington, pp. 9-29.
- Tursini, L., 1953, 'Leonardo da Vinci and the problems of navigation and naval design'. Trans. Inst. Naval Arch., vol. 95, pp. 97-102.
- Ursell, F., 1960, 'On Kelvin's ship-wave pattern'. J. Fluid Mech., vol. 8, pp. 418-431.
- Ursell, F., 1984, 'Mathematical note on the fundamental solution (Kelvin source) in ship hydrodynamics'. IMA J. Appl. Math., vol. 32, pp. 335-351.

- Vossers, G., 1962, 'Wave resistance of a slender ship'. Schiffstechnik, vol. 9, pp. 73-78.
- Watson, G.N., 1944, A treatise on the theory of Bessel functions. Cambridge Univ. Press, Cambridge, 2nd edn.
- Weber, H., 1981, 'Numerical computation of the Fourier transform using Laguerre functions and the Fast Fourier Transform'. Num. Math., vol. 36, pp. 197-209.
- Wehausen, J.V., 1963, 'An approach to thin-ship theory'. Proc. Int. Sem. Theor. Wave Resistance, Ann Arbor, pp. 819-852.
- Wehausen, J.V., 1969, 'Use of Lagrangian coordinates for ship wave resistance (first- and second-order thin-ship theory)'. J. Ship Res., vol. 13, pp. 12-22.
- Wehausen, J.V., 1973, 'The wave resistance of ships'. Adv. Appl. Mech., vol. 13, pp. 93-245.
- Wehausen, J.V., 1976, 'Some further remarks (a bibliography of wave resistance of ships)'. Proc. Int. Sem. Wave Resistance, Tokyo and Osaka, pp. 19-29.
- Wehausen, J.V. and Laitone, E.V., 'Surface waves'. Handbuch der Physik, Springer-Verlag, Berlin, Bd. IX, pp. 446-778.
- Weinblum, G., 1963, 'On problems of wave resistance research'. Int. Sem. Theor. Wave Resistance, Ann Arbor, pp. 1-44.
- Wigley, W.C.S., 1942, 'Calculated and measured wave resistance of a series of forms defined algebraically, the prismatic coefficient and angle of entrance being varied independently'. Trans. Inst. Naval Arch., vol. 86, pp. 41-56.

- Wigley, W.C.S., 1949, 'L'Etat actuel des calculs de resistance de vagues'.
Bull. Ass. Tech. Mar. Aeron., vol. 48, pp. 533-564.
- Wu, Y., 1984, 'Hydroelasticity of floating bodies'. Brunel Univ., Uxbridge,
Ph.D. thesis.
- Yen, S.M. and Chamberlain, R.R., 1983, 'Numerical calculations of the
potential flow about the Wigley hull'. Proc. 2nd DTNSRDC Workshop
Ship Wave-Resistance Comp., Bethesda, pp. 422-440.
- Yeung, R.W., 1972, 'Sinkage and trim in first-order thin-ship theory'.
J. Ship Res., vol. 16, pp. 47-59.
- Yeung, R.W., 1982, 'Numerical methods in free-surface flows'. Ann. Rev.
Fluid Mech., vol. 14, pp. 395-442.
- Yeung, R.W. and Kim, S.H., 1984, 'A new development in the theory of
oscillating and translating slender ships'. Proc. 15th Symp. Naval
Hydrodyn., Hamburg, pp. 195-212.
- Yim, B., 1968, 'Higher order wave theory of ships'. J. Ship Res., vol.12,
pp. 237-245.
- Yim, B., 1981, 'A ray theory for nonlinear ship waves and wave resistance'.
Proc. 3rd Int. Conf. Num. Ship Hydrodyn., Paris, pp.55-71.
- Zienkiewicz, O.C., 1977, The finite element method. McGraw-Hill, London,
3rd edn.

NOMENCLATURE

General conventions

- Nondimensional flow variables in terms of the fluid density, the ship speed and the ship length are used exclusively.
- The coordinate system $Oxyz$ is attached to the moving ship. The origin O is located amidships in the undisturbed sea surface. The positive Ox and Oz axes point toward the ship's bow and vertically upward respectively.
- Whenever the independent variables x, y, z are used as subscripts partial differentiation with respect to x, y, z is implied.
- The definition and notation of mathematical functions is in agreement with Abramowitz and Stegun (1972).

List of symbols

Symbols not included in the list below are only used at a specific place and are explained where they occur.

| | |
|-------------|--|
| b | - beam/length ratio of ship |
| c | - mean water line contour |
| d | - draft/length ratio of ship |
| d_w | - drag force |
| d | - mean flow domain |
| d_i | - interior flow domain |
| g | - acceleration of gravity |
| h | - mean hull surface |
| i_k | - k-th moment of area of mean water line plane |
| l_w | - lift force |
| m_w | - trimming moment |
| n | - unit vector normal to hull surface |
| \tilde{p} | - fluid pressure |
| q | - aspect ratio |

| | |
|---------------|---|
| s_w | - sinkage |
| s | - undisturbed free surface |
| s_z | - mean water line plane |
| t | - unit vector tangent to water line contour |
| \tilde{u} | - perturbed flow velocity |
| \tilde{x} | - position vector of source point |
| C_t | - total resistance coefficient |
| C_v | - viscous resistance coefficient |
| C_w | - wave resistance coefficient |
| F_n | - Froude number |
| G | - Kelvin wave source potential |
| G_0 | - zero Froude number Green's function |
| G_1 | - infinite Froude number Green's function |
| K | - Kochin's function |
| L | - water line length of ship |
| N | - nearfield disturbance |
| Q | - source strength |
| R_n | - Reynolds number |
| S | - dipole strength |
| U | - flow velocity |
| V | - ship speed |
| W | - wavelike disturbance |
| \tilde{X} | - vector joining the field point and the free surface mirror image of the source point |
| α_{ij} | - influence coefficient |
| β_{ij} | - influence coefficient |
| ζ_w | - wave elevation |
| ν | - kinematic viscosity of fluid |
| ξ | - position vector of field point |
| ρ | - density of fluid |
| ϕ | - disturbance potential |
| ϕ^i | - interior potential |
| ϕ_0 | - zero Froude number (double body) potential |
| ψ | - explicit potential approximation |
| Φ | - velocity potential |

ACKNOWLEDGEMENT

I gratefully acknowledge the encouragement of Dr. R.K. Burcher (Chief Superintendent, ARE, Haslar) during the development of this work which has been carried out with the support of the Procurement Executive (MOD).

I am grateful to Dr. R.N. Andrew (Defence Staff, MOD, Whitehall, formerly ARE) who provided encouragement support and experimental data, as well as a memorable dinner in the Painted Hall of the Royal Naval College, Greenwich.

Prof. W.G. Price (my supervisor at Brunel University) provided valuable guidance, advice and encouragement, as well as kind hospitality in Gosport. Jenny Price did the typing with amazing speed and accuracy. Her help is gratefully acknowledged.

Prof. J. Gerritsma (Delft University of Technology), who taught me ship hydrodynamics, suggested my specialisation at Brunel University and I am indebted to him for thus enriching my life with 'the English experience'.

The interest and cooperation of my past and present colleagues at Brunel is gratefully acknowledged. Dr. F. Noblesse (DTNSRDC, Bethesda) provided valuable discussion, support and encouragement. I am indebted to Prof. J.N. Newman (MIT, Boston) for drawing my full attention to Bessho's remarkable paper as well as supplying the Chebyshev series expansions of the nearfield disturbance.

The musical accompaniment of Bach et al during hours of contemplation and reflection was much appreciated.

Finally, none of this would have been possible without the support, encouragement and patience of my wife, whose confidence never failed.